RMZ

MATERIALS and GEOENVIRONMENT

MATERIALI in GEOOKOLJE

RMZ – M&G, **Vol. 65**, No. 2
pp. 079–114 (2018)

Ljubljana, June 2018

RMZ – Materials and Geoenvironment
RMZ – Materiali in geookolje
ISSN 1408-7073

Old title/Star naslov
Mining and Metallurgy Quarterly/Rudarsko-metalurški zbornik
ISSN 0035-9645, 1952–1997

Published by/Izdajatelj
Faculty of Natural Sciences and Engineering, University of Ljubljana/
Naravoslovnotehniška fakulteta, Univerza v Ljubljani

Associated Publisher/Soizdajatelj
Institute for Mining, Geotechnology and Environment, Ljubljana/
Inštitut za rudarstvo, geotehnologijo in okolje
Velenje Coal Mine/Premogovnik Velenje
Slovenian Chamber of Engineers/Inženirska zbornica Slovenije

Editorial Address/Naslov uredništva
RMZ – Materials and Geoenvironment
Aškerčeva cesta 12, p. p. 312
1001 Ljubljana, Slovenija
Tel.: +386 (0)1 470 46 10
Fax.: +386 (0)1 470 45 60
E-mail: rmz-mg@ntf.uni-lj.si

Published/Izhajanje
4 issues per year/4 številke letno

Partly funded by Ministry of Education, Science and Sport of Republic of Slovenia./Pri financiranju revije sodeluje Ministrstvo za izobraževanje, znanost in šport Republike Slovenije.

Articles published in Journal "RMZ M&G" are indexed in international secondary periodicals and databases:/Članki, objavljeni v periodični publikaciji „RMZ M&G", so indeksirani v mednarodnih sekundarnih virih: CA SEARCH® – Chemical Abstracts®, METADEX®, GeoRef.

Annual subscription for individuals in Slovenia: 20 EUR, for institutions: 30 EUR. Annual subscription for the rest of the world: 30 EUR, for institutions: 50 EUR/Letna naročnina za posameznike v Sloveniji: 20 EUR, za inštitucije: 30 EUR. Letna naročnina za tujino: 30 EUR, inštitucije: 50 EUR

Transaction account/Tekoči račun
Nova Ljubljanska banka, d. d., Ljubljana: UJP 01100-6030708186

VAT identification number/Davčna številka
24405388

Online Journal/Elektronska revija
www.rmz-mg.com
www.degruyter.com/view/j/rmzmag

Table of Contents

Kazalo

Historical Review

More than 90 years have passed since the University Ljubljana in Slovenia was founded in 1919. Technical fields were united in the School of Engineering that included the Geologic and Mining Division, while the Metallurgy Division was established only in 1939. Today, the Departments of Geology, Mining and Geotechnology, Materials and Metallurgy are all part of the Faculty of Natural Sciences and Engineering, University of Ljubljana.

Before World War II, the members of the Mining Section together with the Association of Yugoslav Mining and Metallurgy Engineers began to publish the summaries of their research and studies in their technical periodical Rudarski zbornik (Mining Proceedings). Three volumes of Rudarski zbornik (1937, 1938 and 1939) were published. The War interrupted the publication and it was not until 1952 that the first issue of the new journal Rudarsko-metalurški zbornik – RMZ (Mining and Metallurgy Quarterly) was published by the Division of Mining and Metallurgy, University of Ljubljana. Today, the journal is regularly published quarterly. RMZ – M&G is co-issued and co-financed by the Faculty of Natural Sciences and Engineering Ljubljana, the Institute for Mining, Geotechnology and Environment Ljubljana, and the Velenje Coal Mine. In addition, it is partly funded by the Ministry of Education, Science and Sport of Slovenia.

During the meeting of the Advisory and the Editorial Board on May 22, 1998, Rudarsko-metalurški zbornik was renamed into "RMZ – Materials and Geoenvironment (RMZ – Materiali in Geookolje)" or shortly RMZ – M&G. RMZ – M&G is managed by an advisory and international editorial board and is exchanged with other world-known periodicals. All the papers submitted to the RMZ – M&G undergoes the course of the peer-review process.

RMZ – M&G is the only scientific and professional periodical in Slovenia which has been published in the same form for 60 years. It incorporates the scientific and professional topics on geology, mining, geotechnology, materials and metallurgy. In the year 2013, the Editorial Board decided to modernize the journal's format.

A wide range of topics on geosciences are welcome to be published in the RMZ – Materials and Geoenvironment. Research results in geology, hydrogeology, mining, geotechnology, materials, metallurgy, natural and anthropogenic pollution of environment, biogeochemistry are the proposed fields of work which the journal will handle.

Editor-in-Chief

Zgodovinski pregled

Že več kot 90 let je minilo od ustanovitve Univerze v Ljubljani leta 1919. Tehnične stroke so se združile v Tehniški visoki šoli, ki sta jo sestavljala oddelka za geologijo in rudarstvo, medtem ko je bil oddelek za metalurgijo ustanovljen leta 1939. Danes oddelki za geologijo, rudarstvo in geotehnologijo ter materiale in metalurgijo delujejo v sklopu Naravoslovnotehniške fakultete Univerze v Ljubljani.

Pred 2. svetovno vojno so člani rudarske sekcije skupaj z Združenjem jugoslovanskih inženirjev rudarstva in metalurgije začeli izdajanje povzetkov njihovega raziskovalnega dela v Rudarskem zborniku. Izšli so trije letniki zbornika (1937, 1938 in 1939). Vojna je prekinila izdajanje zbornika vse do leta 1952, ko je izšel prvi letnik nove revije Rudarsko-metalurški zbornik – RMZ v izdaji odsekov za rudarstvo in metalurgijo Univerze v Ljubljani. Danes revija izhaja štirikrat letno. RMZ – M&G izdajajo in financirajo Naravoslovnotehniška fakulteta v Ljubljani, Inštitut za rudarstvo, geotehnologijo in okolje ter Premogovnik Velenje. Prav tako izdajo revije financira Ministrstvo za izobraževanje, znanost in šport.

Na seji izdajateljskega sveta in uredniškega odbora je bilo 22. maja 1998 sklenjeno, da se Rudarsko-metalurški zbornik preimenuje v RMZ – Materiali in geookolje (RMZ – Materials and Geoenvironment) ali skrajšano RMZ – M&G. Revijo RMZ – M&G upravljata izdajateljski svet in mednarodni uredniški odbor. Revija je vključena v mednarodno izmenjavo svetovno znanih publikacij. Vsi članki so podvrženi recenzijskemu postopku.

RMZ – M&G je edina strokovno-znanstvena revija v Sloveniji, ki izhaja v nespremenjeni obliki že 60 let. Združuje področja geologije, rudarstva, geotehnologije, materialov in metalurgije. Uredniški odbor je leta 2013 sklenil, da posodobi obliko revije.

Za objavo v reviji RMZ – Materiali in geookolje so dobrodošli tudi prispevki s širokega področja geoznanosti, kot so: geologija, hidrologija, rudarstvo, geotehnologija, materiali, metalurgija, onesnaževanje okolja in biokemija.

Glavni urednik

Original scientific paper

Received: Jun 25, 2017
Accepted: Nov 29, 2017
DOI: 10.2478/rmzmag-2018-0010

Design of underground structures and analysis of self-support capacity

Projektiranje podzemnih objektov in analiza samonosilnosti hribine

Matej Nagy[1,*]
[1] Salini Impregilo S.p.A. Via dei Missaglia, 97 - 20142 Milano
* matejn@ymail.com

Abstract

The complicated rock structures and the stability of surrounding rocks of the underground powerhouse are key ground mechanical challenges for hydropower projects.

In this paper, an example of contributing self-support capacity of rock mass to evaluate optimised support for long-term usage of structure is given. It describes importance of investigations in the initial in situ stress distribution, rock mechanical and geological properties, engineering rock mass classifications by different methods, numerical modelling, comparison of tools for stability and support analysis and proper stability control for rock excavation and support.

The results show that after underground excavations in hard rock, detailed analysis of measures to investigate deformation and self-supporting capacity creation is useful and a cost-saving procedure.

Key words: Hydropower tunnel, Power house cavern, Self-support capacity, Underground Excavation, Support installation

Povzetek

Kompleksna struktura tal in stabilnost hribine pri gradnji velike podzemne strojnice so ključni inženirski izzivi pri projektiranju hidroelektrarn. V tem prispevku je prikazan primer, ki prispeva k razumenvanju karakteristik samonosilnosti hribine, ocenjevanje optimalnih podpornih ukrepov za dolgoročno obratovanje objekta. Prikazan je pomen preliminarnih raziskav o porazdelitvi napetosti v izkopu, mehanskih in geoloških lastnostih kamnin, geomehanske klasifikacije po različnih inženirskih metodah, numeričnem modeliranju in primerjavi orodij za analizo stabilnosti in podporanja, ustrezen monitoring stabilnosti pri gradnji.

Rezultati kažejo, da je pri podzemnih gradnjah v trdnih kamninah, podrobna analiza ukrepov za spremljanje in preiskovanje deformacij ter lastnosti samonosilnosti hribine, koristen proces, ki predstavlja ekonomičnost uporabe podpornih ukrepov.

Ključne besede: Dovodni tunel, podzemna strojnica, samonosilnost hribine, podzemne gradnje, vgradnja podporja

Introduction

The demand of hydropower projects has been increasing significantly since last few years in countries with hydropower potential. At the same time, standards for environmentally and economically favourable design of power plants have been set at higher levels. As a consequence, power plant underground structures with cross-sectional area more than 1500 m^2 are under construction with an increasing number. In this paper, some reliance concerning important decisive technical solutions for the design of power caverns and intake tunnels is introduced. Images (Figure 1) may provide a first idea concerning required size of underground excavations in hard rock for required power capacity and support systems, which depend on understanding of right rock mass behaviour [1,2].

In the design of underground excavation projects, the main approach is to adjust and minimise rock support to achieve limit state of actual rock mass strength and acceptable displacements.

With technological development in observing deformations, material analysing, and modelling during the design stage, understanding of self-support capacity to achieve acceptable strength has become much easier, which is required to investigate deeper in material behaviour. This method and a more precise interpretation provide a set of parameters for geotechnical design of underground structure and define conditions for precise support installation, which means economical optimisation of used supporting elements. When excavating large underground structures, the cost control is even more important. In large hydropower projects, there are usually excavated complex massive underground structures such as powerhouses, waterway tunnels and shafts. These structures are designed to transport water under a high variable pressure of up to 100 bars, and potential of erosion and dynamic loads are much higher than known from transportation infrastructure (Figure 2a and 2b). Leakage of water has to be controlled with detailed construction and grouting works; hard rock strength could be significantly improved with grout injection in empty spaces.

Main geotechnical and geological challenges allied to the construction of underground

Caverns are stability problems for long-term uninterrupted energy generation. In addition, all technical and economic conditions have to be considered when evaluating suitable

Figure 1: *A view on existing cofferdam (50 m high), valley to be filled and underground structures in the hydropower project of a future main dam (330 m high).*

Figure 2 *(a and b): Waterway tunnel portals and foundation construction of connection tunnels.*

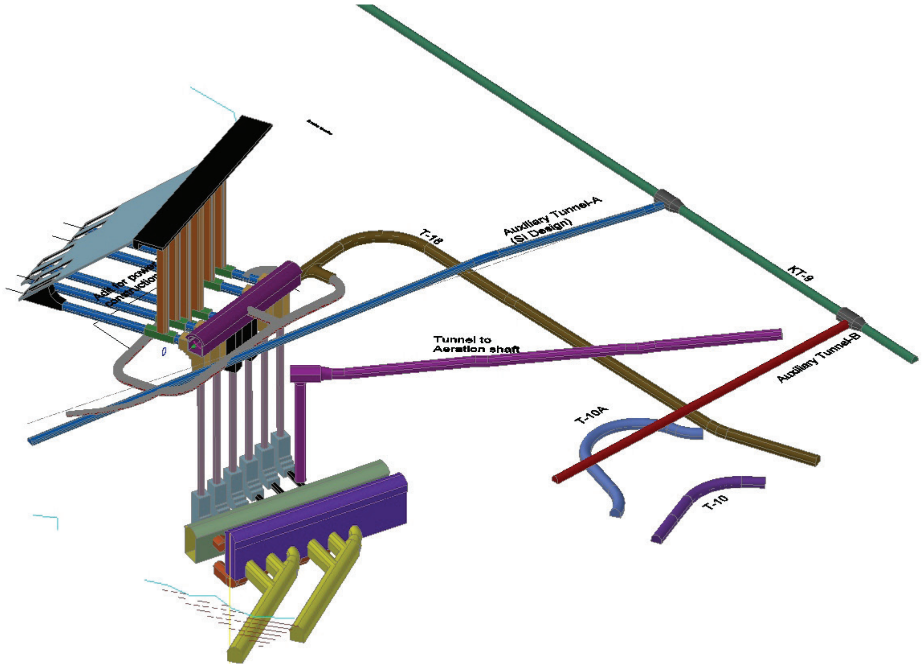

Figure 3: *3D model of underground powerhouse cavern and connection tunnels.*

location and orientation of the underground power cavern (Figure 3).

With correct selection of excavation technology and planning sequences, there are many projects where self-supporting capacity of the rock mass is fully used. Practice shows some cases without concrete lining or some cases used only in distressed sections where a tunnel crosses highly fractured or fault zones.

The underground power house with a cross-section of 22 m × 50 m is taken as an example in this paper.

Positioning of the power house cavern is selected taking into examination the geometry of structural discontinuities in the rock mass. For improvement of self-stability of the crown and side walls, also to minimise issues with blasting over breaks, the excavation direction of underground cavern and waterway tunnels should be intersecting strike orientation of principal discontinuities. Usually some compromises have to be made in the structural design when it is not possible to align it in the perfect direction to achieve minimal influence by discontinuities. According to the project, most suitable positioning of power house cavern has to take consideration of in situ stress measurement and stress directions (Figure 4). It is important to analyse range of *s*H (maximum horizontal principle

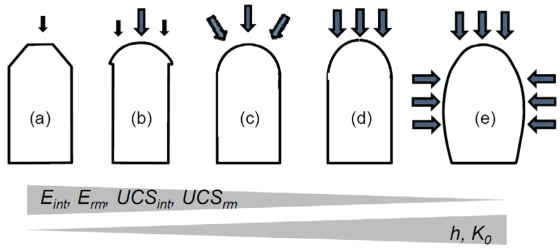

Figure 4: *Different cavern shapes and their applicability according to rock mass properties and stress conditions [3].*

stress), which can cause tensional cracks on the upper part of excavation along the length.

Stability control

In hard rock underground excavation, failures occur on roof and side walls in heavily jointed rock or when the material is exposed to high in situ stress. Wedge or rock blocks failure is the most common type of failure in hard rock excavation where three or more structural intersecting planes form a block with excavation boundary as the fourth plane (Hammett and Hoek, 1981). When wedges are free to fall, the whole stability of cavern will decrease rapidly, causing further progressive rock fall, which leads to reduced rock mass strength. This effect will cause the other wedges to be destabilised, and the failure process will continue until natural shape stage is reached. Orientation of discontinuities, the shape of the cavern and condition of the structural features, i.e. friction and weathering, will influence the structurally controlled instability.

For unfavourable geological conditions, engineering measures have been proven to be successful:

- concrete layer for water tunnels combined with anchors;
- concrete replacement in faults combined with anchor cables;
- systematic installation of anchor cables in the roof and sidewalls of main underground powerhouse and
- careful treatment of open joints with grouting works.

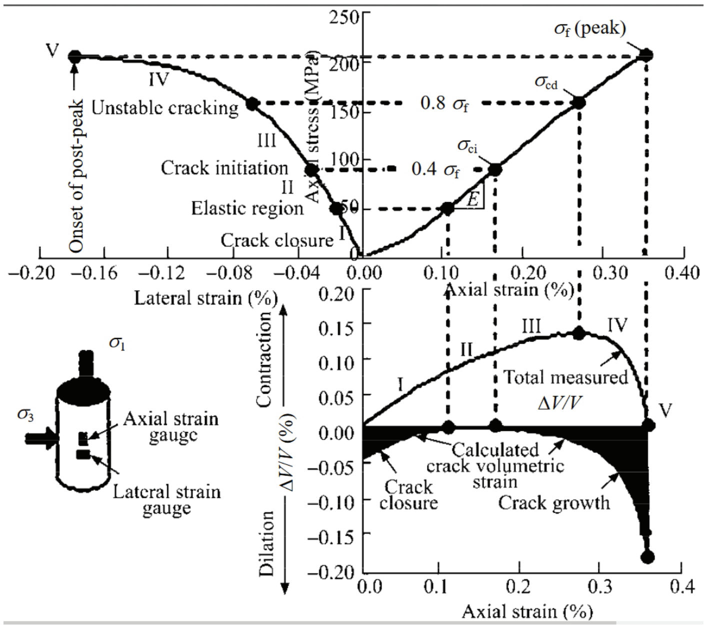

Figure 5: *Stress–strain curves obtained from a single uniaxial test [4].*

It is also important to investigate the failure mechanism process of brittle rock using the laboratory scale. Detailed monitoring of rock sample using compression tests shows crack development behaviour. Stress–strain curve of a brittle rock sample could be divided into four stages:

- crack closure phase;
- linear elasticity phase;
- stable crack growth phase and
- unstable crack growth phase

Figure 5 shows the definitions of crack initiation stress (σ_{ci}), crack damage stress (σ_{cd}) and peak strength (σ_f). Initiation stress of cracking σci is defined as the stress level marking onset of dilation and the beginning of phase III where the stress–strain curve is deviated from linear-elastic behaviour, indicating the development and growth of stable cracks.

Cracks in this stage are referred as stable cracks until an increase in load is required to raise further cracking, and time-dependent crack growth does not occur under a constant load. The crack damage stress, σ_{cd}, is defined as the stress level marking the beginning of phase IV, where the reversal of volumetric strain curve occurs, indicating that the dilation due to the formation and growth of cracks exceeds the elastic compression of the rock resulting from increasing load. Loading a sample with stress more than σ_{cd} results in time-dependent increases in damage to the material, leading to an ultimate sample failure under a sustained constant load. The crack damage stress, therefore, is believed to be indicative of the long-term strength of the rock [4].

The presence of macrocracks in rock mass leads to discontinuous material behaviour, and then under the effect of high pressure, free fragments start to flow, pores form and swell causes slips and rotating particles between blocks (Figure 6). In this failure mechanism, the theory for continuum calculation does not match and the granular medium theory could be used to calculate the dilatancy of the large-scale rock mass geometric model, which means that it is

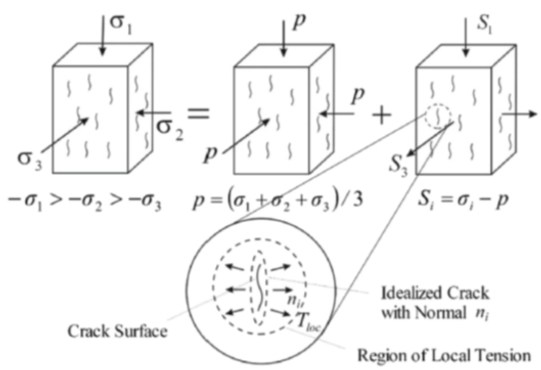

Figure 6: *Relationship between local stress and applied stress [5].*

necessary to use particle flow code (PFC) to demonstrate deformations in the design stage. These phenomena of hard rocks have to be considered in the selection of correct design methodology, especially in projects with large-span underground excavations [5–7].

Self-support capacity

Hard rock mass itself around underground openings has a certain self-support capacity (Figure 7). After tunnelling or larger underground excavation, surrounding rock goes in deformation along the unloading direction, and in the tangential direction, there occurs squeezing of material under the load forces. The inner surrounding rock mass starts to interconnect, and rock mass structure begins to degenerate after an unloading zone is created in the surrounding rock. In the unloaded zone, a self-supporting zone is formed because rock blocks occlude. After displacements, it takes all the load from itself and the above rock mass is integrated with structure [8]. The created zone with new mechanical properties allows the surrounding rock to stabilise in short time. The creation of self-supporting zone is a phenomenon of self-regulation of stress that keeps resistance of deformation in rock mass (Figure 8). Before installation of support systems, it is useful and considerable to control the estimated decompression period correlated with the pre-deformation. The stiffness of the inner zone determines where both curves on the graph intersect. At this stage, equilibrium and compatibility are also completed.

The boundary of self-supporting zone can be determined according to the stress path analysis procedure [9,10].

Figure 7: *Powerhouse cavern under excavation of lower part.*

Design procedure

Complex ground conditions and limit state may affect the stability of caverns and tunnels by the geometry of joints and density of fractures in the surrounded rock mass. With the development of technology and research in numerical analysis of material deformability, comparisons of the calculation obtained by different numerical methods such as finite element method, discrete element method and indirect boundary element method and in case of fractured rock mass also by PFC for better understanding of stress distribution and deformation effects on joins around excavations are numerically studied [5]. In practice, comparisons that indicate the validity of the stress analyses around excavation openings have already been performed.

The influence of model geometry (Figure 9) on each numerical method has to be analysed. Groundwater is one of main issues in underground excavations, where numerical simulation is necessary to estimate the amount of water inflow. A proper scale has high importance for correct analysis in such models. With comparison of analysis, it was found that if the distance between excavation boundary and outer model boundary is too small, then the simulat-

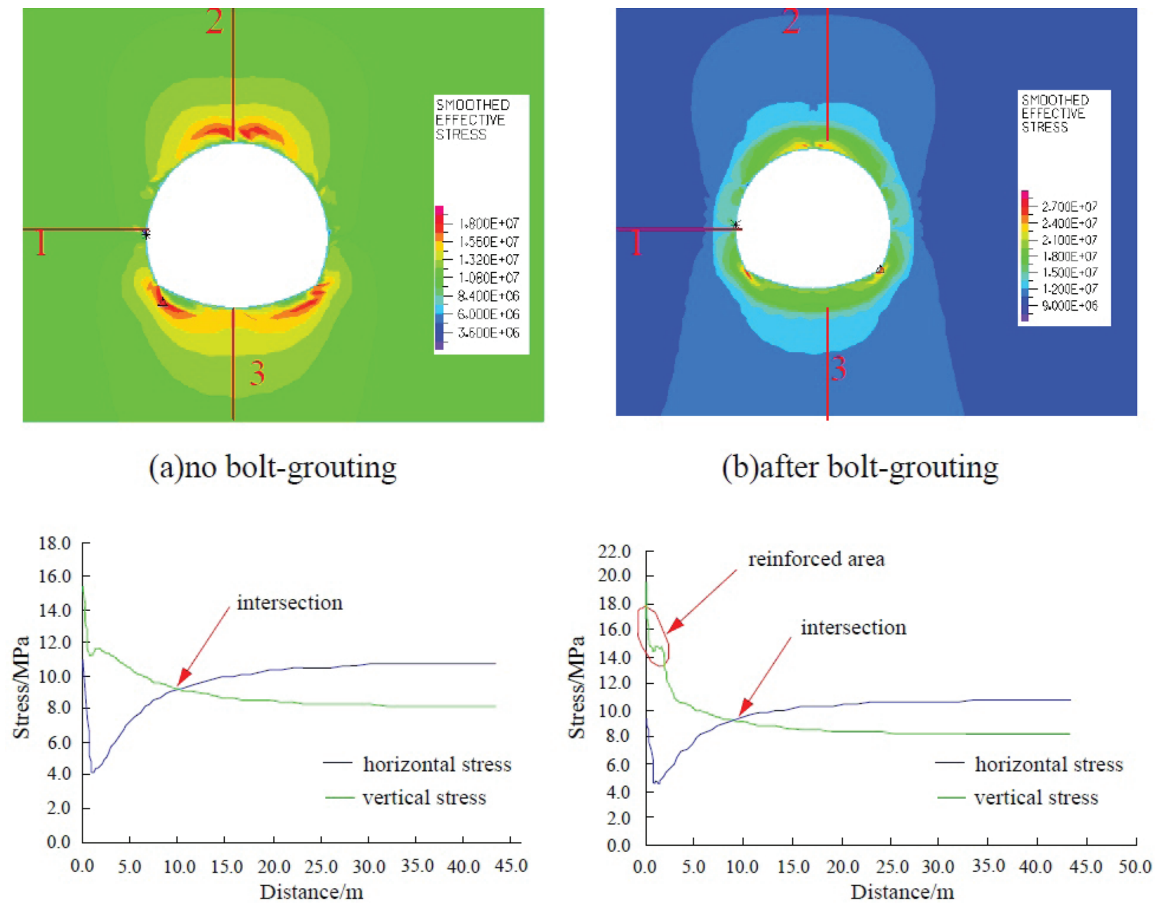

Figure 8: *Stress and distance graph (radial excentre). Example of stress distribution and curves of horizontal stress and vertical stress in self-support arch (before and after rock bolt installation and grouting); horizontal stress is higher than vertical stress, which is applied on side walls of tunnel.*

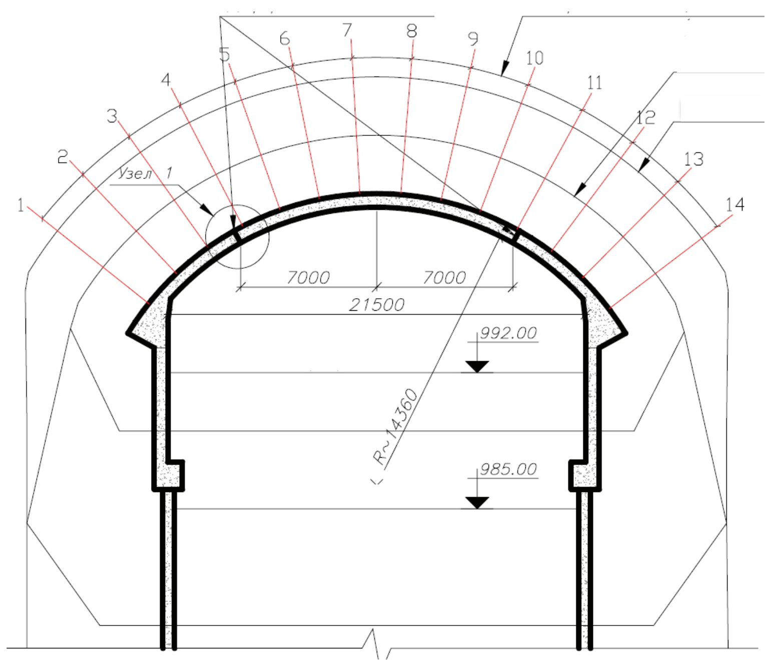

Figure 9: *Cross-section of cavern.*

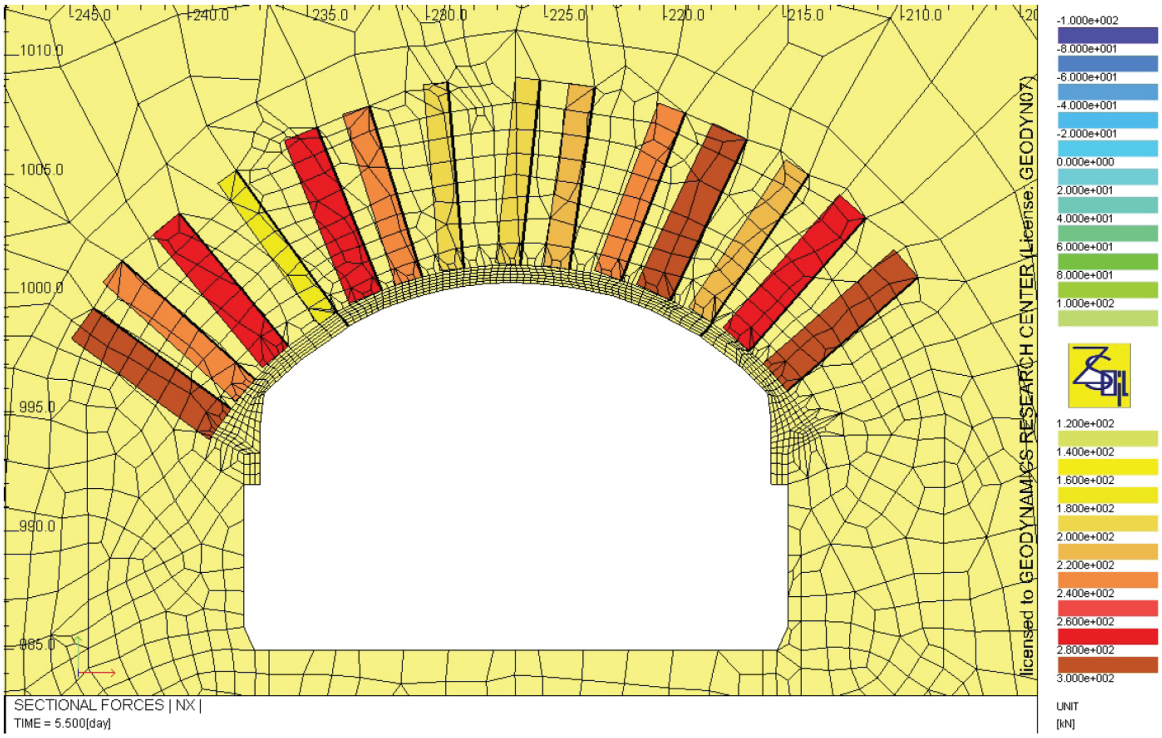

Figure 10: *Distribution of loads (kN) in anchors around arch zone.*

ed water flow rate into the excavation is overestimated.

Similar incorrect results of displacements could be calculated in case of not optimised number of elements and also line assembling boundary or geometry. In case of very large models, it may be difficult to process because of huge operation that has to be done using computer hardware that an average user does not have [11–13].

Estimating stress distribution in self-support zone

Long-term prediction of behaviour of underground structures is a complicated procedure; therefore, a reliable constitutive model is needed, which can interpret the measurement of viscous phenomenon. Because of scale effect, the rock rheological property measured on samples in the laboratory cannot be extrapolated directly to field scale. It is necessary to correlate numerical results with in situ measurement over a long period of time.

In this example, the need for additional anchorage of the arch in large powerhouse cavern, after primary support was completed for temporary protection, is analysed.

For this purpose, a series of numerical calculations of the stress-deformed state of the array distributed around cavern was performed, with the determination of the forces in anchors of the arch. Calculations were performed for siltstone and sandstone rock with GSI = 45, with different capacities of the unloading zone of the massif above the arch.

In addition, it was assumed that the excavation development of cavern is conducted by a mining excavation method of drill and blast in particular sequences.

Analysis of changes in the stress state of concrete lining in the zone of arch was done on the basis of a comparison of the stressed state of the concrete and the loads in the anchors, for example while leaving the existing primary support anchors and when they are completely replaced with new anchors.

It was found that the types of anchors and the distance between them generally correspond to the project requirements. According to the example draft, primary support contains passive rod anchor AGG 8 m long on a grid 2.0 m × 2.0 m. The diameter of the rods is 36 mm, and design-bearing capacity of such type of anchors is 30 tons.

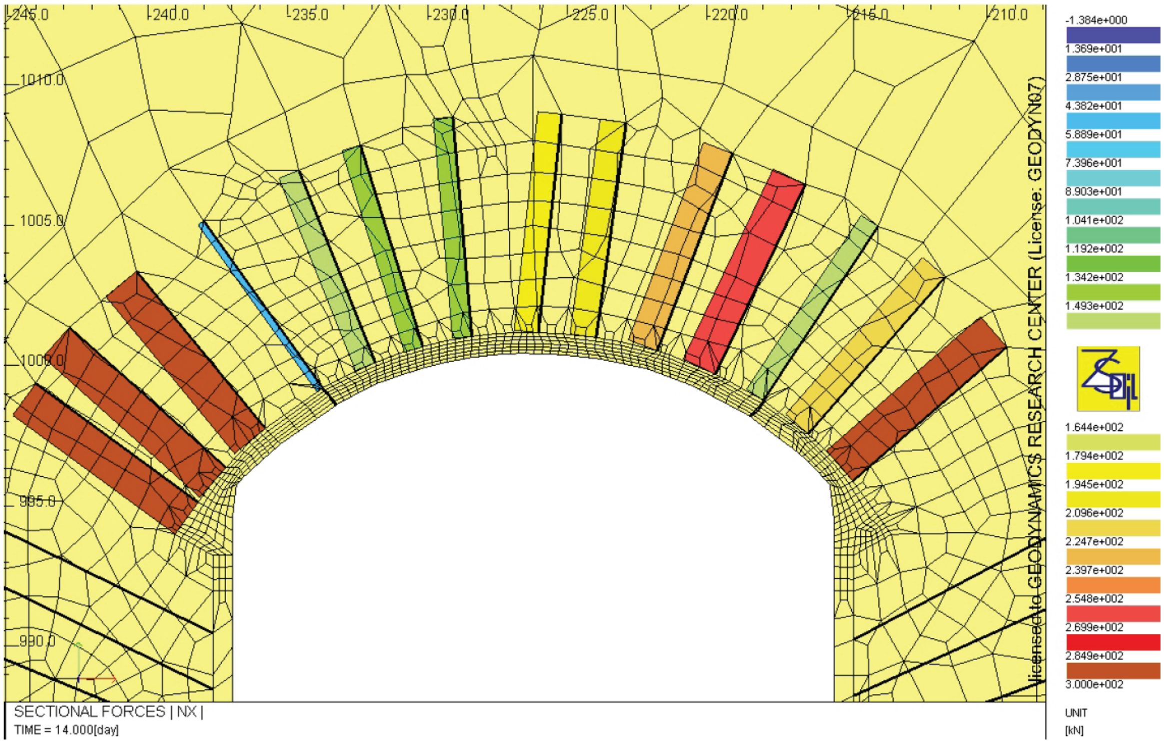

Figure 11: *Anchors' load (kN) decreases after initial displacements.*

The rigid arch is made up of monolithic reinforced concrete with a thickness of 0.7 m, having two deformation seams. Concrete design strength for compression is 13 MPa and for tensile is -0.98 MPa.

The structure was modelled by thin interlayers of a weak material, with a strain modulus E = 2000 MPa. The design of the expansion joint according to the project is shown in Figure 9.

For long-term usage of the structure, the visual inspection shows no significant damage of support concrete layer, which leads to reasonable doubts about the future stability of the structure. During the blasting works and excavation sequences for deepening the power house, some passive anchors in the upper part of side wall were also damaged. Main defects of the structure were visible at joints of side wall and lower part of the arch, practically at the areas where it joins the walls of the turbine hall.

Consideration for two optional support solutions was studied for reinforcement propagation of the zone under higher stress to a depth of 3 m and 6 m, paying attention to calculations in the zone of siltstones.

With design revision noted, the anchor of the arch in the zone of siltstones began to yield already at the initial stage of the cavern deepening excavation works (985.0 m).

This behaviour was observed for both a 3-metre and a 6-metre deep zone. With further excavation in depth of the power house, the change in stresses of the anchors is multidirectional: in one part of the anchors, there is an increase in stress, and in the other part of the anchors, there is a decrease in stress. In some stages of construction distribution of forces in the anchors in the two parts of the zone considered unloading is shown in Figure 10.

The distribution of forces in the anchors is explained by the distribution of radial movements of the arch directed to its geometric centre; in the 3-m zone of relaxation in siltstones and sandstones, it can be seen that largest displacements of 8 and 2 cm occur near its abutment to side walls where the anchors experience maximum loads and failures.

Displacements in arch that occurred during the development of the maximum compressive stresses in the arch were at the junction of the arch with the side wall and, with its external side, near the expansion joints, which were designed for the purpose of achievement of self-support capacity of rock mass (Figure 11).

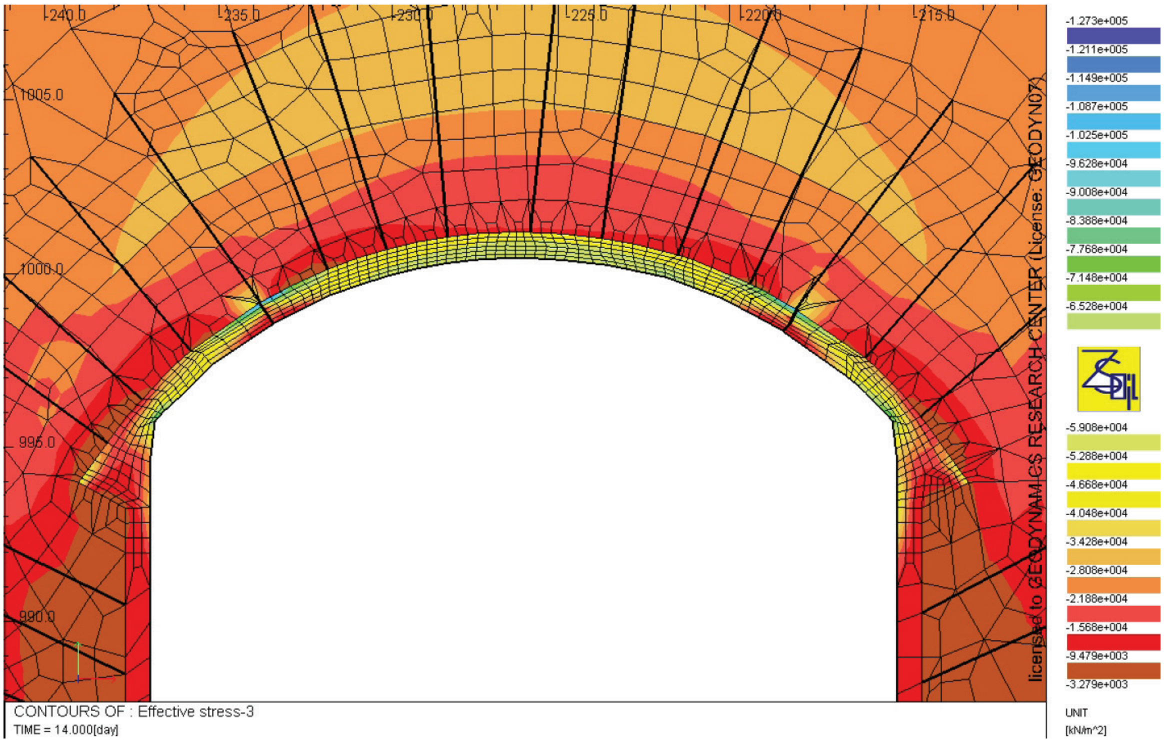

Figure 12: *Distribution of compressive stress (kN/m^2) in the arch.*

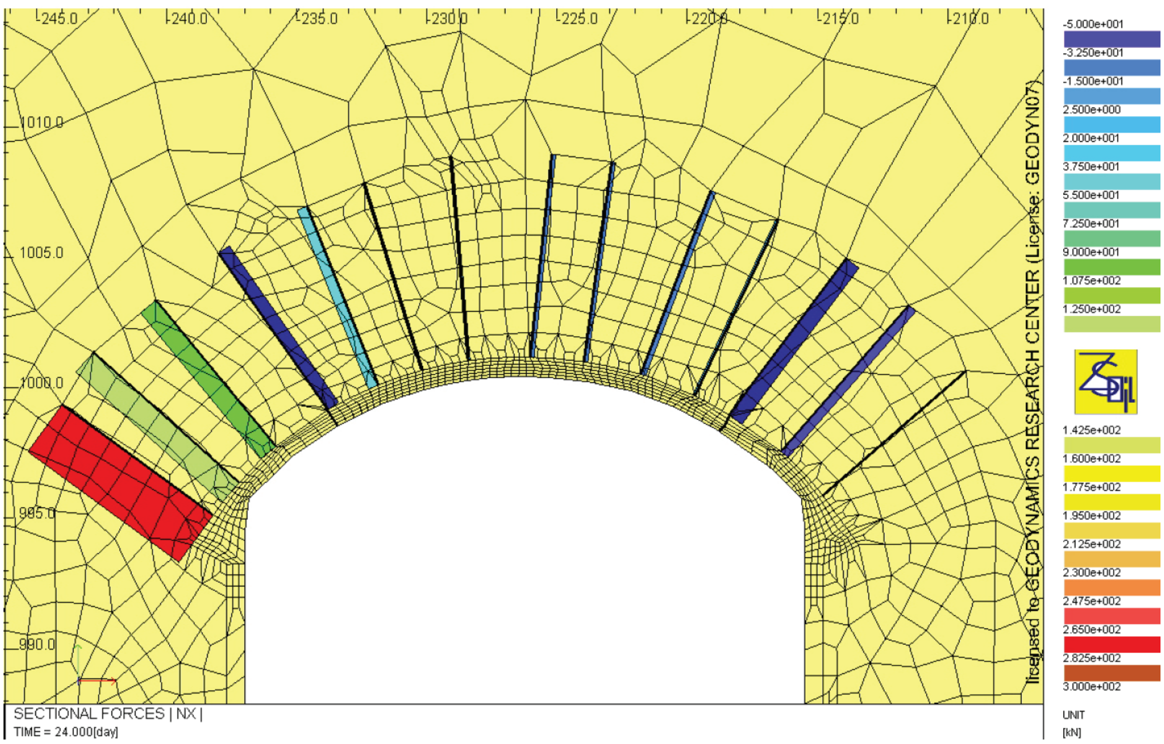

Figure 13: *Load distribution (kN) in case of installation of additional anchors.*

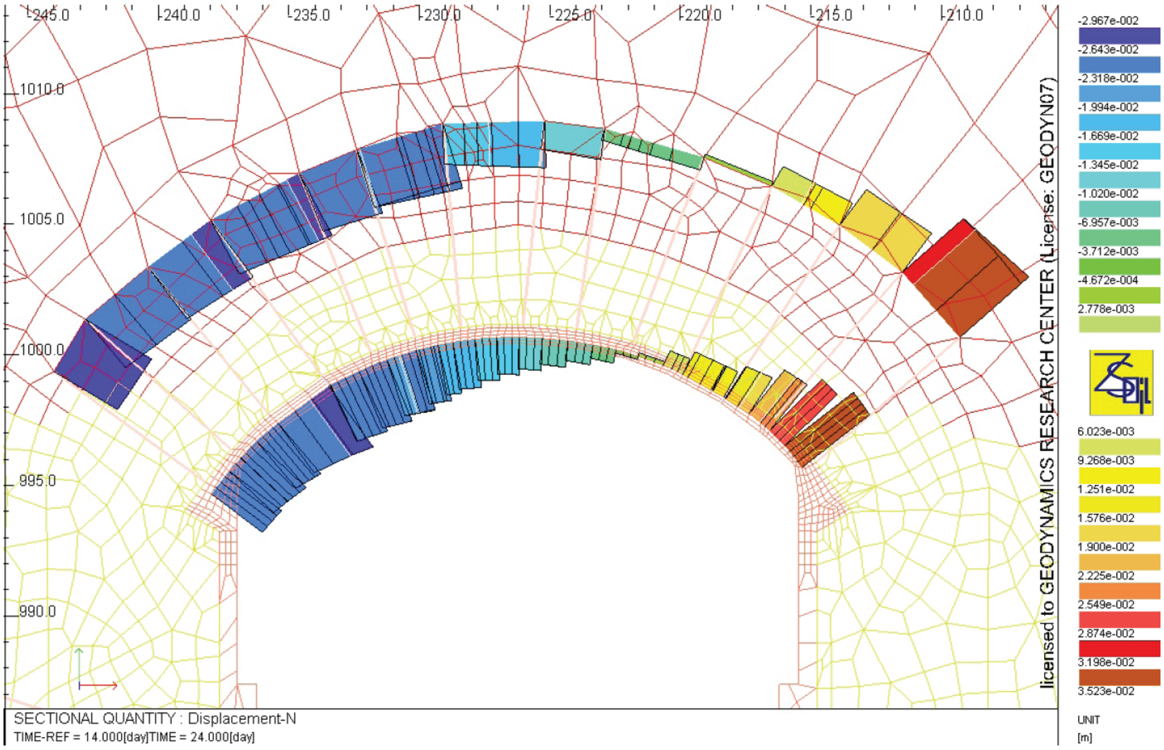

Figure 14: *Radial displacement (m) of the arch array.*

Incensement of stress is a consequence of deformability mechanism of the arch while closing of two expansion joints.

The maximum stresses on the inner surface of the arch develop exactly where the support side wall is acting like a pillar and causing destruction of the protective layer of crown excavation (Figure 12).

To examine the need for additional anchorage of the arch, it was necessary to reanalyse the old design and all changes in the anchors and stresses in the structure for optimised completion of underground structure. These changes consequently considered two options – upgrade of anchorage system or its full replacement before completion of structure.

Calculations show that for the final stage of excavation, the loads on anchors installed in the arch zone do not increase (Figure 13).

Reduction of forces in anchors is caused by a relative convergence of their ends, which leads to a reduction in the previously existing tension. This phenomenon is observed in some anchors of the arched part of the power house. Illustration of this is represented in Figure 14, which shows the radial displacement of the array near both ends of the anchors that occurred during the completion.

Calculations show that maximum tensile forces in additionally installed anchors in the final stage of work would not exceed 60 kN, which is significantly less than the maximal load of 300 kN.

Deformations in the period of completion of excavation at the bottom of cavern differ both qualitatively and quantitatively from those obtained with the preservation of the anchorage.

Analysis of the data presented shows that the additional installations due to displacements of surrounding rock mass do not significantly affect the stability of the arch.

Comparison of stresses in the arch for the final stage of deepening of powerhouse shows that no additional support will be needed because of self-supporting behaviour of rock mass after initial deformation have occurred and primary support distributed all load on side wall part of excavation.

Conclusions

Structural geology and underground infrastructure projects are complex and behave three dimensionally in nature. Rock support design procedure cannot be performed in a systematic manner without taking into account geometric and geological/geomechanical complexities. When performing designs, the selection of a suitable analysis tool, methodology and data judgement should be done and the design should be well understood; otherwise, costly mistakes regularly occur during construction, because of various influence factors outlined in this paper.

Ideal surrounding rock self-supporting arch should be of curvilinear shape, consisting of compound curves in arch and, when necessary, also in invert. This will allow the smooth distribution of stress around caverns or tunnels.

The pressure located at the vault zone and bottom cannot be acceptable as an effective connection.

This kind of distribution often leads to a decrease in surrounding rock self-supporting capacity. Correct selection of support systems, which have to be compared with few alternative solutions to achieve economic and technical best solution, is the right way to improve the stress concentration in exposed zones, and consequently, the capacity of surrounding rock self-supporting arch increases significantly.

References

[1] Stille, H., Holmberg, M., Olsson, L., Andersson, J. (2005): Probability Based Design Methods for Underground Excavations Characterised by Rock – Structural Interaction, Stockholm: SveBeFo; 80 p.

[2] Kiran, K.S., Krishna K.P. (2010): The Use of Self Supporting Capacity of Rock Mass for Sustainable Hydropower: An Analysis of the Middle Marsyangdi, Headrace Tunnel, Nepal. Hydro Nepal, 6, pp. 18–26.

[3] Saurer, E., Marcher, T., John, M. (2013): Decisive design basis and parameters for power plant caverns. World Tunnel Congress 2013, Geneva, pp. 1858–1864.

[4] Chunsheng, Z., Weijiang, C., Ning, L., Yongsheng, Z., Jing, H. (2011): Laboratory tests and numerical simulations of brittle marble and squeezing schist at Jinping II hydropower station, China. Journal of Rock Mechanics and Geotechnical Engineering, 3(1), pp. 30–38.

[5] Cantieni, L., Anagnostou, G. (2009): The interaction between yielding supports and squeezing ground. Tunnelling and Underground Space Technology, 24(3), pp. 309–322.

[6] Bahat, D., Rabinovitch, A., Frid, V. (2005): Tensile fracturing in rocks. Springer: Berlin Heidelberg, pp. 183–185.

[7] Germanovich, L.N., Salganik, L., Dyskin, A.V., Lee, K.K. (1994): Mechanisms of brittle fracture of rock with pre-existing cracks in compression. Pure and Applied Geophysics, 143(3), pp. 117–149.

[8] Vlachopoulos, N., Diederichs, M.S. (2009): Improved longitudinal displacement profiles for convergence confinement analysis of deep tunnels. Rock Mechanics and Rock Engineering, 42 (2), pp. 131–146.

[9] Yuanchun, S., Huaijian, L., Zailiang, X., Bo, G. (2012): Analyzing of Reinforcement Effect of Bolt-Grouting in Squeezing Tunnel. 2nd International Conference on Electronic & Mechanical Engineering and Information Technology; Atlantis Press: Paris, France, pp. 586–589.

[10] Yuan-Chun, S., (2010): Research on mechanism and controlling technologies of surrounding rock in squeezing ground[D], Institute of geology and geophysics Chinese academy of sciences, Beijing, China.

[11] Franzius, J.N., Potts, D.M. (2005): Influence of Mesh Geometry on Three-Dimensional Finite-Element Analysis of Tunnel Excavation. International Journal of Geomechanics, 5(3), pp. 256–266.

[12] Janin, J.P., Dias, D., Emeriault, F., Kastner, R., Le Bissonnais, H., Guilloux, A. (2015): Numerical back-analysis of the southern Toulon tunnel measurements: A comparison of 3D and 2D approaches. Engineering Geology, 195, pp. 42–52.

[13] Svoboda, T., Masin, D. (2011): Comparison of displacement field predicted by 2D and 3D finite element modelling of shallow NATM tunnels in clays. Geotechnik, 34 (2), pp. 115–126.

Original scientific paper
Received: Mar 16, 2018
Accepted: Apr 18, 2018
DOI: 10.2478/rmzmag-2018-0012

Computer-Assisted Design of Sheet Metal Component Formed from Stainless Steel

Računalniško Podprto Načrtovanje Preoblikovanja Pločevinske Komponente iz Nerjavne Pločevine

Tomaž Pepelnjak[1,*], Tomaž Bren[2], Bojan Železnik[2], Mitja Kuštra[1]
[1] Fakulteta za strojništvo Ljubljana, Aškerčeva 6, 1000 Ljubljana, Slovenia
[2] KGL d.o.o., Proizvodnja in obdelava kovinskih izdelkov, Ponoviška cesta 13, 1270 Litija, Slovenija
* tomaz.pepelnjak@fs.uni-lj.si

Abstract

The development of the product from stainless steel, which is produced for the client in large series, is presented. Technological optimisation was mainly focussed on the design of the deep drawing process in a single operation, which proved to be technologically unstable and therefore unfeasible for the prescribed shape of the product. Testing of prototype products showed unacceptable wrinkling due to the cone-shaped geometry of the workpiece. For this purpose, the research work was oriented towards technological optimisation of forming operations and set-up of proper phase plan in order to eliminate the wrinkling of the material. Testing of several different materials of the same quality was performed to determine the appropriate input parameters used for digital analyses. The analyses were focussed towards the set-up of optimal forming process and appropriate geometry of the corresponding tool, which allowed deep drawing of the workpiece without tearing and/or wrinkling of the material. Performed analyses of the forming process in the digital environment were tested with experiments, which showed a good correlation between the results of both development concepts.

Key words: deep drawing, conical part, stainless steel

Povzetek

Predstavljen je razvoj izdelka iz nerjavnega jekla, ki se za naročnika izdeluje v masovni proizvodnji. Tehnološka optimizacija je bila fokusirana predvsem na načrtovanje procesa globokega vleka v eni operaciji, ki se je izkazala za tehnološko nestabilno in zaradi tega neizvedljivo za zahtevano obliko izdelka. Testiranje prototipne serije je pokazalo nedopustno gubanje materiala zaradi konične oblike preoblikovanca. Zaradi tega so raziskave bile usmerjene v tehnološko optimizacijo preoblikovalnih operacij in vzpostavitev ustreznega metodnega plana za odpravo gubanja materiala. Testiranje številnih materialov enake kakovosti so služili izbiri ustreznih vhodnih parametrov digitalnih analiz. Te smo fokusirali predvsem v vzpostavitev optimalnega preoblikovalnega procesa in izbire ustrezne geometrije pripadajočega orodja. Ta omogoča globoki vlek preoblikovanca brez gubanja in/ali trganja materiala. Izvedene analize preoblikovalnega procesa v digitalnem okolju so bile preverjene z eksperimenti, ki so pokazali dobro ujemanje rezultatov obeh razvojnih konceptov.

Ključne besede: globoki vlek, konični izdelek, nerjavna pločevina

Introduction

In the automotive industry, immense use of steel and aluminium sheet metal components is a daily practice. The products are made either from multiple components, which are delivered as an assembly, or a single component, formed and/or machined to the desired shape tolerances and surface quality. Examples of deep drawn and punched products are shown in Figure 1.

Such a product was designed and developed as part of the presented project. The product was made from stainless steel in mass-production series. The customer determined the required demands for the shape of the product, as well as the required surface roughness of the active surfaces, which had to be polished after the process of drawing and stamping of the side holes was done (Figure 2). Owing to the cost-efficient nature of forming technology, the part was planned to be produced by a single-step forming process. However, first, technological trials and forming tests with the prototype tool showed that the conical shape of the product results in high unsupported region of the drawn part with critical tangential stresses, leading to the critical deformation and wrinkling of the conical part during the drawing process [1] (Figure 3). Additionally, the danger of material tearing due to insufficient clearance of the tool and blank holder force during the drawing process was experimentally confirmed.

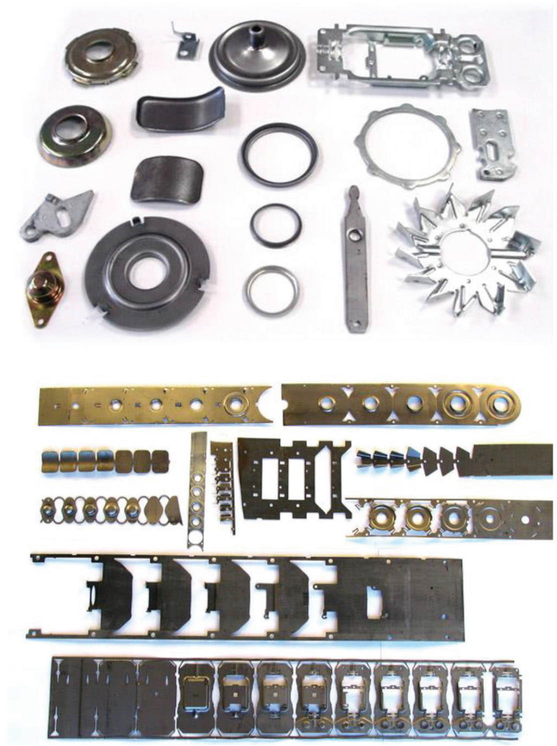

Figure 1: *Referenced stamped and deep drawn parts [6].*

Figure 2: *Finished product [7].*

The most evident error at the developed drawn part was the formation of wrinkles on the conical wall of the product, which is unacceptable for functional and aesthetic reasons and may cause also the die damage. The wrinkling of the formed parts has become a serious problem in recent years with the increased use of thin high strength sheet metals in the automotive industry [2]. The wrinkling phenomenon is directly related to the geometry of the workpiece, stress–strain state, material parameters, and anisotropy and contact conditions [3]. It occurs once the circumferential compressive stress is higher than the critical circumferential compressive stress of the sheet during forming [1]. The magnitude of the compressive stress is usually smaller than that causing the flange wrinkling. Owing to the unsupported region of the analysed part's wall [4], in comparison to the flange, it is more difficult to suppress the wrinkling in this area. However, the usage of stainless steel had beneficial implications, because it has a low value of anisotropy and a high value of hardening rate that consequently means that it has a better resistance to the formation of wrinkles [5].

Figure 3: *Wrinkling on the conical part of the drawn product.*

The resolving of these critical mistakes and the optimisation of the production process were the main focuses of the present research, where the classic planning of the forming technologies and the modern computer-aided technologies with numerical simulations were used together. The optimisation of the forming process involved determining the following parameters:

- the optimal number of forming steps and the intermediate shape of the drawn workpiece after each step;
- the optimal tool clearance and the size of the drawing radii;
- the required blank holder force for the drawing to omit flange;
- minimal drawing steps to form part without cone wrinkling and
- the required calibration force for the shape stabilisation of the cone and embossed detail on the bottom of the product.

The last phase of the technological optimisation was conducted using the hydraulic press in the Forming Laboratory of the Faculty of Mechanical Engineering, University of Ljubljana. In this research phase following the numerical simulations, the fine-tuning of the technological parameters was determined. The experimental work in the last phase of the development also verified the numerical prediction of blank holder force and part calibration. The use of four different steels of the same quality obtained from four different manufacturers also verified the stability of the selected process.

Materials

The material that was chosen for the product was the most widely used stainless steel of 1.4301 quality, which can be easily acquired throughout Europe. This meant that the cost of material supply could be more easily optimised and the mass production could run without delays or interruptions. For quality, numerical analyses of the material and forming properties of the sheet metal had to be evaluated first. The flow curves of two analysed materials of same 1.4301 qualities are shown in Figure 4. Both materials exhibit very similar flow curves. The Ludwik approximation was used for curve fitting.

$$\sigma_f = A + K\varphi_e^n \tag{1}$$

Table 1 contains the information about the anisotropy, which plays an important role in the shaping of the product during the deep drawing process. Furthermore, it also shows the intensity of the material's thinning along the critical cross-section – the higher the anisotropy, the less intensive the localisation. The mean values of anisotropy are calculated according to the equation

$$\bar{r} = \frac{1}{4}(r_0 + 2 \cdot r_{45} + r_{90}) \tag{2}$$

whereas the planar anisotropy is calculated according to the equation

$$\Delta r = \frac{1}{2}(r_0 - 2r_{45} + r_{90}) \tag{3}$$

As it can be seen from Table 1 and Figure 4, both materials exhibit very similar formability properties; therefore, only one value of the plasticity curve and the mean anisotropy value of the material were used to conduct numerical simulations. Because the values for anisotropy rely on the direction of the rolling, we can expect uneven properties of the workpiece along its perimeter and a noncircular flange, which has to be cut-off after the deep drawing process.

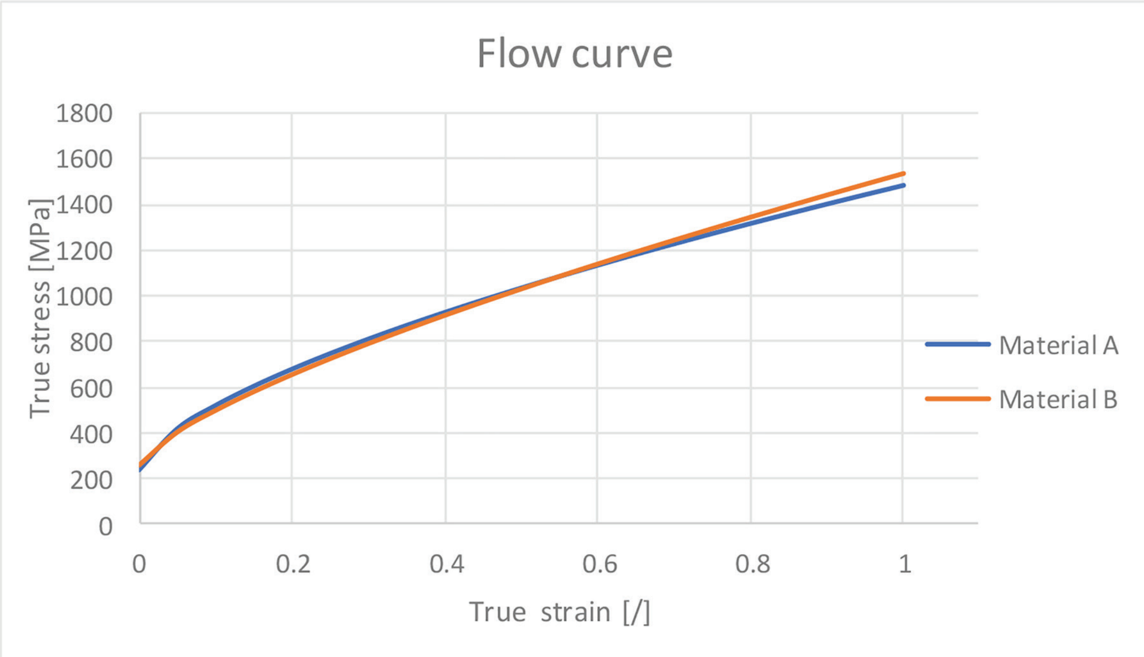

Figure 4: *Flow curves of the analysed materials.*

Table 1: *Anisotropy of the material.*

Specimen position according to the rolling direction	Material A	Material B
0°	0.88	0.81
45°	1.15	1.14
90°	0.77	0.78
Average value of the anisotropy	0.99	0.97
Planar anisotropy	-0.65	-0.69

Finite element model

The objects of the finite element model (FEM) used for the numerical simulation are shown in Figure 5. The FEM model consists of the blank, punch, counter-punch, die and blank holder. The blank was modelled as elastic–plastic, whereas all tool parts were considered as rigid objects. Considering the elastic behaviour of the blank, the Poisson ration of $v = 0.3$ and Young's modulus of $E = 210$ GPa were taken into account. The plastic behaviour followed the flow curve shown in Figure 4, considering also the anisotropic material properties from Table 1. The interaction conditions among all objects in contact followed the Coulomb's law with a coefficient of $\mu = 0.1$. Table 2 presents the element size for each meshed object of the finite element simulation.

Table 2: *Nodes and elements of FEM mesh.*

Model	Nodes	Elements
Blank	8073	7959
Punch	5053	4999
Counter-punch	773	716
Die	882	820
Blank holder	372	330

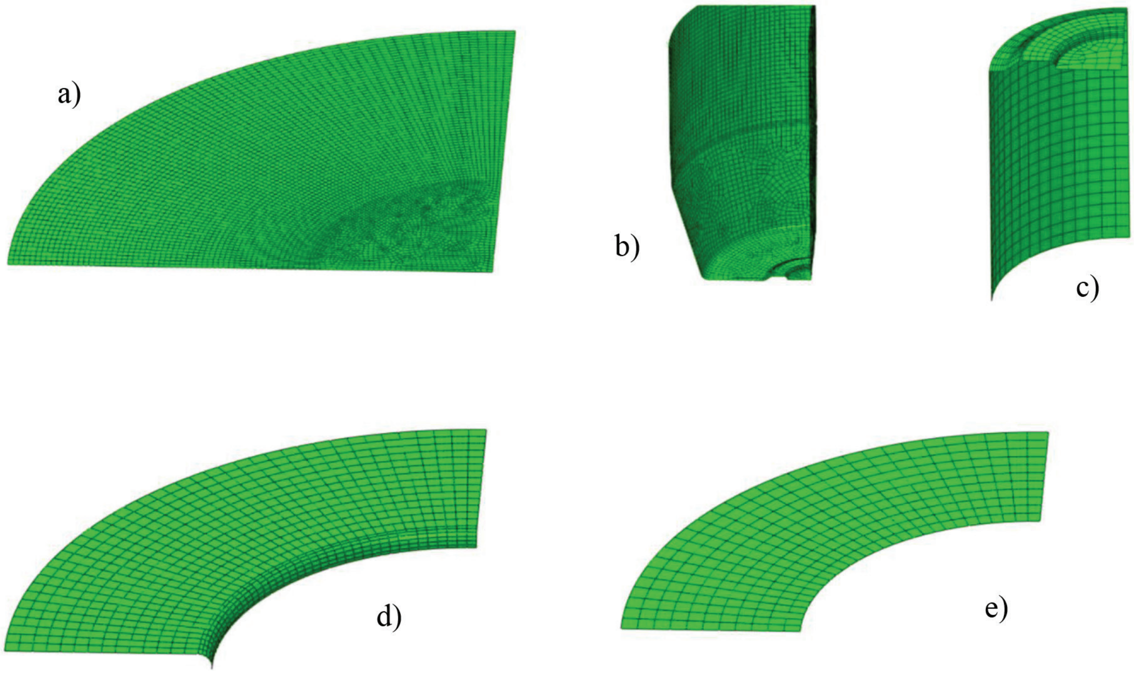

Figure 5: *The FEM used for the numerical simulation: a) blank, b) punch, c) counter-punch, d) die and e) blank holder.*

Results

In order to verify the prediction of the wrinkling occurring in the material during the single-step deep drawing process, the first phase of the development was to check the numerical model. Owing to the axis symmetry of the model, the analysis was done only with one-fourth of the whole workpiece. Through this, the computing time of the numerical analysis was reduced. The unfavourable drawing conditions in the single-step process of the numerical model have also expressed significant wrinkling of the cone-shaped part of the specimen (Figure 6). Some simulations also predicted the intensive thinning of the material at the narrower part of the cone, when certain tool optimisations were implemented (Figure 7). The analysis also focussed on determining a favourable radius of transition between the vertical part and the conical part of the product as well as the calibration of the conical shape of the product. The results show that calibration may reduce wrinkling but cannot eliminate it completely.

The wrinkling analyses on the vertical part and the conical part of the product were carried out using four different models. However, the analyses of the single-step deep drawing process have shown that all four different drawn parts have still measurable wrinkling on the cone-shaped areas of the workpiece, which is shown in Figure 8. It is evident from Figure 8 that none of the optimised geometries could entirely eliminate the wrinkling phenomenon.

The analysis of different forming phase plans has shown that the basic shape of the product cannot be made by a single-step drawing process. Therefore, the technological process was divided into two forming steps. In the first deep drawing phase, the sheet metal was moved into a hat-shaped preform with a straight wall and a large radius on the bottom of the product (Figure 9, top and middle). In the second drawing phase, using the inverted drawing process with a movable die, the workpiece was drawn onto a fixed punch. Doing so, we increased the vertical height and created the conical half of the product (Figure 9, bottom). Using this two-phase approach, the analysis showed that the wrinkling has significantly decreased. The analysed nodes showed a fluctuation of the measured radius below the value of 0.5 mm along the circumference of the product. Because this fluctuation was still not admissible, the product had to be calibrat-

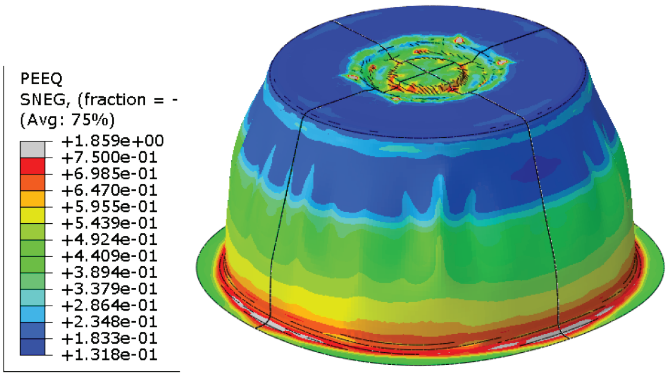

Figure 6: *Analysis of wrinkling – equivalent strain.*

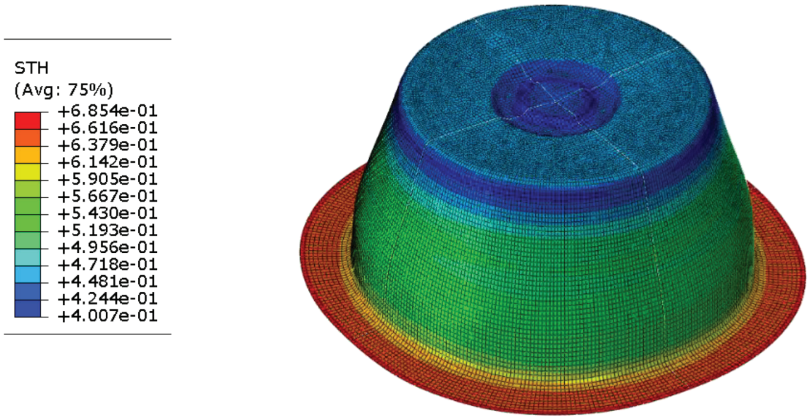

Figure 7: *Analysis of material tearing – sheet thickness (mm) of the drawn part.*

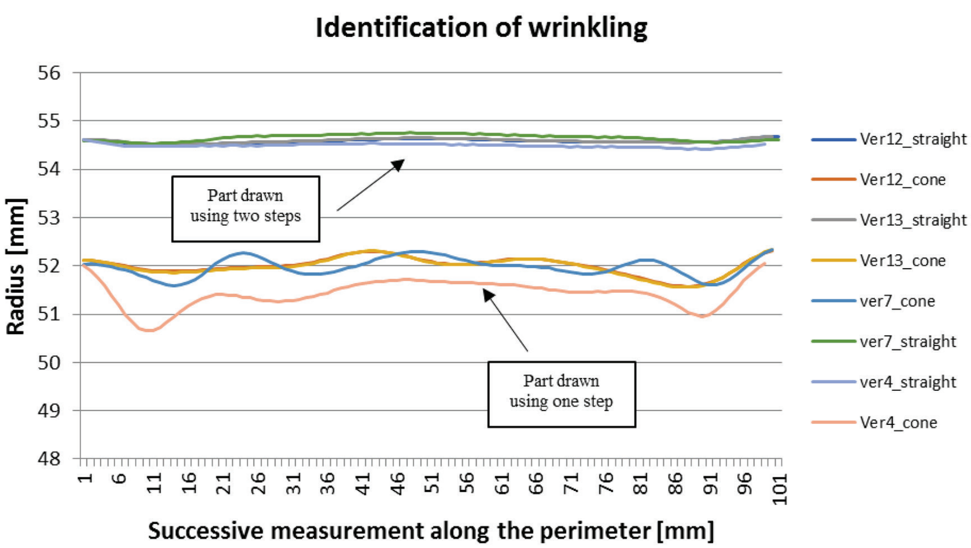

Figure 8: *Analysis of wrinkling along the part's perimeter.*

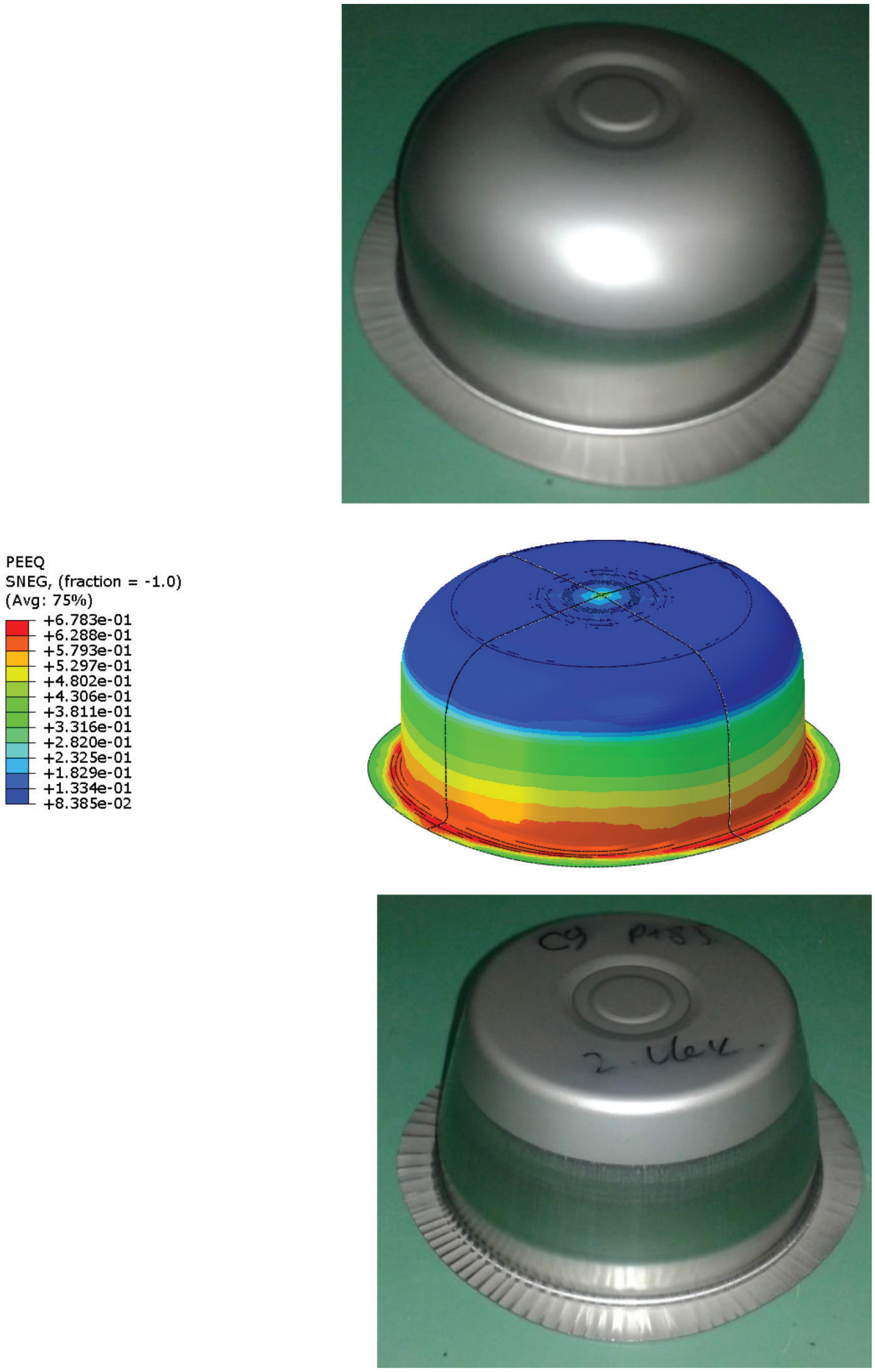

Figure 9: *Chosen technology of the drawing: first drawing (top) and analysis of the comparison deformation of the first drawing (middle) and the second drawing with calibration (bottom).*

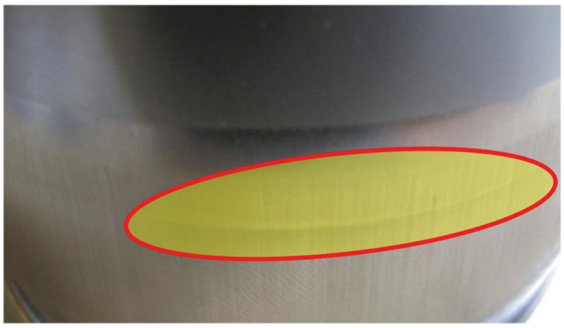

Figure 10: *Detail of the calibrated part area at the end of the punch stroke.*

ed at the middle of the conical part (Figure 10). Doing so, the wrinkling was entirely eliminated. The proper selection of the technological solution was verified using the test tool of the Faculty of Mechanical Engineering of Ljubljana. The fluctuations in the material property and different surface qualities (surface roughness) that arise due to different manufacturers of the 1.4301 steel were also assessed.

Conclusions

Design of the forming process of a conical workpiece made of stainless sheet metal showed the relevance of simultaneously conquering its production technology from the industrial partner supported by academic knowledge and analyses in the digital environment. The layout of the deep drawing process showed that due to the conical shape and successive wrinkling of the product, it is not feasible to perform the forming operation in one step only. For this reason, the two-step deep drawing process was selected, and the final conical shape was obtained in the second drawing phase with implemented calibration at the end of the punch stroke.
The deep drawing phases were followed by the operations of successive forming of the strengthening ribs, cutting, trimming and polishing of the final product. The product is already successfully integrated into the mass production without any tearing or wrinkling problems.

Acknowledgement

The authors acknowledge the support of the Slovenian Research Agency within the framework of programme P2-0248.

References

[1] Shafaat, M.A., Abbasi, M., Ketabchi, M. (2011): Investigation into wall wrinkling in deep drawing process of conical cups. *Journal of Materials Processing Technology*, 211(11), pp. 1783–1795, doi:10.1016/j.jmatprotec.2011.05.026.

[2] Neto, D.M., Oliveira, M.C., Santos, A.D., Alves, J.L., Menezes, L.F. (2017): Influence of boundary conditions on the prediction of springback and wrinkling in sheet metal forming. *International Journal of Mechanical Sciences*, 122, pp. 244–254.

[3] Nan, L., He, Y., Heng, L., Siliang Y. (2016): Plastic wrinkling prediction in thin-walled part forming process: A review. *Chinese Journal of Astronautics*, 29(1), pp. 1–14.

[4] Wang, X., Cao J. (2000): On the prediction of side-wall wrinkling in sheet metal forming processes. *International Journal of Mechanical Sciences*, 42, pp. 2369–2394.

[5] Naryanswamy, R., Sowerby, R. (1995): Wrinkling behaviour of Cold rolled sheet metals when drawing through a tractrix die. *Journal of materials technology*, 49, pp. 199–211.

[6] Železnik T.: KGL d.o.o., Available on: <http://www.kgl.si/stancanje.php - view 5.1.2018>.

[7] Železnik T.: KGL d.o.o., internal company material, Litija, 2017.

Original scientific paper

Received: October 04, 2017
Accepted: December 14, 2017
DOI: 10.2478/rmzmag-2018-0008

SaltMod estimation of root-zone salinity Varadarajan and Purandara Application of SaltMod to estimate root-zone salinity in a command area

Uporaba modela SaltMod za oceno slanosti koreninske cone na namakalnih površinah

Varadarajan, N.*, Purandara, B.K.
National Institute of Hydrology, Visvesvarayanagar, Belgaum 590019, Karnataka, India
* nvarad@gmail.com

Abstract
Waterlogging and salinity are the common features associated with many of the irrigation commands of surface water projects. This study aims to estimate the root zone salinity of the left and right bank canal commands of Ghataprabha irrigation command, Karnataka, India. The hydro-salinity model SaltMod was applied to selected agriculture plots at Gokak, Mudhol, Biligi and Bagalkot taluks for the prediction of root-zone salinity and leaching efficiency. The model simulated the soil-profile salinity for 20 years with and without subsurface drainage. The salinity level shows a decline with an increase of leaching efficiency. The leaching efficiency of 0.2 shows the best match with the actual efficiency under adequate drainage conditions. The model shows a steady increase, reaching the levels up to 8.0 decisiemens/metre (dS/m) to 10.6 dS/m at the end of the 20-year period under no drainage. If suitable drainage system is not provided, the area will further get salinised, thus making the land uncultivable. We conclude from the present study that it is necessary to provide proper drainage facilities to control the salinity levels in the study area.

Key words: waterlogging, SaltMod, root-zone salinity, leaching efficiency, artificial drainage

Povzetek
Poplavljanje in slanost tal sta običajna pojava v mnogih namakalnih projektih. V študiji poročamo o ugotavljanju slanosti v koreninski coni na levem in desnem obrežju kanala namakalnega območja Ghataprabhaza v Karnataki, v Indiji. Postopek določanja slanosti z modelom SaltMod so uporabili na izbranih kmetijskih parcelah v okrajih Gokak, Mudhol, Biligi in Bagalkot za oceno slanosti koreninske cone in učinkovitosti odvodnjavanja tal. V raziskavi so modelirali slanost v talnem profilu v razdobju 20 let ob prisotnosti podpovršinskega odvodnjavanja in brez njega. Slanost upada vzporedno z naraščanjem učinkovitosti odvodnjavanja. Učinkovitost 0,2 najbolje ustreza dejanski učinkovitosti v ustreznih pogojih odvodnjavanja. Model kaže stalno naraščanje do ravni 8,0 - 10,6 deci Siemens/meter na koncu 20-letnega obdobja v pogojih brez odvodnjavanja. Če ni na voljo primernega sistema odvodnjavanja, se naraščanje slanosti v območju nadaljuje, tako da postane zemlja neprimerna za obdelovanje. Iz opravljene študije sledi, da je potrebno na proučevnem območju zagotoviti ustrezno odvodnjavanje, da se zaustavi naraščanje slanosti.

Ključne besede: poplavljanje tal, SaltMod, slanost v koreninski coni, učinkovitost odvodnjevanja, umetno odvodnjavanje

Introduction

Waterlogging is said to occur when the water table rises to within the root zone of crops. Climate, topography and geology play a dominant role in governing the occurrence, movement and storage of water. Any change in the water balance of an area causes a change in water table, leading to either waterlogging conditions or depletion of water table depending upon the nature of the change. Rise or decline in the water table is not desirable because both the phenomena degrade the sub-surface environment, thereby degrading the ground water regime [1]. Direct evaporation of ground water from the capillary fringe leads to salinisation of the soil, and in advanced stages, to the salinisation of ground water as well. Lack of aeration in the root zone, coupled with soil salinity, adversely affect crop yields in waterlogged areas. Seepage losses occurring along the routes used for the transfer of water from available resources has caused waterlogging and development of salinity in many irrigation commands. It is a fact that in some of the major projects, irrigation is in vogue for >3 decades, and the abacus have been stabilised with the farmers enjoying all the benefits, including access to uncontrolled use of surface water through the canals in the case of those in the upper and middle reaches of the projects [2]. With the availability of surface water throughout the year, farmers found it rarely necessary to use the ground water, with the result that ground water utilisation became almost negligible. The net result was a rise in ground water levels, gradually building up the water table, giving rise to waterlogging conditions. In addition, waterlogging also results in the accumulation of salt in the top soil or ground surface, rendering it infertile.

Purandara et al. [3] carried out a study on the waterlogging problems in the canal commands of the hard rock region of the Ghataprabha command and highlighted the problems of waterlogging and salinity in the command area. Dilip et al. [4] analysed the ground water characteristics of the Ghataprabha command under a geographic information system (GIS) environment and reported the acute problem of ground water salinity. National Institute of Hydrology (Roorkee, Uttarakhand, India) and the Remote Sensing Directorate of the Central Water Commission (New Delhi, India) carried out a study of Ghataprabha Command Area using remote sensing and GIS [5] and delineated the waterlogged and salt-affected areas in the command. Hiremath [6] carried out a study on waterlogging and salinity, as well as the impact of major irrigation projects on agriculture land and the reclamation of affected areas in Bagalkot and Biligi taluks of the Ghataprabha Command Area. Varadarajan et al. [7] highlighted the status of salinity in the aquifers of the Ghataprabha Command Area due to a combination of various hydro-geochemical processes contributed by increase in mineralised water, rock weathering and agricultural activities.

Bahceci et al. [8] simulated the effect of different drain depths on the amount of drainage water, root zone salinity and depth of water table in the Konya–Çumra Plain, Turkey, by using SaltMod. Simulation results indicated that the leaching efficiency is 0.7 and the natural drainage is 0.120 m/year in the test area. Khan et al. [9] used SaltMod for suggesting remedial measures to the highly salt-affected areas. The predicted values showed very good correlation with the observed conditions, thereby indicating the applicability of SaltMod as a management tool. Hebsur [10] made detailed ground-water quality studies in the Malaprabha and Ghataprabha canal command areas using SaltMod, and the model predicted that there is a decrease in the root-zone salinity as the irrigation with good-quality water increased in combination with poor-quality waters. Shrivastava et al. [11] applied SaltMod for the Segwa minor canal command. The model predicted fairly accurate trends in the region and it was found that SaltMod is an effective tool to forecast various situations once the model is calibrated and validated for use in a given agro-climatic situation. Poornima et al. [12] estimated the root-zone salinity of salt-affected areas of some parts of Gokak and Ramdurg taluks of Belgaum District and Mudhol Taluk of Bagalkot District, Karnataka, India, using SaltMod. The model simulated the soil-profile salinity for 20 years under different conditions, viz. with and without sub-surface drainage. The salinity level shows a decline with an increase of leaching efficiency. This study aims to estimate the

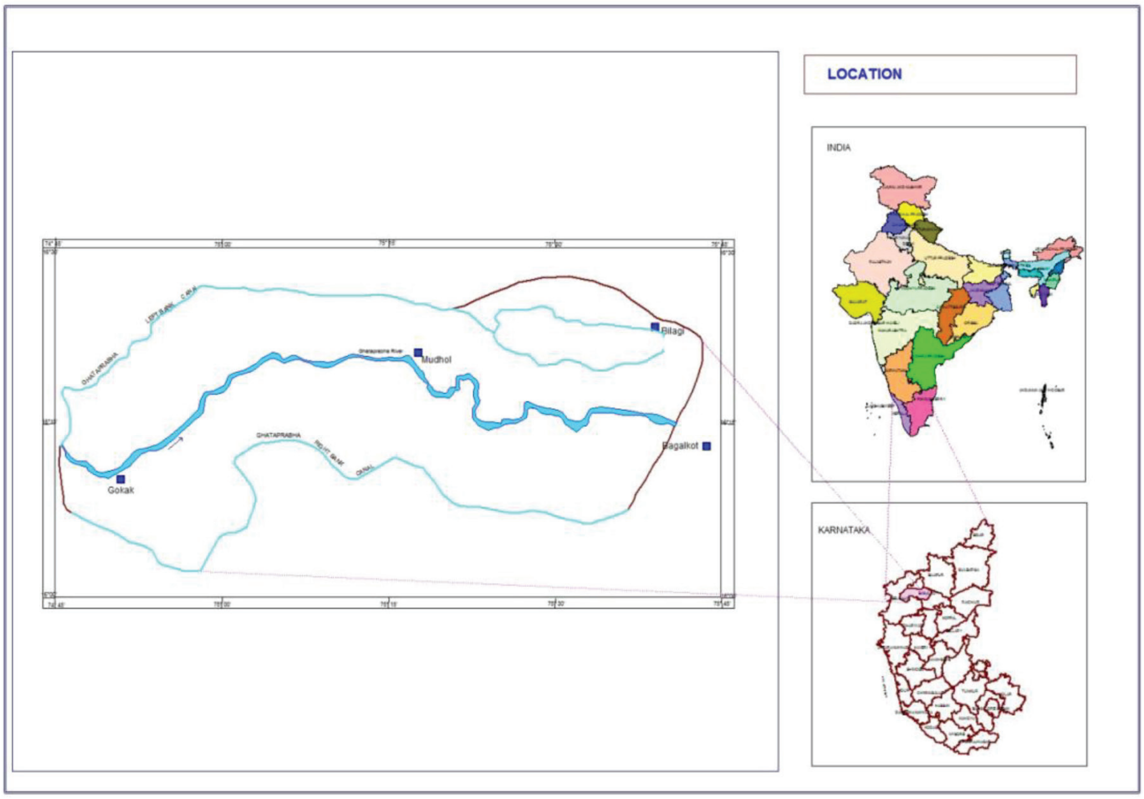

Figure 1: *Index map of the study area.*

root-zone salinity and leaching efficiency of the salt-affected areas of the left and right bank canal commands of Gokak, Mudhol, Biligi and Bagalkot taluks of Ghataprabha irrigation command. The hydro-salinity model 'SaltMod' was applied for this study area, which computes the salt and water balance for the root zone, transition zone and aquifer zone.

The command area of Ghataprabha reservoir is located between 16°0′8″N and 16°48′9″N latitudes and between 74°26′43″E and 75°56′33″E longitudes, covering an area of 317430 ha divided between the Belgaum and Bijapur districts of Karnataka. The index map of the study area is shown in Figure 1. The study area is bound by the Krishna River in the north, Maharashtra state to the west, the confluence of Krishna River and Malaprabha River in the east and the basin boundary between the Ghataprabha and Malaprabha rivers in the south. The existing canal command area (net command area is 161871 ha) is served by the Ghataprabha Left Bank Canal (GLBC) and six branch canals, with a number of major and minor distributaries. The proposed right bank canal is expected to irrigate an area of about 155000 ha.

The topography of the area is undulating with table lands and hillocks typical of the Deccan Traps. General topographic elevation varies between 500 and 900 m above mean sea level with a gradual fall from the West towards the East. The catchment boundary between the rivers Krishna and Ghataprabha follows the GLBC up to Biligi. The command area essentially lies within the Krishna river basin and is drained by the Ghataprabha River. The Ghataprabha River is one of the right bank tributaries of the river Krishna in its upper reaches. The river originates from the Western Ghats in Maharashtra at an altitude of 884 m and flows westwards for about 60 km through the Ratnagiri and Kolhapur districts of Maharashtra. In Karnataka, the river flows for about 216 km through Belgaum District.

The command area falls in the semi-arid zone and falls under drought-hit areas. The average annual rainfall is about 700 mm, with vide variation in time and space. The command area is underlain predominantly by sedimentary rocks of the Deccan Traps. Soils in the left bank canal command area are rich in clay and bases due to hydrolysis, oxidation and carbonation. However, soils in the right bank canal command area are developed due to weathering of sedimentary rocks. Soils in the area can be classified based on the geological formations. Soil depth varies from 25 cm to 30 cm in the case of shallow soils with high permeability. Deep soils with dark grey colour are found between 45 and 90 cm depth. Black cotton soils with an average pH of 8.0–8.5 generally occupy the low-lying areas. These soils exhibit high water-holding capacity but poor permeability.

The hydro-geology is complex as the Deccan Traps occupy major portions of the study area. River alluvium is found only along the course of rivers. Ground water occurs in the weathered and fractured hard rocks, as well as in the vesicular horizons in the traps. Unconfined to semi-confined conditions are observed in weathered/semi-weathered rocks. Confined conditions can be encountered when the fractures are deep seated or in vesicular horizons underlain by massive traps.

Materials and Methods

SaltMod is a computer programme for the prediction of the salinity of soil moisture, ground water and drainage water, the depth of the water table, as well as the drain discharge in irrigated agricultural lands, using different (geo) hydrologic conditions, varying water management options, including the use of ground water for irrigation, and several cropping rotation schedules. The water management options include irrigation, drainage and the use of sub-surface drainage water from pipe drains, ditches or wells for irrigation. The computer programme was originally made in FORTRAN by Oosterbaan and Isabel Pedroso de Lima at the International Livestock Research Institute (ILRI), the Netherlands [13]. A user shell in Turbopascal was developed by Ramnandanlal, and improved by Kselik of ILRI, to facilitate the management of input and output data. The schematic representation of SaltMod is shown in Figure 2.

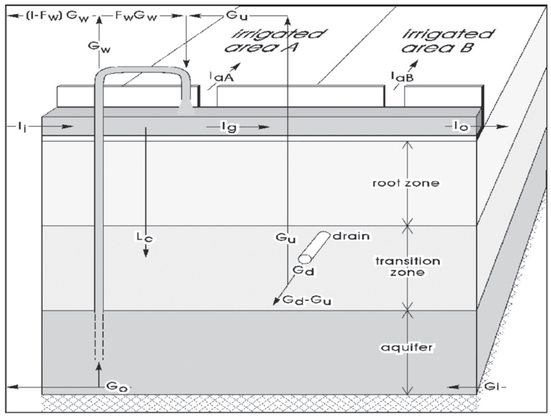

Figure 2: *Schematic diagram of SaltMod.*

The hydro-salinity model 'SaltMod' was applied for this study area, which computes the salt and water balance for the root zone, transition zone and aquifer zone. The computation method SaltMod is based on seasonal water and the salt balance of agricultural lands, which can be expressed by the general water balance equation as follows:

Incoming water = Outgoing water ± Change in storage (1).

Results and Discussion

The model was applied to the selected agriculture plots at Gokak, Biligi, Mudhol and Bagalkot taluks for the estimation of root-zone salinity and leaching efficiency. The model was calibrated and validated by using field-based data collected from the University of Agricultural Sciences, Dharwad, Karnataka, India. The detailed method consists of a number of iterative calculations of water and salt-balance equations to find out the final equilibrium in each zone separately. The method calculates the salt balance for each zone, based on the water balance of the individual zone and using the respective salt concentrations of the incoming and outgoing water flows. The model was run for two seasons (kharif and rabi), with full cropping rotations (the rotation index Kr = 4) being adopted. There are two groups of crops, viz., A and B, per season. The Group A crop consists of sugarcane, jowar, maize and bajra; and Group B consists of sugarcane, wheat, cotton, pulses and groundnut.

Table 1: *Season-wise input parameters of Gokak, Biligi, Mudhol and Bagalkot*

S. No.	Parameters	Season 1	Season 2	Season 3
1	Duration	4 months	5 months	3 months
2	Crop grown	Sugarcane, cotton, jowar, maize, groundnut, sunflower, pulses	Sugarcane, jowar, wheat, cotton, pulses, groundnut, maize	No irrigation
3	Water sources	Canal, well	Canal, well	Nil
4	Fraction of area occupied (irrigated)	1.00	1.00	0.00
5	Fallow/barren	0.00	0.00	1.00
6	Rainfall (m^3/season/m^2)	0.60	0.00	0.00
7	Water used for irrigation (m^3/season/m^2)	1.00	1.00	0.00
8	Percolation losses from the irrigation canal system (m^3/season/m^2)	0.01	0.01	0.00
9	Incoming ground water flow through the aquifer (m^3/season/m^2)	0.50	0.30	0.00
10	Outgoing ground water flow through the aquifer (m^3/season/m^2)	0.30	0.20	0.00
11	Potential evaporation (m^3/season/m^2)	0.10	0.16	0.00
12	Ground water pumped from wells in the aquifer (m^3/season/m^2)	0.50	0.50	0.00
13	Fraction of water pumped by wells from the aquifer used for irrigation (m^3/season/m^2)	0.30	0.30	0.00
14	Outgoing surface runoff (m^3/season/m^2)	0.60	0.00	0.00

The data required by the model are the following: seasonal average values of the areal fractions of the crops; rainfall; depth of different soil layers; values of leaching efficiency; initial salinity of the different soil layers, ground water and irrigation water; evaporation; surface runoff; reuse of drainage water and so on. The model takes the input data of each year as an average over two seasons, a wet and a dry season. The leaching efficiency of the root zone/transition zone is defined as the salt concentration of the water percolating from the root zone/transition zone into the underground divided by the average salt concentration of the soil water in the root zone/transition zone. Leaching efficiencies of the root zone (Flr) are given a range of arbitrary values, and the corresponding salinity results of the programme are compared with the values actually measured. The efficiency producing the best match is assumed to be the actual efficiency. The arbitrary Flr values are taken as 0.05, 0.1, 0.2, 0.3 and 0.4. The model was calibrated by using the data for the period 2001–2005 from the University of Agricultural Sciences (Dharwad), the Agriculture Department, the Irrigation Department and the Department of Mines and Geology [14]. Further, the validation was done by using the data from 2006 to 2010.

The root-zone salinity was simulated for 20 years using SaltMod under different conditions, such as with and without sub-surface drainage. For the prediction period, it was assumed that there will be no significant yearly deviations of the input parameters, such as rainfall, irrigation, evaporation, cropping pattern, etc., from the observed data given as the average input to the model for the period 2006–2010. The seasonal input and other data are shown in Tables 1 and 2 for all the locations.

Table 2: *Input parameters corresponding to soil and aquifer properties*

S. No	Parameters	Gokak	Biligi	Mudhol	Bagalkot
1	Storage efficiency	0.60	0.60	0.60	0.60
2	Depth of root zone (m)	0.60	0.60	0.60	0.60
3	Depth of transition zone (m)	2.00	2.00	2.00	2.00
4	Depth of aquifer (m)	15.0	12.0	10.0	15.0
5	Total porosity of root zone (m/m)	0.30	0.30	0.30	0.30
6	Total porosity of transition zone (m/m)	0.30	0.30	0.30	0.30
7	Total porosity of aquifer (m/m)	0.30	0.30	0.30	0.30
8	Effective porosity of root zone (m/m)	0.05	0.05	0.05	0.05
9	Effective porosity of transition zone (m/m)	0.05	0.05	0.05	0.05
10	Effective porosity of the aquifer (m/m)	0.20	0.20	0.20	0.20
11	Initial salt content of the soil moisture (dS/m) at field saturation in				
	Root zone	2.75	4.25	4.40	5.25
	Transition zone	2.15	3.65	4.20	5.00
	Aquifer	-	-	-	-
12	Mean salt concentration of irrigation water in the pilot area (dS/m)	0.50	0.50	0.50	0.50
13	Initial depth of water table from ground surface (m)	1.00	1.00	1.00	1.00
14	Critical depth of water table for capillary rise (m)	2.00	2.00	2.00	2.00

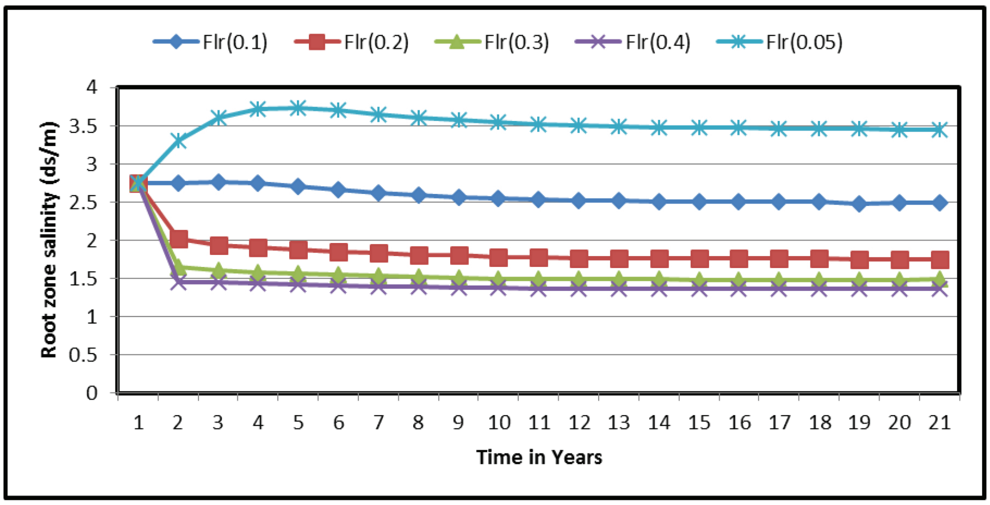

Figure 3: *Predicted root-zone salinity at Gokak (with drainage).*

SaltMod was applied to predict the salinity levels for the selected sites in the Ghataprabha command. This will be highly useful for taking up management decisions in the salinity-affected areas. The salinity level shows a decline with an increase of leaching efficiency. Prediction of root-zone salinity for 20 years with sub-surface drainage system is shown in Figures 3–6.

From the analysis, it is certain that the root-zone salinity declines after 3–5 years to the acceptable limits of 2.0–3.0 dS/m and became constant after 10 years for all the locations. The leaching efficiency of 0.2 shows the best match with the actual efficiency under adequate drainage conditions. However, without a sub-surface drainage system, there is a drastic increase in salinity over the years, thereby indicating the

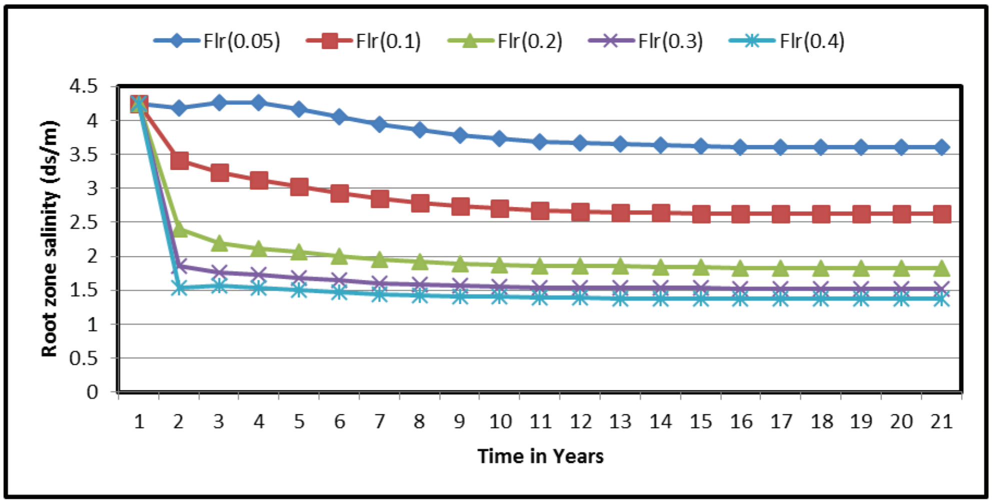

Figure 4: *Predicted root-zone salinity at Biligi (with drainage).*

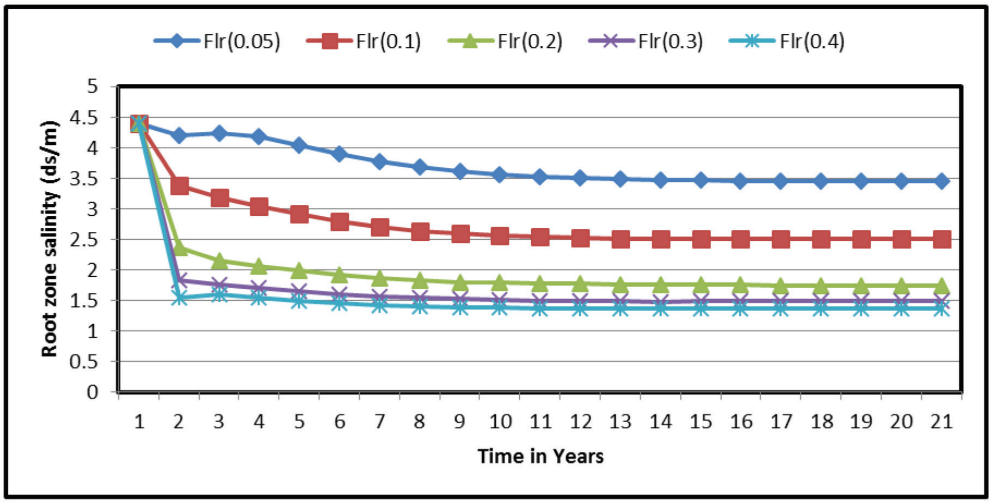

Figure 5: *Predicted root-zone salinity at Mudhol (with drainage).*

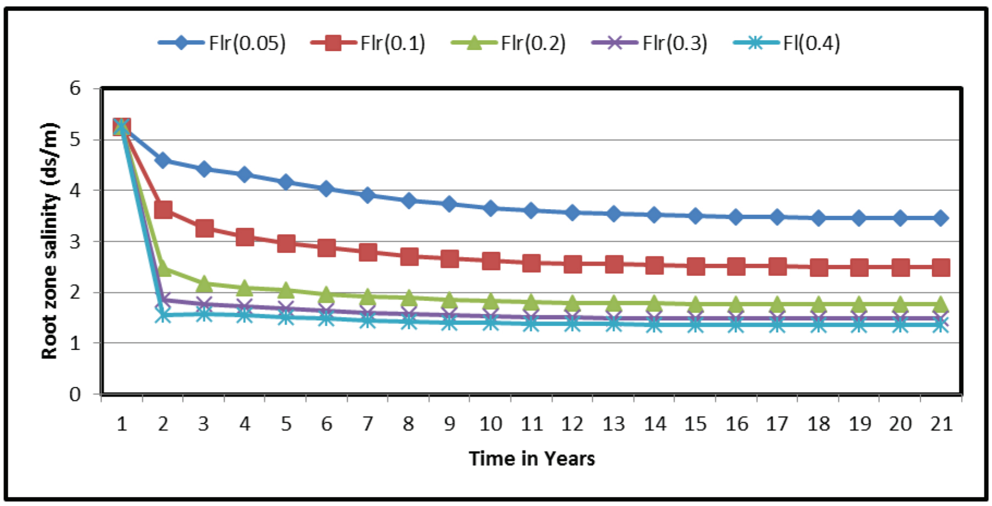

Figure 6: *Predicted root-zone salinity at Bagalkot (with drainage).*

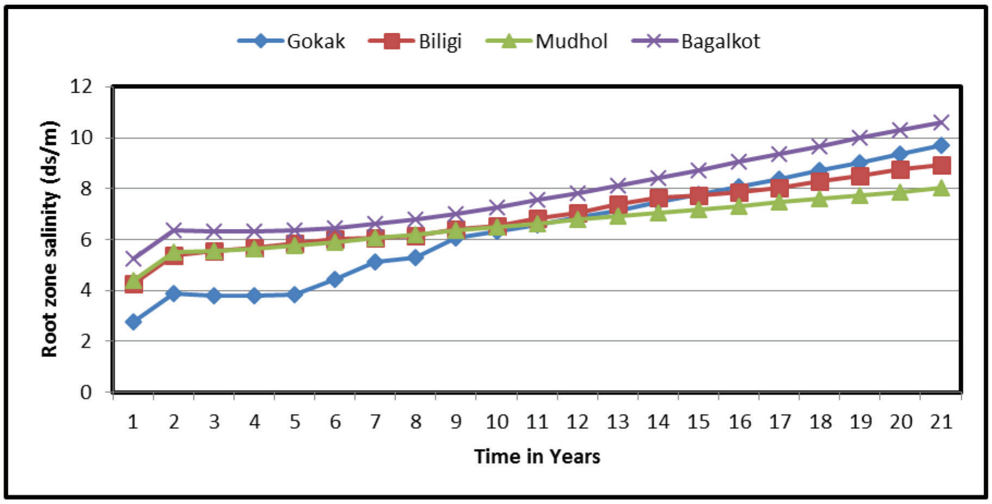

Figure 7: *Predicted root-zone salinity (without drainage).*

necessity of an artificial drainage system. The predicted salinity levels of the root zone without a sub-surface drainage system are shown in Figure 7 for all the locations. The model shows a steady increase, though at a slow pace over the years, reaching levels up to 8.0–10.6 dS/m at the end of the 20-year period. If a suitable drainage system is not provided, canal command areas will further get salinised, thus making the land uncultivable. From the present study, it is evident that it is necessary to provide proper drainage facilities to control the salinity levels in the command area.

Conclusions

SaltMod, a mathematical model is applied to predict the root-zone salinity and leaching efficiency. The model simulated the soil-profile salinity for 20 years under different conditions, viz. with and without sub-surface drainage. The salinity level shows a decline with an increase of leaching efficiency. The leaching efficiency of 0.2 shows the best match with the actual efficiency under adequate drainage conditions. The root-zone salinity shows a decline after a period of 3–5 years to the acceptable limits of 2.0–3.0 dS/m and remains constant after 10 years. However, without drainage, there is a drastic increase in salinity over the years, thereby indicating the necessity of an artificial drainage system. The model shows a steady increase, though at a slow pace over the years, reaching the levels of 8.0–10.6 dS/m at the end of the 20-year period. If a suitable drainage system is not provided, canal command areas will further get salinised, thus making the land uncultivable.

Acknowledgements

The authors acknowledge the National Institute of Hydrology for carrying out this study as a part of the work programme at the Regional Centre, National Institute of Hydrology, Belgaum. The authors are thankful to the Director, National Institute of Hydrology, Roorkee, India; Dr. Sudhirkumar, Co-coordinator; and Dr. B. Venkatesh, Head, of the National Institute of Hydrology, Belgaum, for their valuable encouragement in the preparation and presentation of this technical paper.

References

[1] Sinha, B.P.C. (1986): Water-logging and drainage problems in India-an over view. In: Proceedings of the Seminar on Conjunctive Use of Surface and Ground Water Resources, Central Ground Water Board, Ministry of Water Resources, Government of India, New Delhi; pp.1–13.

[2] Central Ground Water Board, Ministry of Water Resources, Govt.of India, (1997): *Report on Studies on*

Conjunctive Use of Surface and Groundwater Resources in Ghataprabha Irrigation Project, Karnataka, 180 p.

[3] Purandara, B.K., Venkatesh, B., Varadarajan, N. (1997): Water Logging problems in canal commands of Hard Rock region. In: Proceedings of Brain Storming Session on Hydrological problems of Hard Rock Region, organized by NIH, Belgaum on15th March, 1997, pp. 1–4.

[4] Dilip, G.D., Varadarajan, N., Purandara, B.K. (2002): Mapping of Groundwater Quality Parameters in GIS Environment. In: Proceedings on International Conference on Hydrology and Watershed Management held at Jawaharlal Nehru Technological University, Hyderabad during 18–20 December, pp. 568–577.

[5] National Institute of Hydrology, Central Water Commission, (2003): *Report on Study of Ghataprabha Command Area using Remote Sensing and GIS,* September 2003, pp.1–65.

[6] Hiremath, C.B. (2005): *Water Logging and Salinity-Impact of Major Irrigation Projects on Agriculture Land and Reclamation of Affected Areas,* M.Tech. Thesis, Visvesvaraya Technological University, Belgaum 2005, 120 p.

[7] Varadarajan, N., Purandara, B.K., Kumar, B. (2010): Status of Salinity in aquifers of Ghataprabha command Area, Karnataka, India. *RMZ- Materials and Geo-environment,* 57(3), pp. 347–362.

[8] Bahceci, I., Nazmi, D., Tari, A., Ahmet, I.G., Sonmez, B. (2006): Water and Salt balance studies using SALTMOD to improve subsurface drainage in the Konya-Cumra plain, Turkey. *Journal of Agricultural Water Management*, 85(3), pp. 261–271.

[9] Khan, N.M., Basir Ahmad, M., Latif, Y.S. (2004): Application of SALTMOD to Evaluate Preventive measures against Hydro-Salinization in Agricultural Rural Areas. *Quarterly Science Vision*, 9(3–4), pp. 111–117.

[10] Hebsur, N.S. (2005): *Groundwater Quality Appraisal of Malaprabha and Ghataprabha Command areas and its impact on crop production and soil health*, University of Agricultural Sciences, Dharwad, 230 p.

[11] Shrivastava, P.K., Patel, A.M., Oosterbaan, R.J. (2003): Saltmod Validation and Application in Segwa minor canal command area, In: Proceedings the 9th International Drainage Workshop, Utrecht, The Netherlands, September 10–13, Paper No 041.

[12] Poornima, K.B, Shiva Keshava Kumar, P., Varadarajan, N., Purandara, B.K. (2014): Estimation of Root zone salinity using SALTMOD – a case study. *International Journal of Advanced Research,* 2(9), pp. 858–870.

[13] [13] Oosterbaan, R.J. (2000): SALTMOD*, Description of Principles, Users Manual and Examples of Application,* Special Report, ILRI, Wageningen, The Netherlands, October 2000, pp. 1–80.

[14] Varadarajan, N. (2013): *Ground Water Quality Assessment in the Salinity Affected Areas of Ghataprabha Command Karnataka (India),* PhD. Thesis, Visvesvaraya Technological University, Belgaum, Karnataka, 284 p.

Original scientific paper

Received: August 22, 2017
Accepted: December 14, 2017
DOI: 10.2478/rmzmag-2018-0007

Site Characterization for Construction Purposes at FUNAAB using Geophysical and Geotechnical Methods

Geofizikalna in Geotehnična Ocena Gradbene Lokacije v Funaabu v Nigeriji

Alabi, A.A.[1]*, Adewale, A.O.[2], Coker, J.O.[3], Ogunkoya, O.A.[1]

[1] Department of Physics, College of Physical Sciences, Federal University of Agriculture, Abeokuta (FUNAAB), Nigeria

[2] Department of Science Laboratory Technology, Moshood Abiola Polytechnic, Abeokuta, Nigeria

[3] Department of Physics, Faculty of Science, Olabisi Onabanjo Univesity, Ago Iwoye, Nigeria

* derylab@yahoo.com

ABSTRACT

Geophysical and geotechnical techniques were used to investigate the sub-surface information of a proposed site for a hostel construction at Federal University of Agriculture, Abeokuta. Ten vertical electrical sounding (VES) stations were adopted. Typical sounding curves obtained include the HA, KH, AKH and KQH types, of which the AKH-type consists of 40% of the survey points, and a maximum of five geo-electric sub-surface layers were delineated. Laboratory analyses were performed to investigate particle size distribution, Atterberg limit, compaction limit, California bearing ratio (CBR) and specific gravity. The CBR revealed that all soil samples, except L4, are mechanically stable and have high load-bearing capacity. The Atterberg limit test and the geo-electric section showed that the second layer of VES 4 is composed of sandy clay with high plastic index and low liquid limit, which may pose a threat to the foundation of any engineering structure. VES locations 5, 6 and 8 were identified as high groundwater potential zones suitable for optimum groundwater abstraction. The study area is suitable for both shallow and deep foundations, however VES 4 and VES 5 require reinforcement.

Key words: grain size, California bearing ratio, Atterberg limits, compaction

POVZETEK

Za vrednotenje globinske informacije na predlagani lokaciji za hostel pri Zvezni poljedelski univerzi v Abeokuti so uporabili geofizikalne in geotehnične metode. Podatke so pridobili na desetih postajah z vertikalnim električnim sondiranjem (VES). Izmed značilnih krivulj HA, KH, AKH in KQH obsegajo tiste vrste AKH 40% izmerjenih točk, kar je omogočilo opredeliti v globini pet geoelektričnih plasti. V laboratoriju so opravili preiskavo porazdelitve zrnavosti, Atterbergove konsistenčne meje, kompakcijski preskus, California bearing ratio (CBR) in specifično težo. CBR nakazuje, da so vsi vzorci tal mehansko obstojni in da imajo visoko obremenilno kapaciteto z edino izjemo vzorca L4. Rezultati določitev Atterbergovih mej in geoelektričnih lastnosti pričajo o tem, da vsebuje druga plast VES 4 peščeno glino z visokim indeksom plastičnosti in nizko tekočinsko mejo, kar utegne ogrožati temeljenje. Lege VES 5, VES 6 in VES 8 razlagajo kot cone visokega potenciala podzemne vode, ki so lahko primerne lokacije za črpanje podtalnice. Preiskano območje je primerno tako za plitvo kot tudi globoko temljenje z izjemo lokacij VES 4 in VES 5, na katerih bo potrebno ojačenje.

Ključne besede: zrnavost, preskus California bearing ratio, Atterbergove meje, stisljivost

Introduction

In recent years, reports on collapsed structures have become alarming [1–4], and this phenomenon had led to loss of life and properties. It has been reported [5, 6] that building collapse may be due to inadequate bearing pressure, poor building materials, foundation failures which are traceable to lack or improper geo-technical and geophysical investigations, as well as effects of vibrations or fluctuations in water level. In recent years, collapse of engineered structures have become widespread going by the number of failed structures. Most of these failures can be attributed to insufficient knowledge of the bedrock of the sites, inaccurate top soil profile information, failure to identify sub-surface voids or solution cavities in carbonate rocks and lack of information on competence of the soil strata among others [7, 8]. Part of the concern in the design of structures is the pre-construction investigation of the subsoil which is to be carried out at the proposed location to ascertain the fitness of the host earth materials. The electrical resistivity method is useful in determining the competence of the subsoil layers; the resistivity value of the soil strata is proportional to its competence, and this value is governed by the amount of pore space and the arrangement of the pores, soil particle size and arrangement, among others [9]. Electrical resistivity measurements are preferred because of the wide range of resistivity values that are associated with nature, and it is also cost-effective among other geophysical surveys. The method is suitable for estimating depth of the bedrock and identifying the presence of structural features in the bedrock or potentially hazardous sub-surface conditions before the engineering structure is put in place [10]. The electrical resistivity method had found landmark success in solving a wide variety of engineering and environmental problems [11–19]. Application of 2D electrical resistivity tomography (ERT) in geo-technical investigations of the foundation at Ogudu Lagos, Nigeria [20], showed that the depth to the competent layer that could support a sizeable engineering structure is confined to the second half of the surveyed northeast area at a deeper depth mapped by ERT.
Electromagnetic profiling, dipole–dipole profiling and geo-electric depth sounding were integrated to carry out post-foundation engineering geophysical investigation within the surroundings of the 2,500 capacity auditorium building, Federal University of Technology, Akure, Nigeria [21]. The geo-electric sections and the inverted 2D resistivity structures delineated four sub-surface geo-electric layers, which include the topsoil, weathered layer weathered/fractured basement and the resistive basement bedrock. The study revealed that the sub-surface geologic materials underlying the investigated building are characterized by the presence of heterogeneous near-surface geo-materials, as well as uneven basement topography at shallow depths, where the foundations are usually placed. These features constitute a zone of geo-technical weakness, which may precipitate subsidence-related failure and eventual collapse of the foundation of the building.
Faseki et al. [22] used the geo-technical method to determine the geo-stratigraphy and engineering properties of the soil in shallow formations as foundation material in a proposed construction site along Badore Road, Addo, Lagos, Nigeria. Two boreholes were drilled up to the depth of 30.0 m, while cone penetration tests (CPTs) were deployed up to a depth of 6.0 m. Samples from boreholes were subjected to grain size and Atterberg limit tests. The results revealed that the site is underlain essentially by soft silty sandy clay at the upper layer, characterized by void ratio, unit weight, average standard penetration testing SPT-N and natural water content values, which are indicative of poor foundation material.
Oyedele et al. [23] carried out an integrated geophysical and geo-technical survey on a proposed engineering site at Ikoyi, Lagos, Nigeria. The investigation used CPT and SPT. Geophysical and geo-technical tests showed good agreement. Four to five sub-surface layers were delineated within the study area: the topsoil loose sand, peat/clay, sandy clay, sand and clay, which indicate good correlation with the soil layers in the bore logs. The existence of loose sand, peat and clay near the surface is capable of being inimical to building structures.
Site characterization involves determination of the nature and behaviour of all those aspects of

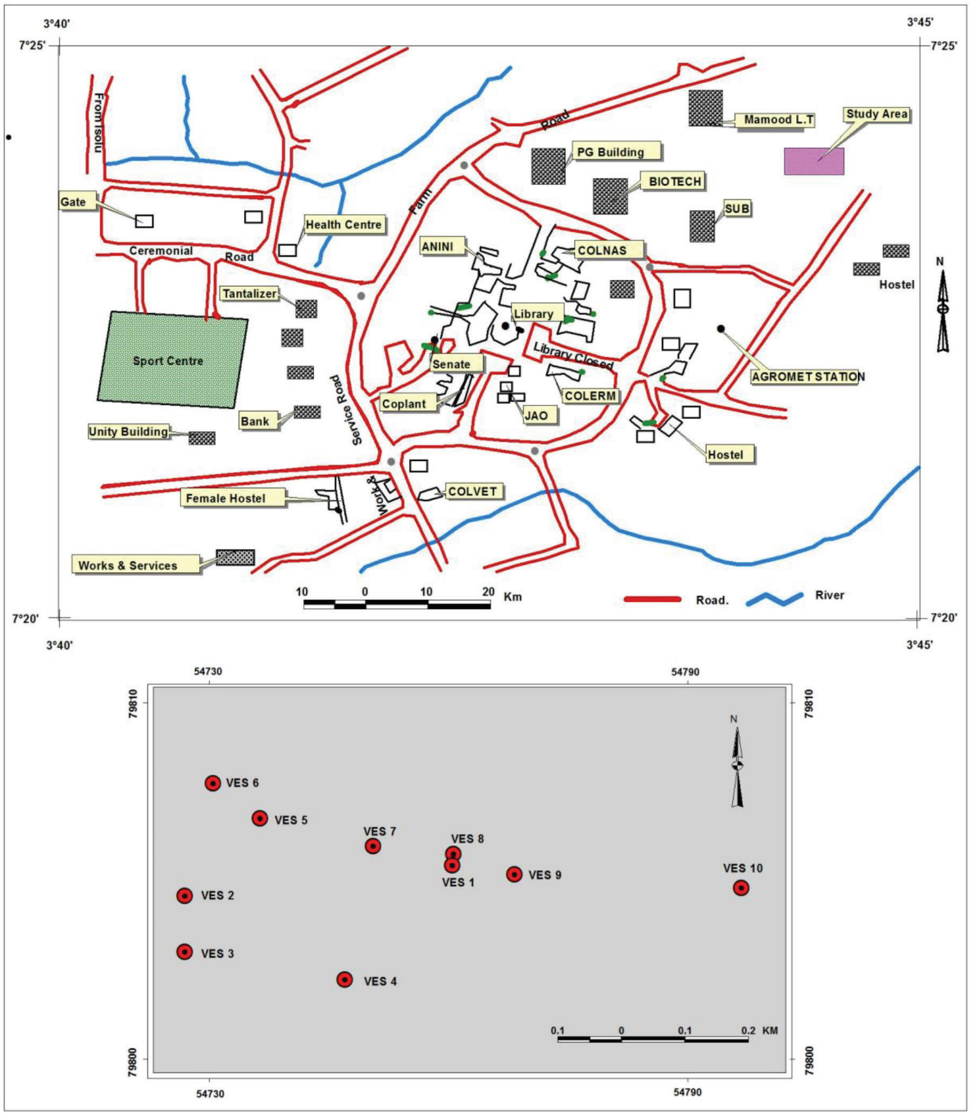

Figure 1: *The Topography Map of the Study Area.*

a site and its environment that could significantly influence or be influenced by an engineering construction project. The main reason for site characterization is to have adequate, dependable information of the sub-surface and site conditions, which will assist in taking decisions during the consideration, design and execution of an engineering construction project. The aim of this work is to investigate the nature and engineering properties of the proposed site for the proper designing of the foundation for the proposed hostel building at Federal University of Agriculture Abeokuta (FUNAAB). The study used geophysical and geotechnical techniques to probe the sub-surface competence and structural disposition in terms of load bearing in the context of building construction.

Materials and Methodology

Description of the Study Area

The study area is a proposed site for students` hostel located near the student union building within FUNAAB campus in Odeda Local Government Area of Abeokuta, Ogun State, Southwest Nigeria (Figure 1). It is located between latitudes 7°12′00″ and 7°30′00″ and between longitudes 3°15′00″and 3°45′00″.

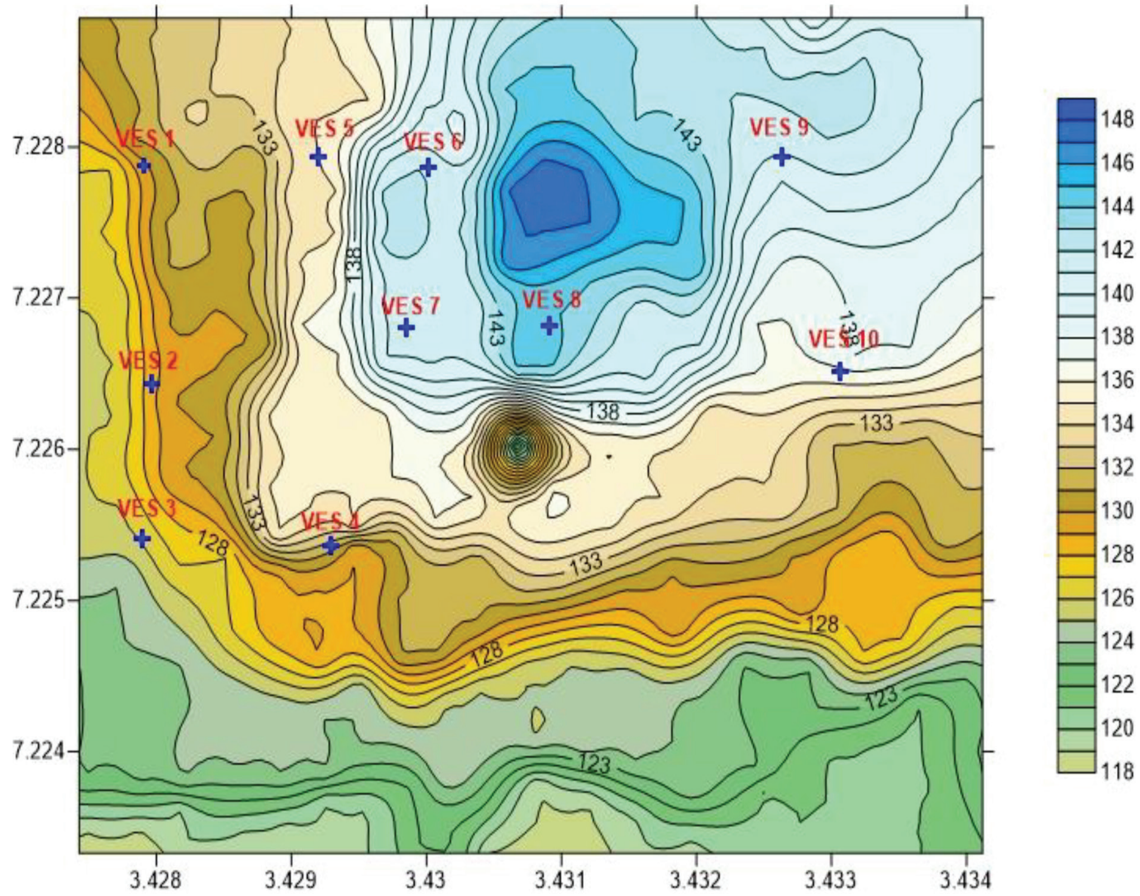

Figure 2: *Digital Elevation Model in Three Dimensions.*

Geology and Hydrological Settings of the Study Area

The ground elevation around the site of investigation ranges from 371 to 379 m above sea level (Figure 2), with the top soil mainly composed of sand, sandy clay and laterite. The topography of the area is slightly even, with some areas sloping gently. The climate is hot and humid, influenced by rain-bearing southwest monsoon winds from the ocean and dry northwest winds from the Sahara Desert. The study area, which falls within the Precambrian basement complex of Southwestern Nigeria [24–26], is underlain by crystalline rocks. The lithological units include magmatic gneiss complex, granitic gneiss and charnockites (Figure 3). Boulders of gneiss and granitic gneiss occur in the western part of the study area. Fracture bedrock generally occurs in a typical basement terrain [27]. The study area lies within the basement complex rocks. These rocks are from the Precambrian age to the early Palaeozoic age, and they extend from the north-eastern part of Ogun State (to which Abeokuta belongs), running in the southwest direction and dipping towards the coast [28].

Field Work Procedure for Geophysical Survey

The vertical electrical sounding (VES) approach of the electrical resistivity technique was adopted to determine the electrical resistivity and depths of the sub-surface layer with a highly sensitive terrameter (ABEM 300) using Schlumberger electrode arrangement (Figure 4). When the ratio of the distance between the current electrodes and the potential electrodes became too large, the potential electrodes were displaced outwards; otherwise, the potential difference may become too small to be measured with sufficient accuracy [29, 30]. Measurements

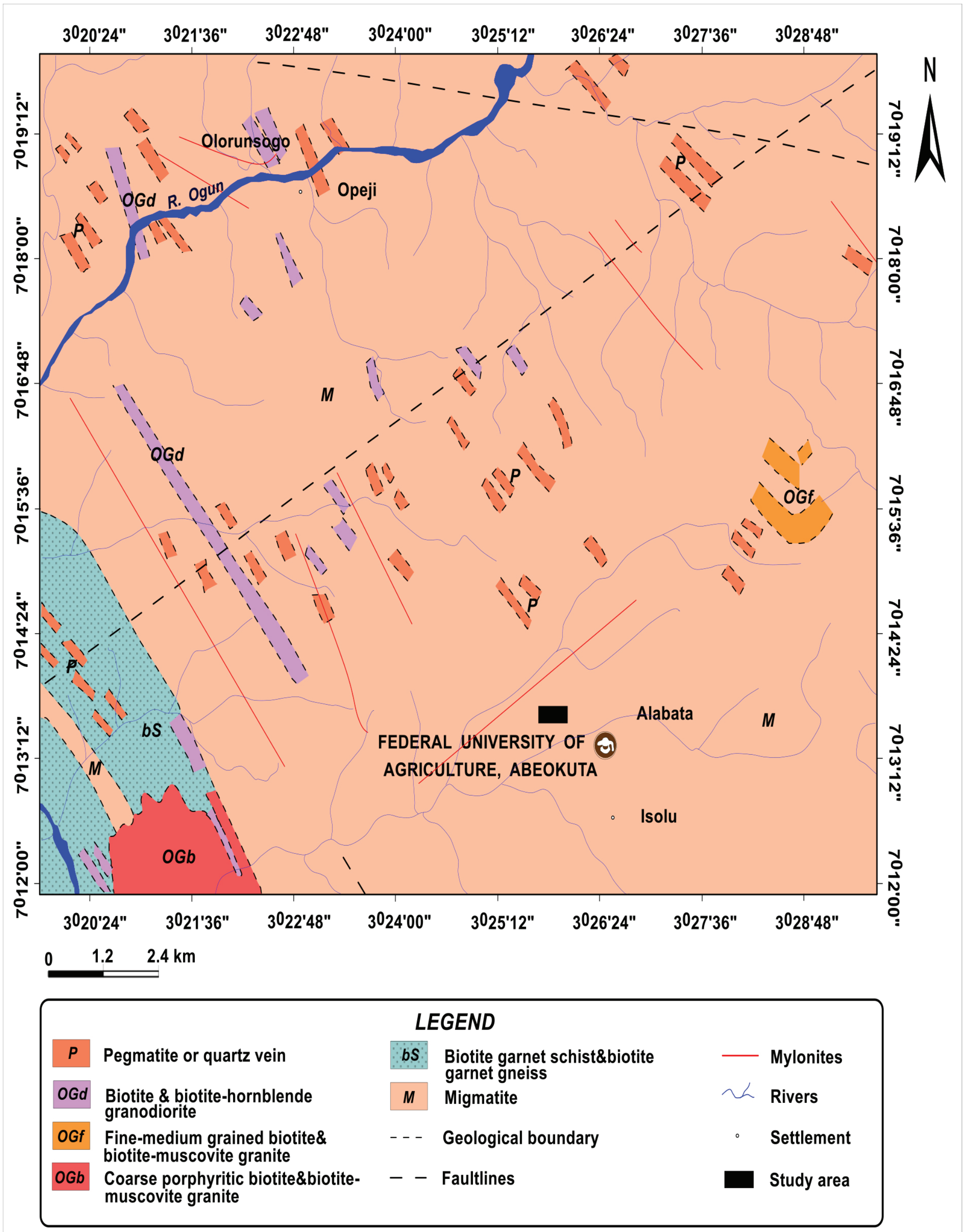

Figure 3: *Geological Map of the part of Abeokuta showing the study area.*

of current and the potential electrode positions were marked such that AB/2e $\frac{MN}{2}$, where AB/2 = current electrode spacing and MN/2 = potential electrode spacing. The value of AB/2 increased as the measurement progressed, while the potential electrodes' separations were guided accordingly. The potential electrodes were kept at small separations relative to the current electrodes' separations [30, 31]. One of the major advantages of this method relative to other methods is that only the current electrodes

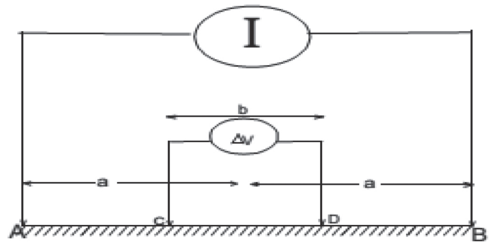

Figure 4: *Schlumberger array configuration, where I is the current, a is the midpoint between the current electrodes, b is the distance between the potential electrodes and ΔV is the potential difference between the two potentials C and D.*

need to be moved to new positions for most readings, while the potential electrodes are kept constant for up to three or four readings [30, 32]. During the field work sounding, the earth resistivity meter performs automatic recording of both voltage and current, stacks the results, computes the resistance in real time and digitally displays them [30, 33].

The apparent resistivity value is the product of the geometric factor and the resistance recorded in the resistivity meter. Several soundings and apparent resistivity values would be obtained by progressively expanding the current electrodes' spacing with fixed steps to enable sufficient penetration to the sub-surface earth and enhance structural responses as specified by Schlumberger arrays.

Laboratory Tests for Geo-technical Survey

Disturbed soil samples (15 kg each) were collected at each of the locations of the seven VES stations – L2 (VES2), L4 (VES4), L5 (VES5), L6 (VES 6), L7 (VES7), L8 (VES8) and L10 (VES10) – within the site. The samples were put inside black polythene bags, labelled and packed under controlled temperature to prevent the escape of moisture. The analysis was carried out at Civil Engineering Laboratory, Federal University of Agriculture, Abeokuta. Analysis of samples was extended to include California bearing ratio (CBR) test, specific gravity determination, grain size analysis (sieve analysis) test, compaction test and Atterberg limits test. Samples were prepared depending on the investigation types and procedures used. Some samples were wet and compacted, some were oven-dried and sieved with a specific sieve number, some were soaked in distilled water, some were pulverised and run through a known sieve, while some were crushed with a rubber-headed pestle and sieved before the analysis was carried out on them. Laboratory equipment deployed for the analysis were electric oven, sieve shaker, plastic mortar and pestle, Casagrande's liquid limit (LL) apparatus, density bottle with distilled water and gassing machine.

The CBRs of soaked and unsoaked soils were determined using a standard method (*American Society for Testing and Materials* [ASTM] D1883). The test was carried out on the top and bottom layers of the compacted wet soil, and the average was taken as the actual CBR. A water pycnometer-based standard test (ASTM D854-00) was used to determine the specific gravity of the soil.

The specify gravity of the soil solids was calculated using Equation (1):

Specify gravity,

$$G_S = \frac{w_O}{w_O + (w_a - w_b)} \tag{1}$$

where

w_o = weight of sample of oven-dry soil, $g = w_{ps} - w_p$, w_a = weight of pycnometer filled with water and w_b = weight of pycnometer filled with water and soil.

The grain sieve analysis was performed to determine the percentage by weight of the grains passing through a 75 µm sieve (sieve no. 200). Samples of approximately 500 g were used for determining grain size distribution. The percentages of particles retained and particles passing were calculated using Equations (2) and (3).

$$R = \frac{M_r}{T_m} * 100 \tag{2}$$

$$P = 100 - R \tag{3}$$

$$Q_p = T_m - M_r \tag{4}$$

where T_m = total mass of the soil, R = % retained, P = % passing, M_r = mass retained, Q_p = quantity passing.

The compaction test was used to investigate the moisture–density relationship of the soil samples. Standard methods (ASTM D698 and ASTM D1557) were used for estimating the laboratory compaction characteristics of soil using, respectively, standard effort (6,000 kN-m/m^3) and modified effort (27,000 kN-m/m^3) for the determination of the moisture–density relationship. The moisture content of each compacted soil specimen was calculated by finding the average of the two water contents.

The Atterberg limit test was carried out using Casagrande's apparatus and following the procedure described in ASTM D4318. The LL, the plastic limit (PL) and the plasticity index (PI) of the soil were determined.

Data Processing and Interpretation

Characteristics of the VES Layers (Schlumberger Array)

The summary and interpretation of the results, iterated using the IP2 computer software, are displayed in Table 1. The results of the resistivity curves and the geo-electric sections, i.e. thickness of layers, resistivity, depth, inferred lithology and curve type values, are shown in Table 1.

The shape of a VES curve depends on the number of layers in the bedrock, the thickness of each layer and the ratio of the resistivity of the layers [34]; it also reflects the different lithological attributes in the study area. The results of the quantitative interpretation suggest that the sites are characterized by four types of resistivity curves, which are 4-AKH, 3-KH, 2-HA and 1-KQH. For example, curve AKH of the layer resistivity sections ($\rho1 < \rho2 < \rho3 > \rho4 > \rho5$) for VES-1, 2, 3 and 9 – after quantitative treatment and analysis – were delineated to five distinct geo-electric layers in the study area (top soil, laterite, which extends to the third geo-electric layer at some sites, and a fourth layer, which is sandy clay, with basement rock being the fifth layer).

Typical sounding curves and geo-electric section layers from the site include the HA ($\rho_1>\rho_2>\rho_3<\rho_4$), KH ($\rho_1<\rho_2>\rho_3<\rho_4$), AKH ($\rho_1<\rho_2<\rho_3>\rho_4<\rho_5$) and KQH ($\rho_1<\rho_2>\rho_3>\rho_4<\rho_5$) curve types, with four to five geo-electric layer combinations. The AKH curve type predominates, constituting 40% of the total number of curves, while the KH, HA and KQH types constitute 30%, 20% and 10% of this total, respectively. Concisely, a maximum of five geo-electric sub-surface layers were identified in the area, comprising the topsoil with resistivity values ranging from 47.8 to 381 Ω-m and thickness varying from 0.701 to 1.08 m; the lateritic layer with resistivity values between 116 to 1,095 Ω-m and thickness varying from 0.596 to 2.08 m; lateritic hard pan layer with resistivity values ranging from 22.5 to 480 Ω-m and thickness varying from 1.94 to 27 m; and the fresh basement with resistivity range of 455 to 921 Ω-m which is assumed to be infinitely thick. The second layer in VES 4 and VES 5 is filled with sandy clay (Table 1); the two locations would not support engineering structures, except when the foundation is reinforced.

Results of Geotechnical Tests

Compaction Limit Test

The maximum dry density (MDD) for the soil samples ranged from 1,697 to 2,158 kg·m^{-3} while the optimum moisture content (OMC) ranged from 8.74% to 17.74% (Table 2). The values of the MDD for all samples were within the specifications of the Federal Ministry of Works and Housing, Nigeria [35], which recommends that the MDD should be >1,680 kg·m^{-3}and the OMC <18%. The strength of the soil and the density of the soil mass are interrelated generally: the strength of a soil increases as its dry density increases. The potential for the soil to take on water at later times is decreased by higher densities, which is due to the decreased presence of air space in the soil mass. The in-place moisture content of a soil is often used, along with the soil classification, to determine the suitability of the material. Generally, as the moisture content of a soil increases, its strength decreases and its potential for deformation and instability increases.

Sieve Analysis Test

The percentage passing, percentage retained and the quantity of the soil passing were calculated using Equations 2, 3 and 4.

The percentages of soil samples L2, L4, L5, L6, L7, L8 and L10 by weight that passed through No. 200 sieve were within the specification lim-

Table 1: *Summary of the results of the VES for the study area*

VES	Location	Layer	Apparent resistivity (ρ)	Thickness (m)	Depth (m)	Inferred lithology	Curve type
1	Lat 7°13′38.49″ Long 3°25′50.87″	1 2 3 4 5	180.0 417.0 464.0 59.0 712.0	0.70 2.08 1.94 23.80	0.70 2.78 4.72 28.50	Topsoil Lateritic Lateritic hard pan Sandy clay Basement rock	AKH
2	Lat 7°13′36.32″ Long 3°25′40.36″	1 2 3 4 5	180.0 414.0 472.0 61.5 841.0	0.79 1.95 1.98 23.80	0.79 2.74 4.72 28.5	Topsoil Lateritic Lateritic hard pan Sandy clay Basement rock	AKH
3	Lat 7°13′33.48″ Long 3°25′40.52″	1 2 3 4 5	189.0 417.0 480.0 63.5 731.0	0.70 1.84 2.06 25.60	0.70 2.54 4.60 30.20	Topsoil Lateritic Lateritic hard pan Sandy clay Basement rock	AKH
4	Lat 7°13′32.31″ Long 3°25′46.56″	1 2 3 4	285.0 116.0 101.0 610.0	0.78 0.64 14.60	0.78 1.41 16.00	Top soil Sandy clay Saturated sandy clay Basement rock	HA
5	Lat 7°13′40.36″ Long 3°25′43.47″	1 2 3 4	381.0 190.0 25.4 445.0	1.01 0.79 10.00	1.01 1.80 11.80	Top soil Sandy clay Saturated sandy clay Basement rock	HA
6	Lat 7°13′42.23″ Long 3°25′41.48″	1 2 3 4	139.0 178/0 22.5.0 496.0	1.01 0.59 7.38	1.01 1.60 8.98	Top soil Lateritic Sandy clay Basement rock	KH
7	Lat 7°13′38.95″ Long 3°25′47.59″	1 2 3 4	81.5 120.0 47.1 494.0	0.74 2.06 27.10	0.74 2.80 29.90	Top soil Lateritic Sandy clay Basement rock	KH
8	Lat 7°13′38.91″ Long 3°25′50.87″	1 2 3 4 5	129.0 186.0 67.8 24.0 656.0	0.74 1.56 9.51 19.40	0.74 2.30 11.80 31.20	Top soil Lateritic Sandy clay Saturated sandy clay Basement	KQH
9	Lat 7°13′37.46″ Long 3°25′53.07″	1 2 3 4 5	47.8 120.0 157.0 48.7 494.0	1.08 1.70 3.86 29.1	1.08 2.78 6.64 35.70	Top soil Lateritic Lateritic hard pan Sandy clay Basement rock	AKH
10	Lat 7°13′36.77″ Long 3°26′1.76″	1 2 3 4	600.0 1,095.0 53.0 921.0	0.79 0.81 18.10	0.79 1.60 19.70	Top soil Lateritic Sandy clay Basement rock	KH

Table 2: *Results of the Compaction Limits Determined for the Soil Samples*

Sample Number	Optimum Moisture Content (%)	Maximum Dry Density (kg·m^{-3})
L 2	13.16	1,812
L 4	8.74	2,158
L 5	12.83	1,697
L 6	11.00	2,012
L 7	11.70	2,076
L 8	12.40	2,115
L 10	17.74	1,764

Table 3: *Summary of Results of Sieve Analysis*

	Sieve Number	4	8	16	30	50	100	200	Pan
	Diameter (μm)	475	236	118	600	300	150	75	
L2	% Retained	13.22	15.28	18.54	12.61	18.83	16.86	3.25	1.4
	% Passing	86.78	71.5	52.96	40.35	21.51	4.65	1.4	0
L4	% Retained	4.50	4.15	11.24	15.72	29.42	28.86	3.39	2.48
	% Passing	95.50	91.35	80.11	64.39	34. 79	6.11	2.72	0.24
L5	% Retained	11.49	13.12	24.19	11.99	17.79	15.46	2.47	3.28
	% Passing	88.51	75.39	51.2	39.21	21.42	5.96	3.49	0.21
L6	% Retained	14.80	14.42	25.78	12.91	16.05	11.25	3.46	1.33
	% Passing	85.20	70.78	45	32.09	16.04	4.79	1.33	0.00
L7	% Retained	10.03	11.72	20.03	12.11	19.76	18.94	4.02	2.35
	% Passing	89.97	78.25	58.22	46.11	26.35	7.41	2.39	0.04
L8	% Retained	15.43	13.49	20.34	14.49	27.8	0.33	6.88	1.23
	% Passing	84.57	71.08	50.74	50.74	36.25	8.45	8.12	1.24
L10	% Retained	9.06	11.66	24.79	11.12	18.09	20.9	2.61	1.77
	% Passing	90.94	79.28	54.49	43.37	25.28	4.38	1.77	0.00

it, and they were 1.40%, 2.72%, 3.49%, 1.33%, 2.39%, 8.12% and 1.77% (Table 3). The values were less than the stipulated maximum limit of 35% based on the specification requirement [35] in Clause 6201.

Specific Gravity Test

Table 4 shows the results of determination of the specific gravity of the soil samples.

Soil samples L2, L4, L5, L6, L7, L8 and L10 had specific gravities of 2.69, 2.41, 2.64, 2.80, 2.54, 2.67 and 2.47, respectively. The specific gravity of the samples was within the limit of specification [35] in Clause 6201, which ranges from 2.5 to 2.75, except samples L4 and L6, which had values lower than and greater than the limit, respectively. The specific gravity of soil grains depicts vital information on the features of a soil, whether it can withstand engineering structures or not [36]. The closer the specific gravity of the soil to the upper limit of the standard of the soil, the better it is for construction purposes.

Table 4: *Results of the Average Specific Gravity Determination of Soil Samples*

Sample Designation	L 2	L 4	L 5	L 6	L 7	L 8	L 10
First	2.71	2.43	2.57	2.80	2.50	2.67	2.50
Second	2.67	2.38	2.71	2.80	2.57	2.67	2.43
Average SP	2.69	2.41	2.64	2.80	2.54	2.67	2.47

Table 5: *Liquid limit, average plastic limit and plasticity index percentage for the soil samples*

Station	Liquid Limit at N	Average Plastic Limit	Plasticity Index %
L2	23.54	14.75	8.79
L4	41.25	31.84	9.74
L5	17.20	0.00	17.20
L6	21.83	16.10	5.73
L7	30.49	12.91	8.79
L8	34.74	22.95	11.79
L10	32.74	21.04	11.70

Table 6: *Results of the Determined California bearing ratio test for the soil samples.*

Sample Number	Unsoaked CBR (%)	Soaked CBR (%)
L 2	97.82	22.40
L 4	56.78	4.20
L 5	108.00	13.70
L 6	94.48	15.78
L 7	96.34	22.90
L 8	110.00	29.50
L 10	120.00	19.30

Atterberg Limit Results

The values of LL, PL and PI are presented in Table 5.

All soil samples except L4 and L5 satisfied the specification requirement [35] in clauses 6201 and 6252 since both the LL and PI (Table 5) of all the samples did not exceed the stipulated values of 35% and 12%, respectively. The PI of soil sample L5 was above the standard limit; therefore, it is considered to be highly plastic (i.e. it is clayey), which may pose a threat to the structure (leading to structural failure) since the soil usually has the ability to retain appreciable amount of water (moisture), especially by absorption, thereby decreasing its permeability and hydraulic conductivity (K).

CBR Test

The overall CBR for soaked (CBR_s) and unsoaked (CBR_u) soil samples were within the specified limits except the sample at L4 (Table 6).

The specification requirement [35] is that the minimum strength of the material shall not be <80% for CBR_u, while the minimum strength of the material shall not be <10% after at least 48 hours of soaking (CBR_s). The CBR_s and CBR_u values for L4 were 4.20% and 56.78%, respectively. These values indicate that the soil at VES 4 is a clayey lateritic soil, which does not support heavy structures. In addition, moisture influx would be highly detrimental to the structure constructed at this position.

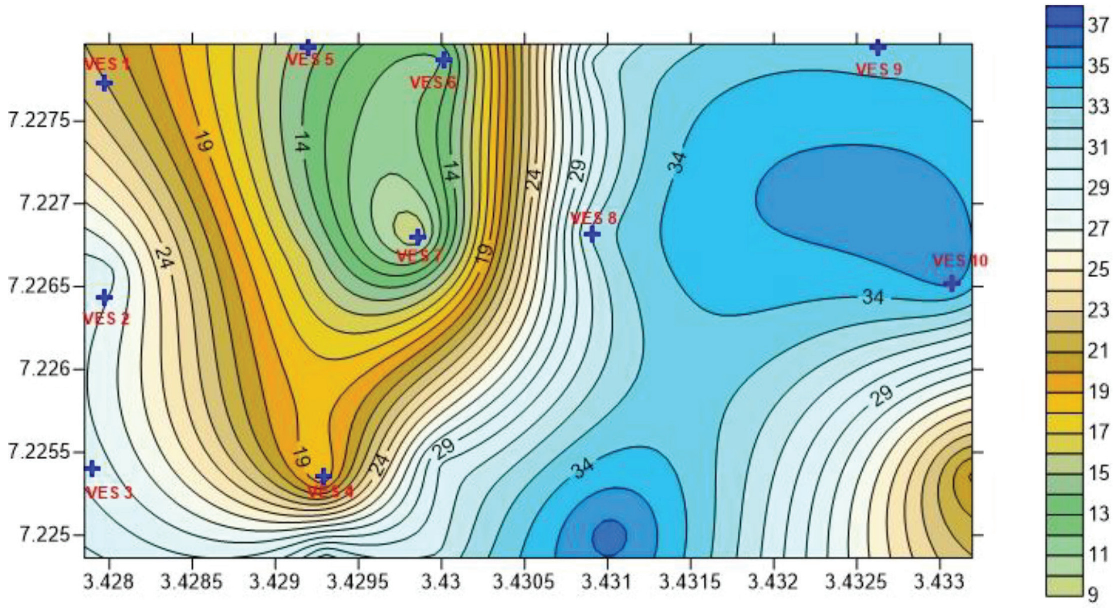

Figure 5: *Overburden thickness map of the study area.*

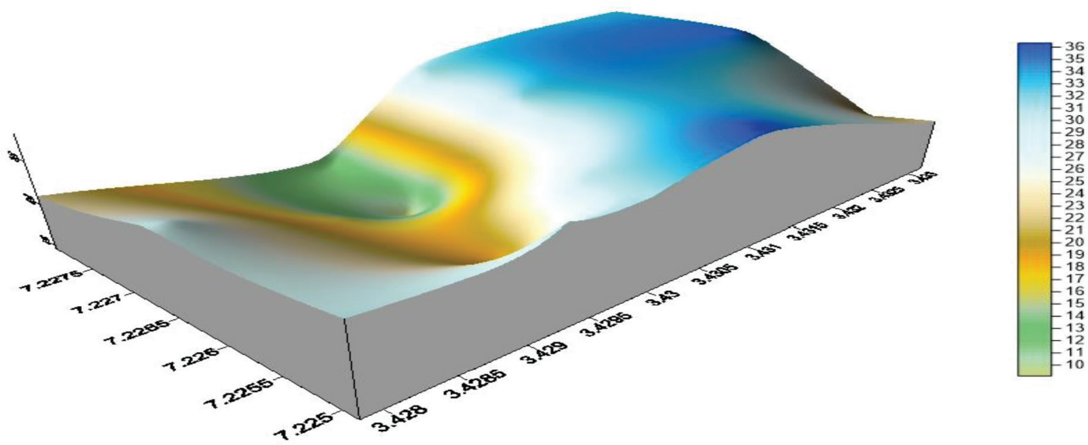

Figure 6: *Basement relief map of the study area.*

Hydrogeological Implication

It is possible to make qualitative hydro-geological deductions from the curve types [37]. The aquiferous zones are found within the layer with relatively low resistivity values (Figure 5). This zone is interpreted as the underlying groundwater level. Consequently, because of the low resistivity of the aquiferous units in Table 1, the positions VES 5, VES 6 and VES 8 are favourable points for locating a well. Basically, the absolute value of electrical conductivity has been effectively used. The overburden thickness map of the area (Figure 6) indicates the zones of relatively thick overburden (i.e. >16 m) and zones of relatively thin overburden (i.e. <16 m). From studies in similar basement terrain [38], areas with thick overburden cover are identified as high-groundwater-potential zones. Likewise, the analysis of the bedrock relief map of the site (Figure 5) has hydro-geological significance in a basement setting [39]. Basement depression zone (i.e. area at lower elevation on the bedrock) is delineated at the eastern part of the study area. The thick overburden and depression zones constitute priority areas for groundwater development.

Geotechnical Implication

The engineering competence of the sub-surface formation in the study area was evaluated qualitatively from layer resistivity characteristics: the higher the layer resistivity, the higher the competence [40]. The relatively low resistivity anomaly (116 Wm) beneath VES 4 depicts a fracture or weak shear zone, which is a potential hazard to settlement of buildings and may cause collapse of overlying structures if remedial engineering action is not considered.

Conclusion

The geophysical and geotechnical methods of foundation investigations carried out at the proposed site for a hostel in the campus of Federal University of Agriculture, Abeokuta, have been effective in characterising the sub-surface materials that underlie the study area as well as the depth to bedrock. The results obtained from the VES experiments show a maximum of five geo-electric layers, which include topsoil, lateritic, lateritic hard pan, sandy clay and basement/fractured basement rock. The geo-electric section reveals that the second layer of VES 4 and VES 5 are filled with sandy clay, which is not suitable for structure foundation. The CBR test reveals that all the soil samples tested – except L4 (taken at VES 4) – are mechanically stable and have high load-bearing capacity, which is suitable for both shallow and deep foundations without the need for reinforcement. However, reinforcement is highly required in the design and construction of the foundation in VES 4. The Atterberg limit test and the geo-electric section reveal that the second layer of VES 4 is filled with sandy clay with high PI and low LL, which may pose a threat to the foundation (leading to structural failure), since the soil usually has the ability to retain appreciable amount of water (moisture) especially by absorption, thereby decreasing its permeability and hydraulic conductivity. The positions of VES 5, VES 6 and VES 8 are identified as high-groundwater-potential zones in the study area, which are suitable locations for hand-dug wells and boreholes for optimum groundwater abstraction. The results from the application of geophysical and geotechnical methods on site characterization reveal that the study area is suitable for both shallow and deep foundations, except at VES 4 and VES 5, where reinforcement is required to support shallow and deep foundations.

References

[1] Marshall, R., Martin, M. (1993): Defect Prevention Research Project*. Canada Mortgage and Housing Corporation/Ontario New Home Warranty Program.*

[2] Fagbenle, O.I., Oluwunmi, A.O. (2010): Building Failure and Collapse in Nigeria: the Influence of the Informal Sector, *Journal of Sustainable Development,* 3(4), pp. 268–276.

[3] Dimuna, K.O. (2010): Incessant Incidents of Building Collapse in Nigeria: A Challenge to Stakeholders. *Global Journal of Researches in Engineering*, 2 (4), pp. 75–84.

[4] Adebowale P.A, Gambo, M.D., Ankeli, I.A., Daniel, I.D. (2016): Building Collapse in Nigeria: Issues and Challenges. Conference of the International Journal of Arts & Sciences*,* 9(1), pp. 99–108.

[5] Leonards, G.A. (1982): Investigation of failures. *Journal of Geotechnical Engineering*, ASCE, 108, pp. 187–246.

[6] Chendo, I.G., Obi, N.I. (2015): Building collapse in Nigeria: the causes, effects, consequences and remedies. *International Journal of Civil Engineering, Construction and Estate Management*, 3(4), pp.41–49.

[7] Robert, J.N., (2010): Geotechnical Site Characterization and Field Investigation Methods; Anticipate and Identify Subsurface Conditions to Manage Risks. *Whitlock dalrymple poston & associates, p.c.*

[8] Oyedele, K.F., Oladele, S., Adedoyin, O. (2011): Application of Geophysical and Geotechnical Methods to Site Characterization for Construction Purposes at Ikoyi, Lagos, Nigeria. *Journal of Earth Sciences and Geotechnical Engineering*. 1(1), pp. 87–100.

[9] Wightman, W.E., Jalinoos, F., Sirles, P., Hanna, K. (2003): Application of Geophysical Methods to Highway Related Problems. Lakewood. *Federal Highway Administration, Central Federal Lands Highway Division, Publication.*

[10] Soupios, P.M., Georgakopoulos, P., Papadopoulos, N., Saltas, V., Andreadakis, A., Vallianatos, F., Sarris, A., Makris, J.P. (2007): Use of engineering geophysics to investigate a site for a building foundation. *Journal of Geophysics and Engineering,* 4, pp. 94–103.

[11] Abu-Shariah, M.I.I. (2009): Determination of cave geometry by using a geo-electrical resistivity inverse model. *Engineering Geology*, 105, pp. 239–244.

[12] El Mahmoudi, A.S., Khalied, M.A., Massoud, A.M. (2010): 2-D electrical tomography for mapping of aquifer at the new campus of King Feisal University, Al Hassa, KSA. *4th International Conference on Water Resources and Arid Environments (ICWRAE4)*, pp. 267–280.

[13] Olorunfemi, M.O., Ojo, J.S., Ojelabi, E.A. (2002): Geophysical Site Investigation of the premises of Idu Flow Station. *Nigerian Agip Company (NAOC) Limited. (For multipurpose Oil Services Company Limited, Port Harcourt). Technical Report*.

[14] Adeoti, L., Kehinde, I., Adegbola, R.B., Sovi, S.T. (2009): Foundation Investigation using Electrical Resistivity Method: A Case Study of Iponri, Lagos State, Nigeria. *Journal of Engineering Research,* 14(1), pp. 50–57.

[15] Ayolabi, E.A., Folorunso, A.F., Oloruntola, M.O. (2010): Constraining Causes of Structural Failure using Electrical Resistivity Tomography (ERT): A Case Study of Lagos, Southern Western, Nigeria. *Journal of Geophysics/Mineral Wealth,* 156/210, pp. 7–18.

[16] Adeyemo, I.A., Omosuyi, O.G. (2012): Hydrogeologic, Electrical and Electromagnetic Measurements for Geotechnical Characterization of Foundation Beds at Afunbiowo, near Akure, Southwestern Nigeria. *Indian Journal of Science and Technology,* 5(2).

[17] Salami, B.M, Falebita, D.E, Fatoba, J.O, Ajala, M.O. (2012): Integrated Geophysical and Geotechnical Investigation of A Bridge Site – A Case Study of A Swamp/Creek Environment in Southeast Lagos, Nigeria. *Ife Journal of Science,* 14(1), pp. 75–82.

[18] Fatoba, J.O., Alo, J.O., Fakeye, A.A. (2010): Geoelectric Imaging for Foundation Failure Investigation at Olabisi Onabanjo University Minicampus, Ago-Iwoye, Southwestern Nigeria. *Journal of Applied Sciences Research*, 6(12), pp. 2192–2198.

[19] Bharti, A.K., Pal, S.K., Priyam, P., Pathak, V.K., Kumar, R., Ranjan, S.K. (2016): Detection of illegal mine voids using electrical resistivity tomography: The case-study of Raniganj coalfield (India). *Engineering Geology,* 213, pp. 120–132.

[20] Ayolabi, E.A., Folorunso, A.F., Jegede, O.E. (2012): An Application of 2D Electrical Resistivity Tomography in Geotechnical Investigations of Foundation Defects: A Case Study. *Journal of Geology and Mining Research*, 3(12), pp. 142–151.

[21] Bayode, S., Omosuyi, G.O., Abdullahi, H.I. (2012): Post –foundation Engineering Geophysical investigation in Part of the Federal University of Technology, Akure, Southwestern Nigeria. *Journal of Emerging Trends and Engineering Apply Science,* 3(1), pp. 203–210.

[22] Faseki, O.E., Olatinpo, O.A, Taiwo, O.B. (2016): Ground Investigation of an Engineering Site at Point Road, Apapa, Lagos, Nigeria. *Journal of Engineering and Energy Research*, 6(1), pp. 1–20.

[23] Oyedele, K.F., Adeoti, L., Oladele, S. Kamil, A. (2014): Investigation of a Proposed Four Story Building Sites Using Geophysical and Laboratory Engineering Testing Methods in Lagos, Nigeria. *International Journal of Scientific Research in Knowledge*, 2(2), pp. 83–91.

[24] Grant, N.K. (1978): Structural Distinction between a Metasedimentary Cover and an underlying Basement in the 600 m. y. old Pan African domain of Northwestern Nigeria, West Africa. *Geological Society of American Bulletin,* 89, pp. 50–58.

[25] Rahaman, M.A. (1976): *Review of the Basement Geology of South-Western Nigeria*. In: Kogbe CA (ed.) Geology of Nigeria, 2nd ed. Elizabethan Publishers, Lagos, pp. 41–58.

[26] Adegoke, A., Ajayi, O.W. (1988): Groundwater Prospects in Basement Complex Rock of South Western Nigeria. *Journal of African Earth Sciences*, 7(1), pp. 227–235.

[27] Odusanya, B.O, Amadi, U.N.P. (1990): An Empirical Resistivity Model for Predicting Shallow Groundwater in the Basement Complex Water Resources. *Journal of Nigerian Association of Hydrologists*, 2, pp. 77–87.

[28] Ako, B.D. (1979): *Geophysical prospecting for groundwater in parts of South-western Nigeria*. Unpublished PhD Thesis. Department of Geology, University of Ife, Ile-Ife, Nigeria. 371 p.

[29] Koefoed, O. (1979): *Geo sounding Principles Resistivity: Sounding measurements.* Elsevier Scientific Publishing Company, Amsterdam, 275 p.

[30] Alile, O.M, Amadasun, C.V.O, Evbuohuwan, A.I. (2008): Application of Vertical Electrical Sounding Method to Decipher the Existing Subsurface Stratification and Groundwater Occurrence Status in a Location in Edo North of Nigeria. *International, Journal of Physical Sciences*, 3(10), pp. 245–249.

[31] Milson, J. (1939): *Field Geophysics; a handbook of geophysical society of London.* John Wiley and Sons, New York, Toronto, Singapore.

[32] Reinhard, K.F. (1974): Combined geo-electrical and Drill-hole investigation for detecting fresh-water aquifers in Northern western Missouri. *Geophysics,* 39, pp. 340–352.

[33] Dorbrin, M.D., King, R.F. (1976): *Introduction to Geophysical Prospecting*. Me Graw-Hill book, New York, 630 p.

[34] Schwarz, S.D. (1988): Application of Geophysical Methods to Groundwater Exploration in the Tolt River Basin, Washington State. *Geotechnical and Environmental Geophysics*, 1, pp. 213–217. http://dx.doi.org/10.4133/1.2921817.

[35] Federal Ministry of Works and Housing (1997): General specifications for Roads and Bridges. *Vol II, Federal Highway Department, FMWH, Lagos, Nigeria,* 168 p.

[36] Gidigasu, M.D. (1976): Laterite Soil Engineering. *Elsevier Scientific Publishing Company, Amsterdam,* 554 p.

[37] Worshington, P.R. 1977: Geophysical Investigations of Groundwater Resources in the Kalahari Basin. *Geophysics,* 42(4), pp. 838–849.

[38] Omosuyi, G.O., Ojo, J.S., Enikanselu, P.A. (2003): Geophysical Investigation for Groundwater around Obanla –Obakekere in Akure Area within the Basement Complex of South-Western Nigeria. *Journal of Mining and Geology,* 39(2), pp. 109–116.

[39] Bala, A.C. Ike, E.C., (2001): The Aquifer of the Crystalline Basement Rocks in Gusau Area, Northwestern Nigeria. *Journal of Mining and Geology*, 37(2), pp. 177–184.

[40] Hunt, R.E. (2007): *Geotechnical Investigation Methods: A Field Guide for Geotechnical Engineers.* Taylor & Francis Group, LLC. pp 48.

Original scientific paper

Received: Aug 07, 2017
Accepted: Mar 09, 2018
DOI 10.1515/rmzmag-2018-0006

A Resistivity Survey of Phosphate Nodules in Oshoshun, Southwestern Nigeria

Raziskava Upornosti Nahajališča Fosfatnih Gomoljev v Oshoshunski Formaciji v Jugozahodni Nigeriji

Oluseun Adetola Sanuade[1],*, Abayomi Adesola Olaojo[2], Adesoji Olumayowa Akanji[3], Michael Adeyinka Oladunjoye[4], Gabriel E. Omolaiye[5]

[1] Department of Geophysics, Federal University Oye-Ekiti, Ekiti State, Nigeria
[2] Earth Sciences Department, Ajayi Crowther University, Oyo, Nigeria
[3] Geoexperts Nigeria Ltd, Rockstone Ville Estate, Badore, Ajah, Lagos, Nigeria
[4] Department of Geology, University of Ibadan, Ibadan, Nigeria
[5] Crustcut and Minerals Limited, 16 Odudu Eleyiwo Street, Victoria Island, Lagos State, Nigeria
*sheunsky@gmail.com

Abstract

This geophysical study was carried out to determine the occurrence of phosphate nodules in the Oshoshun Formation of the Dahomey Basin, Southwestern Nigeria. The electrical resistivity method, comprising 1D vertical electrical sounding (VES; using Schlumberger array) and 2D geoelectrical imaging (using Wenner array), was used to determine the nature and depth of occurrence of the phosphate nodules. Six profile lines were established within the study area, and inverted sections were generated from the apparent resistivity data using DIPRO inversion algorithm. Five VES points were also acquired in the study area, and WinResist programme was used to process and interpret the field resistivity data. Four pits were dug along the profiles to verify the interpreted results. The results obtained by both techniques reveal similar geoelectric units: the top soil, clay, clayey sand and clay at different depths. These layers host pockets of phosphate nodules (78–≥651 Ωm) with varying thicknesses. The strong correlation between the lithology profiles obtained from the pits and the interpreted results of the inverted apparent resistivity sections demonstrates the efficacy of the electrical resistivity method in characterising phosphate occurrence within the formation.

Key words: imaging • inversion • Oshoshun • phosphate nodules • resistivity

Povzetek

Namen te geofizikalne raziskave je bil opredeliti nahajališče fosfatnih gomoljev v oshoshunski formaciji dahomejske kadunje v jugozahodni Nigeriji. Z uporabo metode električne upornosti so določili naravo in globino nahajališča fosfatnih gomoljev, in sicer z 1D vertikalnim električnim sondiranjem ob uporabi Schlumbergerjevega razporeda in z 2D geoelektrično preiskavo z Wennerjevim razporedom. Na raziskovanem območju so izmerili šest profilov in izdelali iz podatkov navidezne upornosti prognozne preseke ob uporabi inverzijskega algoritma DIPRO. Na proučevaneem ozemlju so izvedli tudi pet vertikalnih električnih sondiranj (VES). Za obdelavo in interpretacijo terenskih meritev upornosti so uporabili program WinResist. Za preverbo interpretiranih rezultatov so izkopali ob profilih štiri jaške. Rezultati obeh postopkov so podobni, razkrivajo navzočnost vrhnjih tal, gline in glinenega peska v različnih globinah. V teh plasteh so žepi fosfatnih gomoljev (78 - ≥651 Ωm) različne debeline. Visoka stopnja ujemanja med litološkimi podatki iz jaškov in rezultati iz interpretiranih profilov navidezne upornosti priča o učinkovitosti električne upornostne metode za ugotavljanje fosfatnih nahajališč v plasteh.

Ključne besede: sondiranje, interpretacija, oshoshunska formacija, fosfatni gomolji, upornost

Introduction

Phosphate rock is a globally accepted but imprecise term describing any naturally occurring geological material that contains one or more phosphate minerals suitable for commercial use. The rock comprises both the unprocessed phosphate ore and the concentrated phosphate products [1]. The phosphorus content or grade of phosphate rocks is commonly reported as phosphorus pentoxide (P_2O_5). The principal phosphate minerals in phosphate rocks are calcium phosphates, mainly apatites. Five major types of phosphate resources are being mined in the world: marine phosphate deposits, igneous phosphate deposits, metamorphic deposits, biogenic deposits and phosphate deposits as a result of weathering [2]. Sedimentary phosphates are of great economic importance because they constitute most of the raw materials for the manufacture of phosphate fertiliser and some phosphorus-based chemicals. Direct application of phosphate rock as phosphate fertiliser has been found to compete favourably well with mineral fertilisers on acidic soils [3–6]. Electrical resistivity surveys have been conducted on some phosphate deposits, and remarkable results have been achieved [7,8].

There are large deposits of phosphate-rich sediments of the Eocene Age in Ogun State of Southwestern Nigeria. Although the slightly older (Paleocene) phosphate deposits of Sokoto State have been extensively worked for agricultural material, the Ogun phosphate rock has received little attention [9,10]. It is important to carry out geophysical characterisation studies of Ogun phosphate rock to ascertain the availability of phosphates. Therefore, this study was carried out to determine the occurrence of phosphate nodules and evaluate the nature and depth of such phosphate beds in the study area.

Location and geology of the study area

The study area is located in Oshoshun village, in Ifo local government area of Ogun State. It is located within the longitudes 7°27′14.1″, 7°27′12.5″, 7°27′07.9″ and 7°27′12.6″ and the latitudes 3°53′40.4″, 3°53′40.7″, 3°53′27.6″ and 3°53′36.5″ (Figure 1). The area is accessible through an untarred road, which branches off from the Lagos–Abeokuta Express Road.

The study area lies within the Oshoshun Formation, which is phosphate bearing. The phosphate within the Oshoshun occurs as discrete bands in the shale, which sometimes at some parts could also be glauconitic, while the gypsum appears as mud-supported gypsiferous

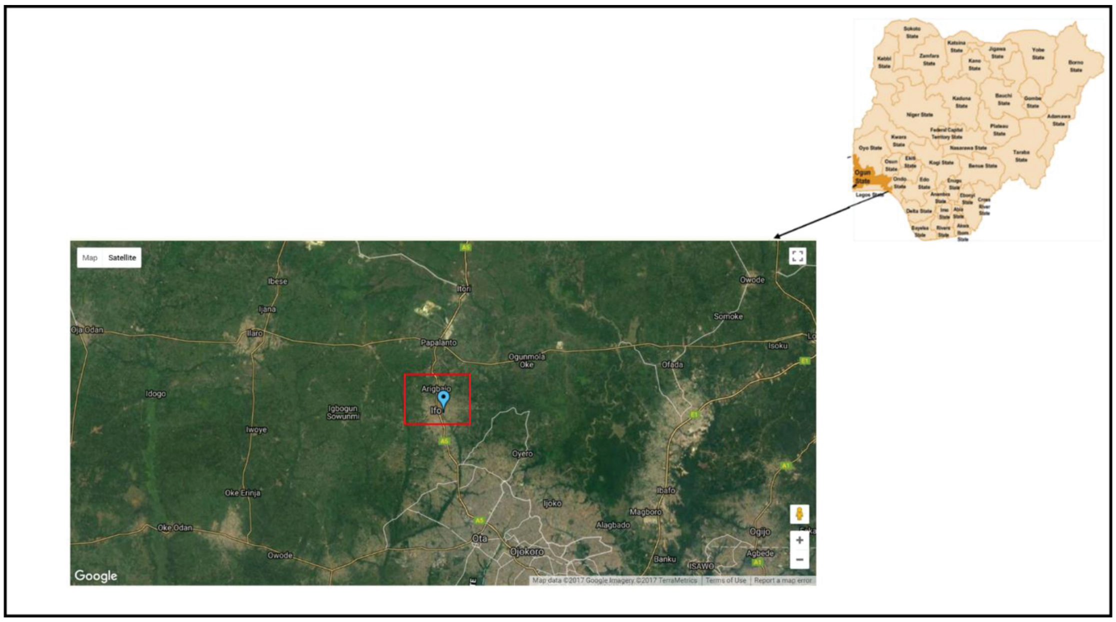

Figure 1: *Map of Nigeria showing the Ifo local government area and its environs.*

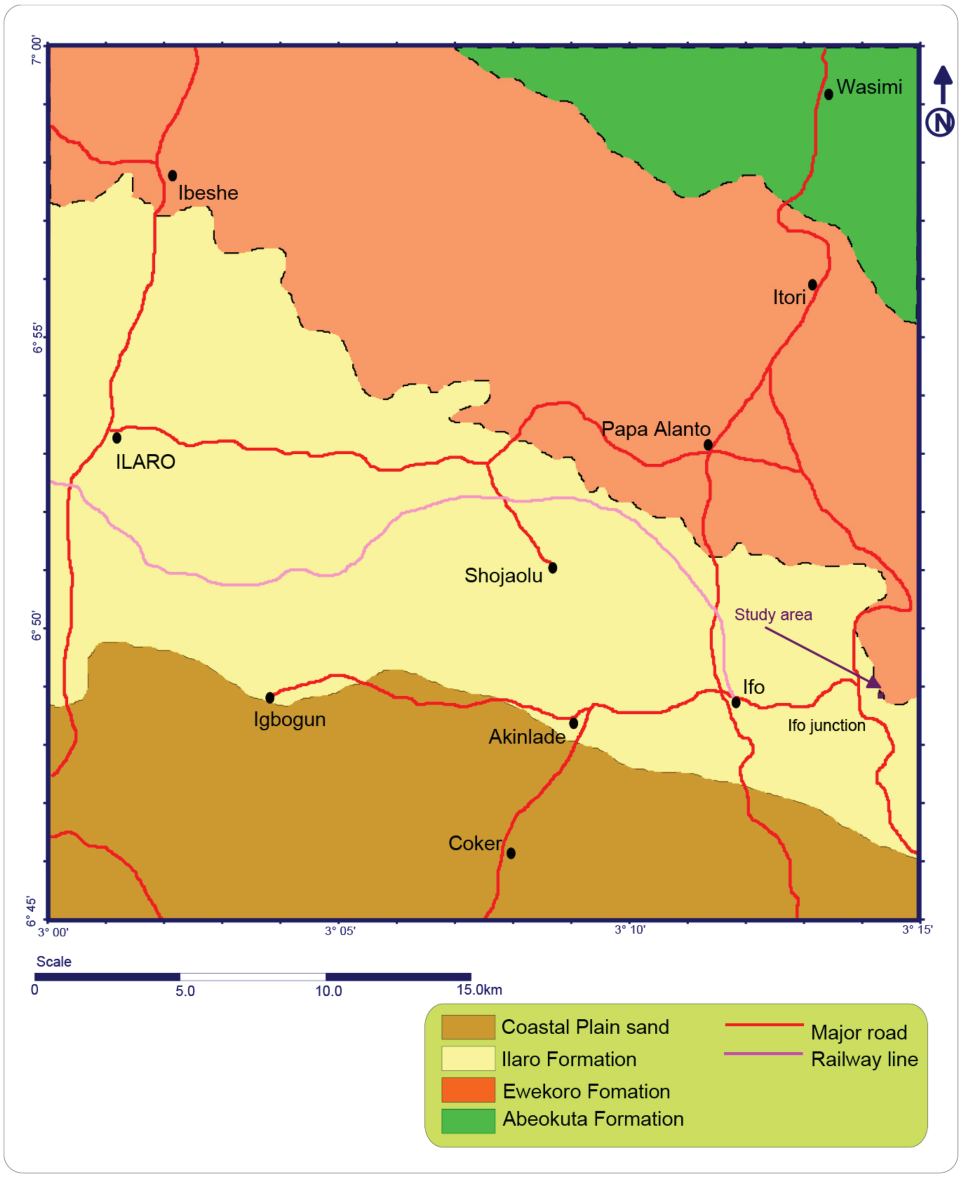

Figure 2: *Geological map of Ifo and environs showing the study area.*

shale. The Oshoshun is overlain by the Ilaro Formation, which is made up of both marine and continental massive yellow and poorly consolidated sandstones (Figure 2). The phosphates occur as nodules at ~3–6 m of depth within the formation.

Methodology

Electrical Resistivity Surveys

Six 2D geoelectrical resistivity profile lines were measured (Figure 3) with the aid of an Ohmega Campus model resistivity meter using the Wenner-alpha array. Each of the 2D traverses was 50 m in length, and they formed an orthogonal set such that the total area covered by the 2D traverses was ~2500 m^2. Five vertical electrical sounding (VES) data were also collected in the site using Schlumberger array to supplement the observed 2D resistivity imaging data and to provide layering information on the lithology of the study area. Figure 3 shows the survey plan with the locations of the traverses and the VES points. The measurements commenced at the east end for the in-lines and at the north end

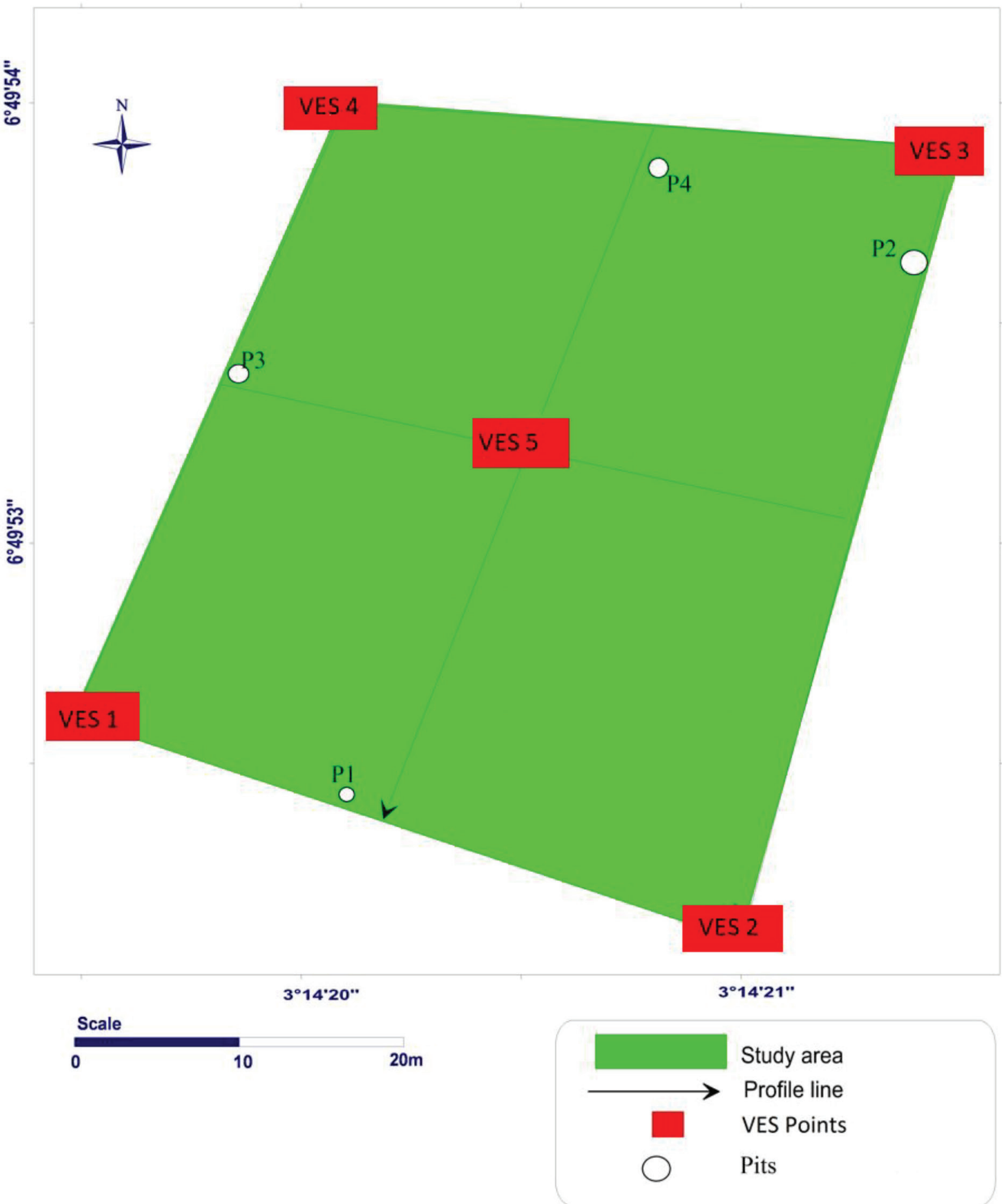

Figure 3: *Map of the study area showing locations of geophysical 1D (VES) and 2D resistivity imaging lines (Profiles 1, 2, 3, 4, 5 and 6) surveys.*

for the cross-lines. Four pits were dug along the profiles 1, 2, 4 and 6 (Figure 3) to verify the interpreted results.

Data Processing and Inversion

The electrical imaging data was processed and interpreted using computer-assisted DIPRO software and presented as inverted sections. The VES curves were quantitatively interpreted by partial curve matching and computer-assisted 1D forward modelling with the WinResist software, version 1.0 [11].

Results and Discussion

Geoelectric Profiles

Figure 4 shows a system of three geoelectric layers from the inverted section. The top soil has resistivity values ranging from 52 to 85 Ωm

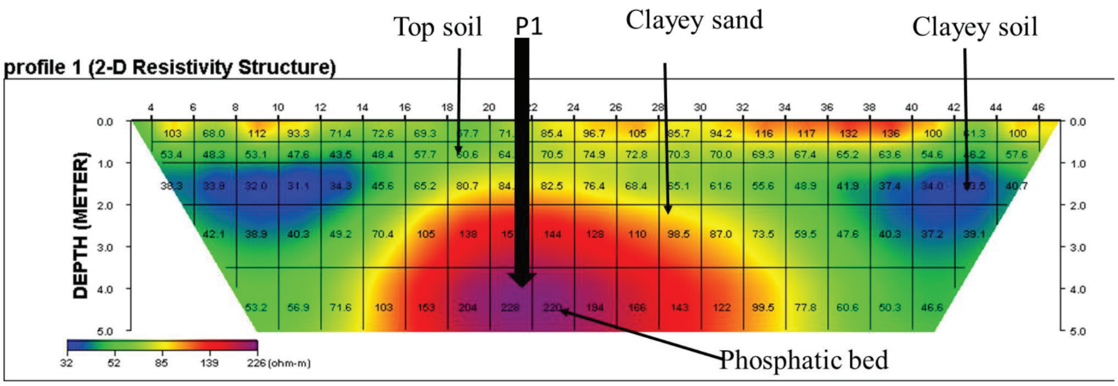

Figure 4: *Inverted model section of Profile line 1.*

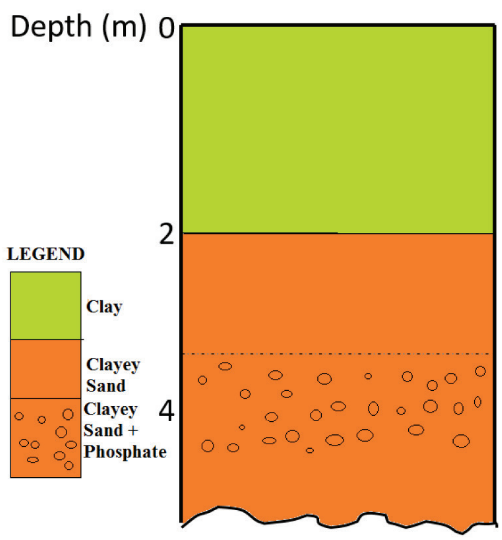

Figure 5: *Soil profile of Pit 1 (P1) dug along Profile 1.*

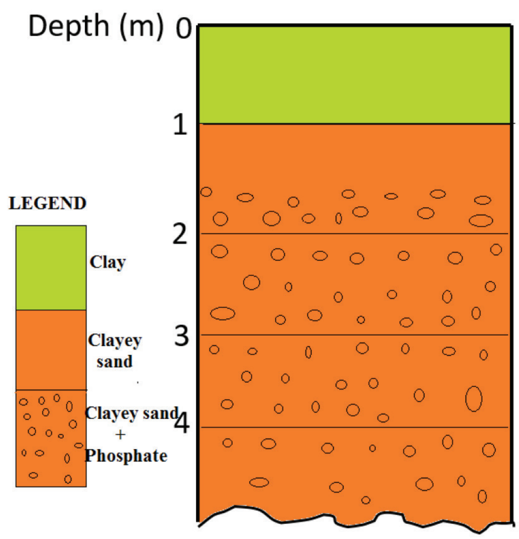

Figure 7: *Soil profile of Pit 2 (P2) dug along Profile 2.*

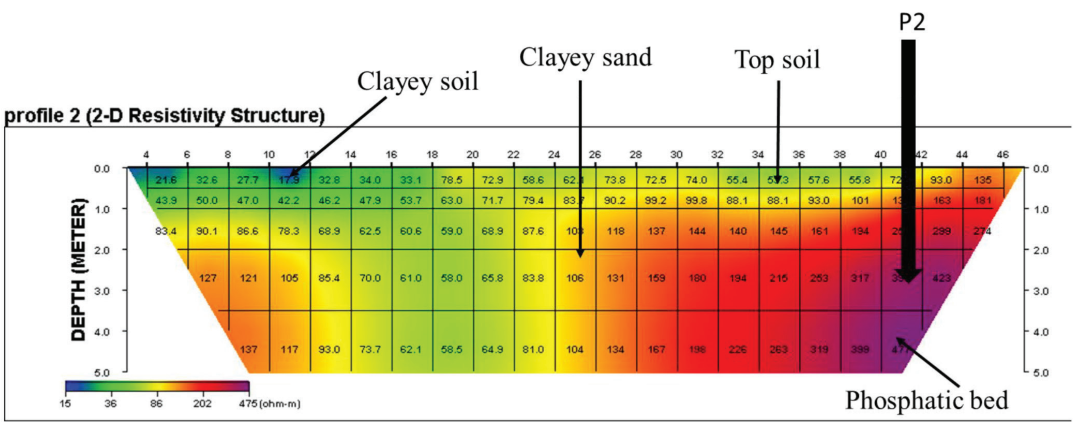

Figure 6: *Inverted model section of Profile line 2.*

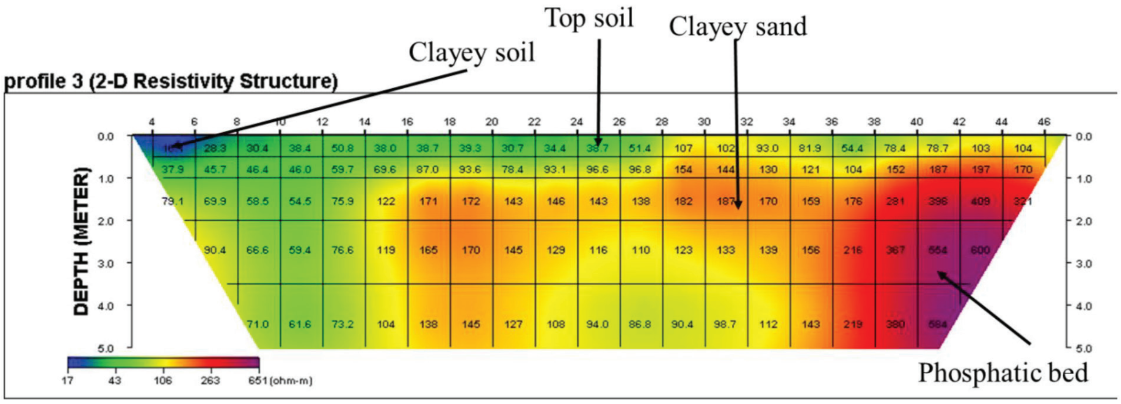

Figure 8: *Inverted model section of Profile line 3.*

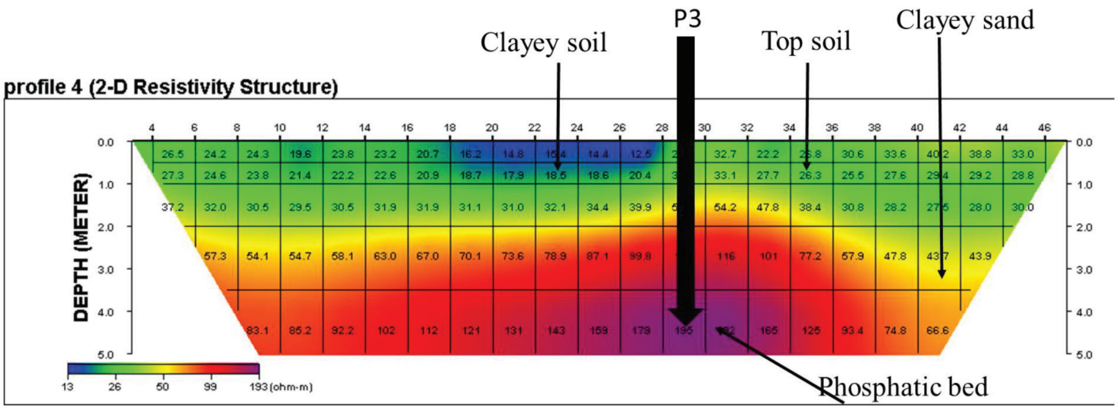

Figure 9: *Inverted model section of Profile line 4.*

extending from the surface to an average depth of 1.0 m; the next layer has resistivity values between 32 and 52 Ωm. This lithology is characterised by the presence of clayey material [12]. The clayey material occurs at both flanks of the traverse line. The third layer has resistivity values increasing from 63 to ≥ 139 Ωm. This indicates the presence of clayey sand [12]. The phosphate-nodule bed (139–≥226 Ωm) occurs within the clayey sand materials in the central lower part of the section.

The lithological column (Figure 5) of Pit 1 dug along Profile 1 reveals two horizons comprising clay (0.1–2 m thick) and clayey sand (2–> 5 m). Phosphate nodules are encountered at ~3.2 m within the clayey sand horizon. This result corresponds with the interpretation of the inverted section.

As observed from the 2D resistivity model in Figure 6, three varying geoelectric layers are

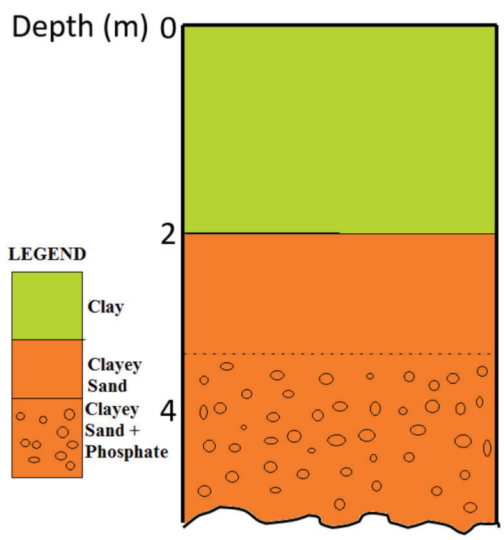

Figure 10: *Soil profile of Pit 3 (P3) dug along Profile 4.*

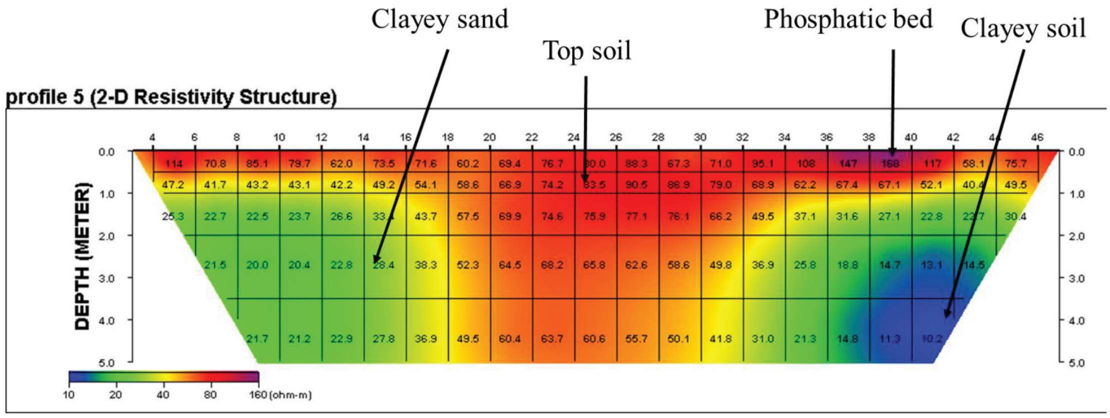

Figure 11: *Inverted model section of Profile line 5.*

detected. The resistivity values of the top soil are between 36 and 86 Ωm, as seen at the beginning of the profile up to the station at distance of 18 m, with an average depth of 1.5 m. The clayey soil layer has resistivity varying from 15 to 36 Ωm between stations at distances of 3 and 12 m. The clayey sand extends to the surface between stations at distances of 42 and 48 m, and its resistivity ranges from 86 to ≥ 202 Ωm; the phosphatic bed (202–≥475 Ωm) is embedded in this layer.

The soil profile (Figure 7) of Pit 2 dug along Profile 2, depicts two layers composed of clay and clayey sand. Phosphate nodules are embedded in the clayey sand at a depth of 1.5–≥4 m. This result corroborates the interpretation from the inverted section.

Profile 3 (Figure 8) shows an ordered arrangement of the geoelectric layers, although the layers tend to dip slightly at an angle. The top soil has resistivity value in the range of 43–106 Ωm, its horizontal extension being between 8 and 28 m. The underlying lithology is suggested to be clayey based on its resistivity value (17–43 Ωm), also occurring at the surface between stations at distances of 3 and 8 m. The clayey sand layer has resistivity values ranging from ≤ 106 to ≥ 263 Ωm. The phosphate-rich sequence is embedded within this layer, thus having resistivity value from 263 to ≥ 651 Ωm. The phosphatic nodule is concentrated at profile distances of 40–46 m.

The inverted section of Profile 4 (Figure 9) exhibits an ordered internal arrangement of the geoelectric layer, and its resistivity value increases with depth. Three geoelectric layers are observed in the inverted section; these include the top soil, clayey soil and clayey sand. The top soil shows that material of low resistivity (14–25 Ωm) is enclosed within a more resistive layer (25–33 Ωm); it extends to an average depth of 2.6 m. The clayey soil has resistivity value between 33 and 59 Ωm, and its thickness is ~1.2 m. The next layer underlying the clayey soil is depicted to be clayey sand, with its resistivity value varying from 59 to ≥ 103 Ωm. This layer hosts the phosphate concentrate (78–≥103 Ωm).

The soil profile (Figure 10) of Pit 3 dug along Profile 4 shows two layers made up of clay and clayey sand. Phosphate nodules are embedded in the clayey sand at a depth of 3.5–≥5 m. This result agrees with the interpretation of the inverted section in Figure 9.

Figure 11 (Profile 5) shows chaotic distribution of resistivities when compared with the distribution in other profiles (1–4): it is characterised by decrease in resistivity values as the depth increases. The top soil is composed of moderate resistive material (40–≥80 Ωm), with pockets of resistive material occurring at the surface. These pockets are referred to as the phosphate nodules. The phosphatic bed has resistivity between 80 and >160 Ωm occurring at stations at distances of 37–40 m. The clayey soil underlying the top soil has resistivity value ranging from 10 to 20 Ωm. The next layer is clayey sand having resistivity between 20 and >40 Ωm.

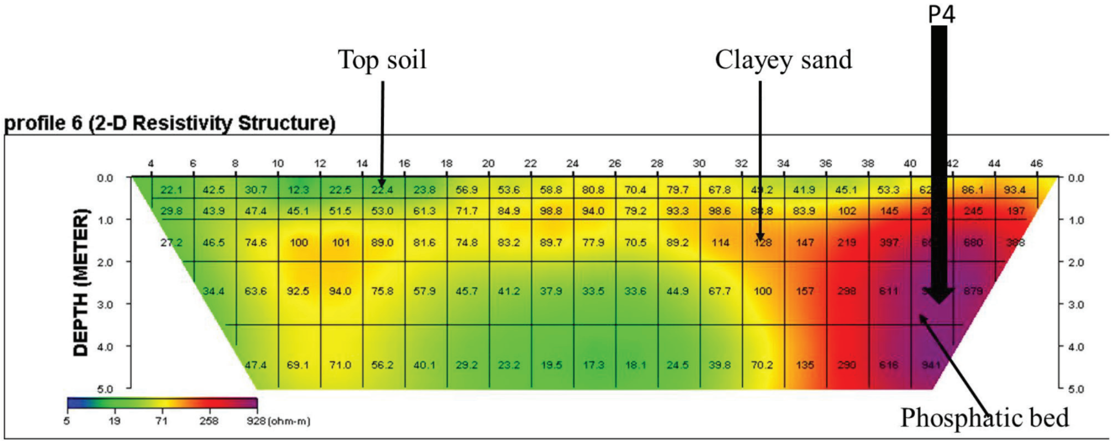

Figure 12: *Inverted model section of Profile line 6.*

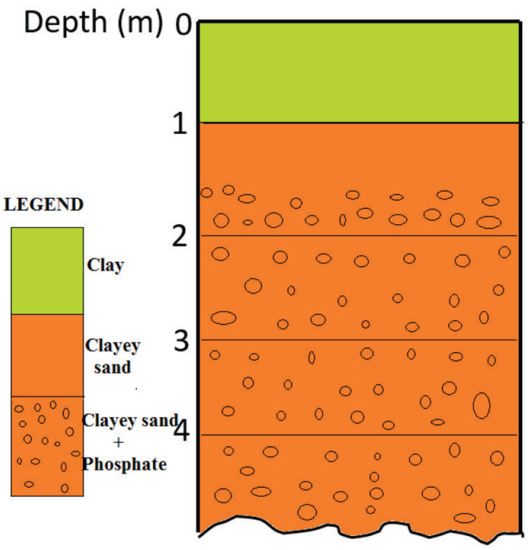

Figure 13: *Soil profile of Pit 4 (P4) dug along Profile 6.*

Profile 6 (Figure 12) shows the gradual transition of one lithology into another as can be assumed from the changing resistivity values horizontally along the profile. The top soil is characterised by resistivity values in the range of 19–71 Ωm. A resistive body is embedded with the clayey sand layer: this resistive body is suspected to be composed of nodules of phosphate. The phosphatic nodules are concentrated at stations at distances of 38–45 m in the top soil.

The soil profile (Figure 13) of Pit 4 dug along Profile 6 reveals two layers made up of clay and clayey sand. Phosphate nodules are encountered in the clayey sand at depth of 1.5–≥5 m. This result agrees with the interpretation of the inverted section.

VES data

The resistivity sounding curves of the five VES stations obtained from the study area have four layers, which are KH-type curves with $\rho_1 < \rho_2 > \rho_3 < \rho_4$ (Figure 14). The analysis and interpretation of the VES curves and the geoelectric parameters indicate that four layers are delineated, including top soil, clay unit, clayey sand and clay. Each litho-unit varies in thickness from one point to another within the study area (Figure 14A–E).

Geoelectric Sections

The 2D view of the geoelectric parameters obtained from the VES data are presented as VES-derived geoelectric sections (Figures 15 and 16). The VES model resistivity values complement the inversion results of the 2D image by distinguishing four different layers.

Geoelectric section 1

Figure 15 is deduced from the joint layer parameters of VES 1, 5 and 3. From the VES geoelectric section, the following layers are obtained: the top soil, clayey sand, clay and clayey sand. The top soil has resistivity value ranging from 62 to 67 Ωm, with an average thickness of 0.93 m. The next layer underlying this unit is clayey sand, its thickness ranges from 3.9 to 7.1 m and the resistivity value of this unit varies

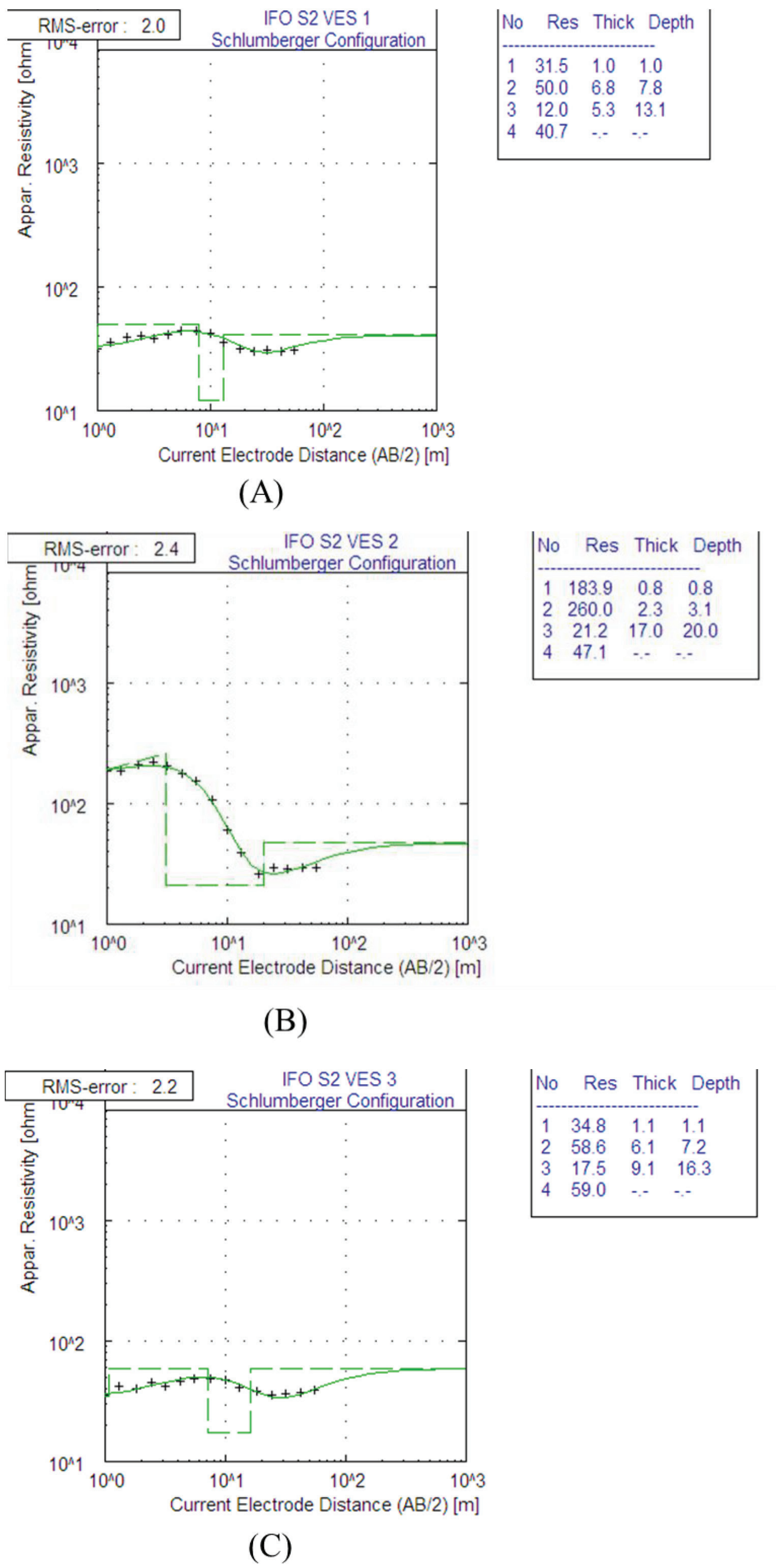

Figure 14: *Schlumberger layer model (A) VES 1; (B) VES 2; (C) VES 3 (all are representatives of KH-type curve: $\rho_1 < \rho_2 > \rho_3 < \rho_4$).*

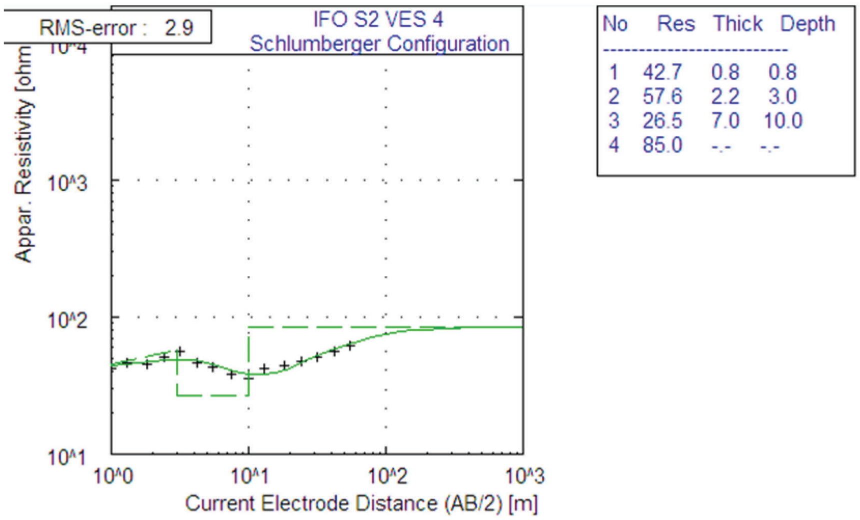

(D)

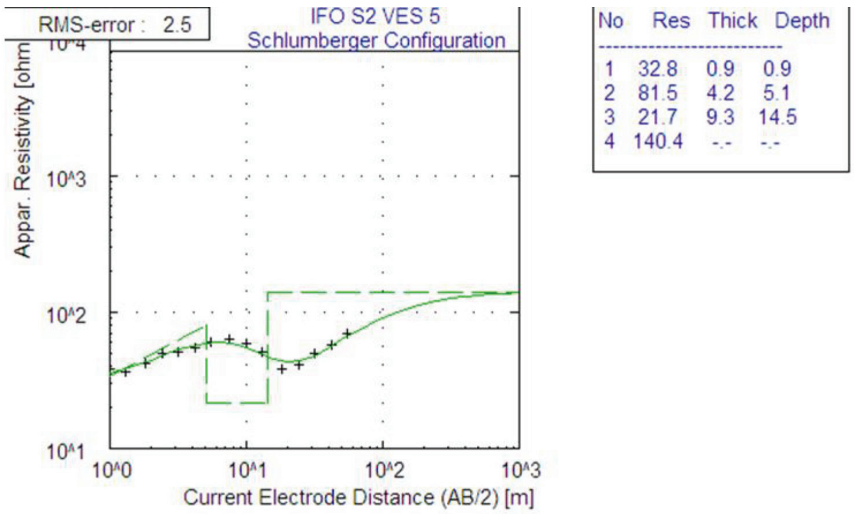

(E)

Figure 14: *Schlumberger layer model (D) VES 4; and (E) VES 5 (all are representatives of KH-type curve: $\rho_1 < \rho_2 > \rho_3 < \rho_4$).*

from 51 to 82 Ωm. The clay unit has resistivity value ranging from 13 to 20 Ωm, it happens to be the thickest unit within this section and its thickness varies from 8.1 to 10.3 m. The last in the sequence is clayey sand; the resistivity value of this layer ranges from 55 to 158 Ωm, which extends from 13.2 m below the surface. The phosphate nodules are embedded within the clayey sand layer.

Geoelectric section 2

The VES-derived geoelectric section (Figure 16) shows four geoelectric units; these include the top soil, clayey sand, the clay unit and clayey sand unit. These sequences tend to alternate with one another with varying thickness and resistivity values. The top soil has thickness ranging from 0.7 to 0.9 m, and the average thickness is 0.83 m. The resistivity value of this unit ranges from 30 to 34 Ωm. Next to this is the clayey sand, and its resistivity varies from 83 to 129 Ωm, with an average thickness of ~3.9 m. The clay unit has the greatest thickness when compared with other units, its resistivity value ranges from 13 to 21 Ωm, it has thickness value ranging from 9.4 to 11.8 m, and thus an

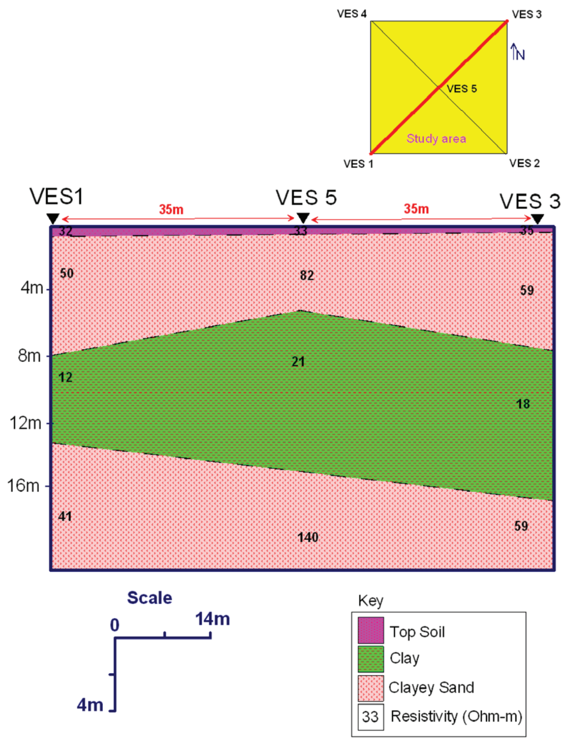

Figure 15: *VES-derived geoelectric section across VES 1, 5 and 3, respectively.*

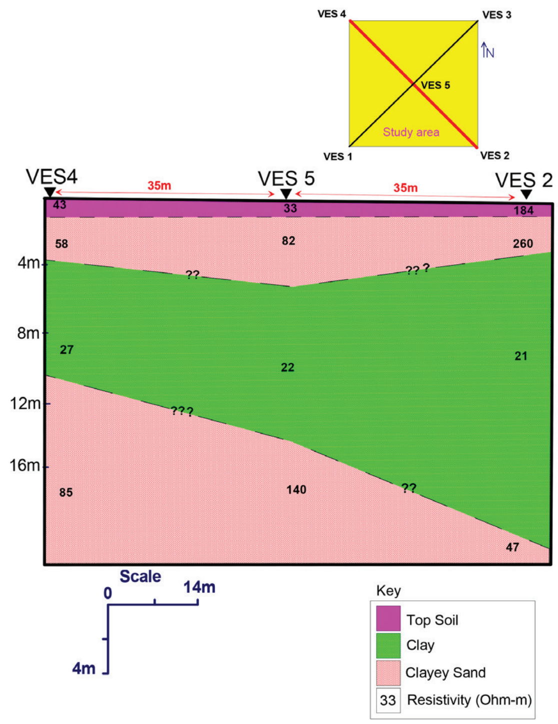

Figure 16: *VES-derived geoelectric section across VES 4, 5 and 2 respectively.*

average thickness of 10.5 m is computed for this unit. The clayey sand has resistivity value ranging from 80 to 130 Ωm and it extends from 13.7 m downwards. The phosphate nodules are also embedded within the clayey sand layer.

Conclusions

Geophysical methods have proven to be effective in delineating the deposits of subsurface raw materials. An integrated geoelectrical study, comprising 1D and 2D resistivity surveys, was used to determine the occurrence of phosphate nodules in the Oshoshun Formation of Dahomey Basin, Southwestern Nigeria. The results obtained by both techniques reveal similar geoelectric units: top soil, clay, clayey sand and clay at different depths. In most cases, clayey sand layers host pockets of phosphate nodules (78–≥651 Ωm) with varying thicknesses. The observed resistivity values of the phosphate nodules at Oshoshun fall in the same range of resistivity values of phosphates from Morocco reported by Bakkali [7]. The strong correlation between the lithology profile obtained from the pits and the interpreted results of the inverted apparent resistivity section demonstrates the efficacy of the electrical resistivity method in characterising phosphate occurrence within the Oshosun Formation. Moreover, geophysical surveys have shown their advantages over other methods, such as drilling, digging pits, etc. Geoelectrical methods are non-destructive, they require short time to survey large areas and the associated costs are thereafter low. The use of geophysical methods is highly recommended in the early stages of reconnaissance for raw materials.

References

[1] Adesanwo, O.O., Dunlevey, J.N., Adetunji, M.T., Adesanwo, J.K., Diatta, S., Osiname O.A. (2010): Geochemistry and mineralogy of Ogun phosphate rock. *African Journal of Environmental Science and Technology*, 4(10), pp. 698–708.

[2] Newman, D.K., Banfield, J.F. (2002): Geomicrobiology: How molecular-scale interactions underpin biogeochemical systems. *Science*, 296, pp.1071–1077.

[3] Bolan, N.S., White, R.E. and Hedley, M.J. (1990): A review of the use of phosphate rocks as fertilizers for direct application in Australia and New Zealand. *Australian Journal of Experimental Agriculture*, 30, pp. 297–313.

[4] Chien, S.H., Sale, P.W.G., Hammond, L.L. (1990): *Comparison of the effectiveness of phosphorus fertilizer products*. In: Phosphorus requirements for sustainable agriculture in Asia and Oceania. Int. Rice Res. Inst., Manila, Philippines, p. 143–156.

[5] Akande, M.O., Aduayi, E.A., Sobulo, R.A., Olayinka A. (1998): Efficiency of Rock phosphate as fertilizer source in South – western Nigeria. *Journal of Plant Nutrition*, 2, pp. 1339–1353.

[6] Adediran, J.A., Oguntoyinbo, F.I., Omonode, R., Sobulo, R.A. (1998): Agronomic evaluation of phosphorus fertilizers developed from Sokoto rock phosphate in Nigeria. *Communications in Soil Science and Plant Analysis,* 29, pp. 2659–2673.

[7] Bakkali, S. (2006): A resistivity survey of phosphate deposits containing hardpan pockets in Oulad Abdoun, Morocco. *Geofísica Internacional,* 45(1), pp. 73–82.

[8] Bakkali, S., Amrani, M. (2008): About the use of spatial interpolation methods to denoising Moroccan resistivity data phosphate “Disturbances” map. *Acta Montanistica Slovaca Ročník,* 13(2), pp. 216–222.

[9] Adegoke, O.S., Ajayi, T.R., Nehikhare, J.I., Rahaman, N.A. (1989): Fertiliser raw material situation in Nigeria. Paper presented at the Workshop Organized by National Fertilizer Company, Durbar Hotel, Kaduna, June, 2–7.

[10] Akintokun, O.O., Adetunji, M.T., Akintokun, P.O. (2003): Phosphorus availability to soybean from an indigenous phosphate rock sample in soil from south – western Nigeria. *Nutrient Cycling in Agroecosystems*, 65, pp. 35–42.

[11] Adelusi, A.O., Akinlalu, A.A., Nwachukwu, A.I. (2013): Integrated geophysical investigation for post-construction studies of buildings around School of Science area, Federal University of Technology, Akure, Southwestern, Nigeria. *International Journal of Physical Science*, 8(15), pp. 657–669.

[12] Loke, M.H. (2000): Electrical imaging surveys for environmental and engineering studies: A practical guide to 2-D and 3-D surveys, 61 p.

Instructions for Authors

RMZ – MATERIALS & GEOENVIRONMENT (RMZ – Materiali in geookolje) is a periodical publication with four issues per year (established in 1952 and renamed to RMZ – M&G in 1998). The main topics are Mining and Geotechnology, Metallurgy and Materials, Geology and Geoenvironment.
RMZ – M&G publishes original scientific articles, review papers, preliminary notes, and professional papers in English. Only professional papers will exceptionally be published in Slovene. In addition, evaluations of other publications (books, monographs, etc.), in memoriam, presentation of a scientific or a professional event, short communications, professional remarks and reviews published in RMZ – M&G can be written in English or Slovene. These contributions should be short and clear.
Authors are responsible for the originality of the presented data, ideas and conclusions, as well as for the correct citation of the data adopted from other sources. The publication in RMZ – M&G obligates the authors not to publish the article anywhere else in the same form.

Specification of the Contributions

Optimal number of pages is 7 to 15; longer articles should be discussed with the Editor-in-Chief prior to submission. All contributions should be written using the ISO 80000.

- Original scientific papers represent unpublished results of original research.
- Review papers summarize previously published scientific, research and/or expertise articles on a new scientific level and can contain other cited sources which are not mainly the result of the author(s).
- Preliminary notes represent preliminary research findings, which should be published rapidly (up to 7 pages).
- Professional papers are the result of technological research achievements, application research results and information on achievements in practice and industry.
- Publication notes contain the author's opinion on newly published books, monographs, textbooks, etc. (up to 2 pages). A figure of the cover page is expected, as well as a short citation of basic data.
- In memoriam (up to 2 pages), a photo is expected.
- Discussion of papers (Comments) where only professional disagreements of the articles published in previous issues of RMZ – M&G can be discussed. Normally the source author(s) reply to the remarks in the same issue.
- Event notes in which descriptions of a scientific or a professional event are given (up to 2 pages).

Review Process

All manuscripts will be supervised shall undergo a review process. The reviewers evaluate the manuscripts and can ask the authors to change particular segments, and propose to the Editor-in-Chief the acceptability of the submitted articles. Authors are requested to identify three reviewers and may also exclude specific individuals from reviewing their manuscript. The Editor-in-Chief has the right to choose other reviewers. The name of the reviewer remains anonymous. The technical corrections will also be done and the authors can be asked to correct the missing items. The final decision on the publication of the manuscript is made by the Editor-in-Chief.

Form of the Manuscript

All papers must be submitted via the online system.
The original file of the Template is available on RMZ – Materials and Geoenvironment Home page address: **www.rmz-mg.com**.

The contribution should be submitted in Microsoft Word. Manuscript should be written in Arial font and 12 pt font with 1.5 line spacing and should contain all figures, tables and formulas. Headings should be written in Arial bold font and shuold not be numbered. Subheadings should be written in Arial italic font. The electronic version should be simple, without complex formatting, hyphenation, and underlining. For highlighting, only bold and italic types should be used.

Annexes

Annexes are images, spreadsheets, tables, and mathematical and chemical formulas. Math formulas should be included in article as editable text and not as images.
Annexes should be included in the text at the appropriate place, and they should also be submitted as a separate document, i.e. separated from the text in the article.
Annexes should be originals, made in an electronic form (Microsoft Excel, Adobe Illustrator, Inkscape, AutoCad, etc.) and in .eps, .tif or .jpg format with a resolution of at least 300 dpi.
The width of the annex should be at least 152 mm. They should be named the same as in the article (Figure 1, Table 1). The text in the annexes should be written in typeface Arial Regular (6 pt).
The title of the image (also schemes, charts and graphs) should be indicated in the description of the image.
When formatting spreadsheets and tables in text editors, tabs, and not spaces, should be used to separate columns.
Each formula should have its number written in round brackets on its right side.
References of the annexes in the text should be as follows: "Figure 1…" and not "as shown below:". This is due to the fact that for technical reasons the annex cannot always be placed at the exact specific place in the article.

Composition of the Manuscript

Title
The title of the article should be precise, informative and not longer that 100 characters. The author should also indicate the short version of the title. The title should be written in English as well as in Slovene..

Information on the Authors
Information on the authors should include the first and last name of the authors, the address of the institution and the e-mail address of the corresponding author.

Abstract
The abstract presenting the purpose of the article and the main results and conclusions should contain no more than 180 words. It should be written in Slovene and English.

Key words
A list of up to 5 key words (3 to 5) that will be useful for indexing or searching. They should be written in Slovene and English.

Introduction

Materials and methods

Results and discussion

Conclusions

Acknowledgements

References

The references should be cited in the same order as they appear in the article. **Where possible the DOI for the reference should be included at the end of the reference.** They should be numbered in square brackets. References should be cited according SIST ISO 690:1996 standards.

Book:
[1] Reynolds, J.M. (2011). *An introduction to Applied and Environmental Geophysics*. New York: Wiley, 710 p.

Unpublished Master thesis or PhD dissertation:
[2] Trček, B. (2001): *Solute transport monitoring in the unsaturated zone of the karst aquifer by natural tracers*. Ph. D. Thesis. Ljubljana: University of Ljubljana 2001; 125 p.

Chapter in an edited book:
[3] Blindow, N., Eisenburger, D., Illich, B., Petzold, H., Richer, T. (2007): *Ground Penetrating Radar*. In: Environmental Geology: Handbook of Field Methods and Case Studies, Knödel, K., Lange, G., Voigt, H.J. (eds.). Springer: Berlin; pp. 283–335.

Journal article : Journal title should be complete and not abbreviated.
[4] Higashitani, K., Iseri, H., Okuhara, K., Hatade, S. (1995): Magnetic Effects on Zeta Potential and Diffusivity of Nonmagnetic Particles. *Journal of Colloid and Interface Science*, 172, pp. 383–388.
[5] Mcmechan, G.A, Loucks, R.G, Mescher, P.A, Xiaoxian, Z. (2002): Characterization of a coalesced, collapsed paleocave reservoir analog using GPR and well-core data. *Geophysics*, 67, pp. 1148–1158. doi: 10.1190/1.1500376

Proceedings Paper:
[6] Benac, Č., Gržančić, Ž., Šišić, S., Ružić, I. (2008): Submerged Karst Phenomena in the Kvarner Area. In: Proceedings of the 5th International ProGEO Symposium on Conservation of the Geological Heritage, Rab, Croatia, Marjanac, T (ed.). Pro GEO Croatia: Zagreb; pp. 12–13.

Electronic source:
[7] CASREACT – Chemical reactions database [online]. Chemical Abstracts Service, 2000, renewed 2/15/2000 [cited 2/25/2000]. Available on: <http://www.cas.org/casreact.html>.

Scientific articles, review papers, preliminary notes and professional papers are published in English. Only professional papers will exceptionally be published in Slovene.

Units

SI System should be used for units. Physical quantities should be written in Italics (e.g. m, l, v, T). Symbols for units should be in plain text with spaces (e.g. 10 m, 5.2 kg/s, 2 s-1, 50 kPa). All abreviations should be spelt out in full on first appearance.

Manuscript Submission

Please submit your article via RMZ-M&G Editorial Manager System. You can find it on the address: http://edmgr.editool.com/rmzmag/default.htm

Log in as an author and submit your article.
You can follow the status of your submission in the system manager and your e-mail.

Information on RMZ – M&G

— Assistant editor
  Jože Žarn
  E-mail address: joze.zarn@ntf.uni-lj.si

— Secretary
  Vukič Nivesč
  Telephone: +386 01 47 04 610
  E-mail address: nives.vukic@ntf.uni-lj.si

These instructions are valid from April 2017.

ISSN 1408-7073